diversity

MDPI

Article

Integrating 3D-Printed and Natural Staghorn Coral (*Acropora cervicornis*) Restoration Enhances Fish Assemblages and Their Ecological Functions

Edwin A. Hernández-Delgado *, Jaime S. Fonseca-Miranda, Alex E. Mercado-Molina and Samuel E. Suleimán-Ramos

Reef Conservation, Vitalization and Ecological Restoration Program, Sociedad Ambiente Marino, San Juan 00927-5133, Puerto Rico; jaimefonseca@sampr.org (J.S.F.-M.); alexmercado@sampr.org (A.E.M.-M.); samuelsuleiman@sampr.org (S.E.S.-R.)

* Correspondence: edwinhernandez@sampr.org; Tel.: +1-939-642-7264

Abstract

Coral restoration is essential for recovering depleted populations and reef ecological functions. However, its effect on enhancing fish assemblages remains understudied. This study investigated the integration of 3D-printed and natural Staghorn coral (*Acropora cervicornis*) out-planting to assess their role in enhancing benthic spatial complexity and attracting fish communities. Conducted between 2021 and 2023 at Culebra Island, Puerto Rico, we employed a before-after-control-impact (BACI) design to test four treatments: natural *A. cervicornis*, 3D-printed corals, mixed stands of 3D-printed and natural corals, and non-restored controls. Fish assemblages were monitored through stationary counts. Results showed that integrating 3D-printed and natural corals enhanced fish assemblages and their ecological functions. Significant temporal changes in fish community structure and biodiversity metrics were observed, influenced by treatment and location. Herbivore abundance and biomass increased over time, especially in live coral and 3D-printed plots. Reefs with higher rugosity exhibited greater Scarid abundance and biomass post-restoration. Piscivore abundance also rose significantly over time, notably at Tampico site. Fishery-targeted species density and biomass increased, particularly in areas with live and 3D-printed coral out-plants. Fish assemblages became more complex and diverse post-restoration, especially at Tampico, which supported greater habitat complexity. Before restoration, fish assemblages showed a disturbed status, with biomass k-dominance curves above abundance curves. Post-out-planting, this trend reversed. Control sites showed no significant changes. The study demonstrates that restoring fast-growing branching corals, alongside 3D-printed structures, leads to rapid increases in abundance and biomass of key fishery species, suggesting its potential role promoting faster ecosystem recovery and enhanced coral demographic performance.

Keywords: biodiversity; coral 3D printing; coral restoration; fish community; fishery target species; phylogenetic diversity; taxonomic distinctness; trophic functional groups

Academic Editor: Bert W. Hoeksema

Received: 25 February 2025
Revised: 15 June 2025
Accepted: 16 June 2025
Published: 23 June 2025

Citation: Hernández-Delgado, E.A.; Fonseca-Miranda, J.S.; Mercado-Molina, A.E.; Suleimán-Ramos, S.E. Integrating 3D-Printed and Natural Staghorn Coral (*Acropora cervicornis*) Restoration Enhances Fish Assemblages and Their Ecological Functions. *Diversity* **2025**, *17*, 445. https://doi.org/10.3390/d17070445

1. Introduction

Coral reefs have declined globally over the last four decades due to numerous human-driven factors, such as sedimentation [1–3], turbidity [4], pollution [5–8], and fishing [9,10]. Additionally, regional and global climate-related changes, including mass coral bleaching [11], coral mortality [12], and ocean acidification [13], have increased coral

loss. These impacts are further compounded by sea level rise (SLR) [14] and stronger hurricanes [15–17]. Recent threats also include invasive and nuisance species [18–20], hypoxia [21,22], virulent coral diseases [23], and mass mortalities [24–26]. Together, these factors threaten the persistence, sustainability, ecological functions, services, ecosystem resilience, and socio-economic benefits of coral reefs. Furthermore, projections of future sea surface warming trends suggest severely compromised coral reef futures and significantly impaired coral restoration outcomes under business-as-usual scenarios as early as the 2030s [27].

Global coral reef degradation requires innovative conservation and restoration approaches. Over the past three decades, numerous global restoration efforts have been implemented, ranging from community-based, small-scale projects [28,29] and various in situ coral nursery designs [30–32], to the integrated use of artificial structures [33,34] and diverse coral gardening techniques [35]. These efforts also include state-of-the-art approaches such as novel land-based nurseries [36], micro-fragmentation [37,38], larval rearing [39], cryopreservation [40,41], and gene banking techniques [42–44]. Additionally, coral restoration has incorporated novel methods like improved gardening techniques [45], ecological engineering [46–48], assisted migration [49,50], assisted evolution [51], assisted microbiome [52,53], epigenetics [54,55], and chimerism [56]. The increasing threats from climate change and SLR on small island developing states (SIDS) necessitate a combination of emerging strategies to enhance resistance to extreme weather disturbances and rising sea levels, including the restoration of green/gray infrastructure, which will require strategies beyond coral restoration [47].

The incorporation of 3D-printing technology has emerged in recent decades as a promising tool for coral reef restoration under some conditions, though its use is still limited. The use of artificial reef substrates and structures in coral reef restoration and recovery of coastal ecosystems in general has been documented since the early 1930s [57,58]. The benefits of artificial structures for fish community enhancement and fisheries management have been largely documented at least since the 1960s [59–67]. Recently, there has been an increase in the use of 3D-printing technology and in the integration of ecofriendly materials [68–70], various textures and shapes [71], sizes, and a wide range of physical designs to promote coral reef biodiversity recovery, and 3D-printed corals offer several benefits that address the ecological, structural, and functional needs of declining coral reefs. Ecologically, they restore habitats by creating complex and detailed structures that mimic natural coral morphology, providing habitats for a wide range of marine organisms, including juvenile fish [72]. This approach can expedite the growth of live coral microfragments, speed up reef transplantation, minimize nursery costs, and allow for flexibility, customization of densities, spatial design, and depth, with a fast return time and enhanced accuracy [73]. These structures provide enhanced shelter, breeding grounds, and feeding areas for fish, invertebrates, and other reef-associated species, helping to restore and maintain biodiversity [72,74,75]. Depending on the materials used, 3D-printed corals also offer suitable surfaces for coral larvae to settle and grow, facilitating the propagation and fusion of out-planted micro-fragments of slow-growing species. This promotes natural coral recruitment, particularly in flattened reef areas with limited spatial relief [76–78]. The micro-textures of 3D-printed structures can be designed to promote the attachment and growth of coral polyps, enhancing growth [79]. However, success in recruitment largely depends on the construction materials and surface roughness [80].

Additionally, 3D-printed corals offer structural benefits that can help rebuild damaged reefs, enhancing their stability and resilience against physical disturbances such as storms. Depending on the materials used, size, configuration, and spatial design, they can absorb wave energy [81], dissipate wave force, and reduce the impact on coastlines, thus

protecting marine and coastal ecosystems [82]. This stability helps prevent coastal erosion and protect shorelines, infrastructure, and lives. Wave numerical modeling has shown a significant reduction in marine flooding and wave height with the implementation of artificial corals [83,84]. Additionally, 3D-printed corals enhance important reef functions. Restored corals, and the use of 3D corals, attract reef fish [85–89], promote nutrient cycling within marine ecosystems, and support the formation of nutrient hotspots [72,85]. By restoring coral structures, essential ecological processes are maintained, leading to enhanced fish recruitment and assemblages [90]. Three-dimensional printing technology provides technological and practical benefits as well. It allows for precise customization of coral shapes, sizes, and surface textures to match the specific needs of different coral species, reef environments, or project objectives. This customization promotes enhanced primary productivity [91] and can replicate natural coral forms and intricate details that traditional restoration methods may find difficult to achieve in the short term [92].

The use of 3D-printed corals offers several technological and practical benefits, including speed, efficiency, and scalability. Key advantages include accessibility in terms of resource availability, cost, and the training required for construction, deployment, and maintenance [90]. Depending on unit size, 3D printing can quickly produce coral structures, allowing for rapid deployment in restoration projects compared to traditional methods of coral transplantation or artificial reef construction. This scalability enables the restoration of larger reef areas in a shorter time frame and, depending on the materials used, it is essential for durability, ease of deployment, and reproduction [90]. Further, 3D-printed corals possess important ecological characteristics, including ecological realism, chemosensory stimulation, and the ability to alter the surrounding physico-chemical environment [90]. Environmentally, they may offer benefits by using sustainable and biodegradable materials compatible with marine environments, thus reducing the ecological footprint of restoration activities. By using synthetic materials, 3D printing reduces the need to harvest live corals or natural substrates from healthy reefs, minimizing the impact on existing ecosystems. Moreover, 3D-printed corals facilitate controlled experiments, monitoring, and adaptation. They provide a consistent platform for scientific research, allowing scientists to study coral growth, behavior, and interactions, as well as fish and invertebrate attraction, in a standardized manner. This approach makes monitoring and data collection easier, helping researchers adapt and optimize restoration strategies based on real-time observations. Recently, the creation of "bionic corals" capable of harboring high densities of endosymbiotic microalgae has shown promise in promoting enhanced net photosynthesis, primary productivity, CO_2 sequestration, and dissolved oxygen production [93–95].

There is a growing development of 3D-printed artificial reef units for various objectives [96]. Coral restoration has been shown to enhance fish assemblages by increasing coral density, colony size, and benthic spatial heterogeneity, which provide shelter and feeding grounds to numerous species [85]. Over time, feedback mechanisms following coral restoration promote enhanced coral growth due to the formation of nutrient hotspots created by fish aggregation in restored areas [97,98]. Based on this principle, the field experiment conducted in this study aimed to test the role of 3D-printed Staghorn coral, *Acropora cervicornis* (Lamarck, 1816), intermingled with natural *A. cervicornis* out-planted colonies to temporarily enhance fish attraction. This approach promotes faster nutrient hotspot formation to accelerate coral growth from the beginning of coral out-planting. Integrating 3D-printed corals with natural corals offers a novel synergistic approach that leverages the strengths of both artificial and natural elements, enhancing coral demographic performance by rapidly improving fish–coral interactions.

This method has numerous benefits, including enhancing benthic structural complexity and stability; 3D-printed corals provide immediate structural complexity in areas

recently restored with natural corals, offering rapid habitat enhancement for marine organisms while natural corals grow. The robust framework of 3D-printed corals serves as a solid foundation for natural coral fragments and larvae to settle and grow, enhancing the overall stability of the reef. This may also promote the attraction and recruitment of fish larvae. The combination of 3D-printed and natural corals accelerates net reef recovery. 3D-printed corals can be produced and deployed quickly, providing immediate benefits to reef ecosystems, whereas natural coral growth alone is a slower process. The presence of 3D-printed structures supports the growth and expansion of natural corals by providing suitable substrates, reducing competition for space, and attracting fish to enhance nutrient hotspots.

This study aimed to understand the before-and-after impacts of a coral restoration experiment on reef fish assemblages. Conducted on Culebra Island, Puerto Rico, it tested the null hypothesis that there would be no significant difference in the response of fish assemblages across four different coral out-planting intervention levels: natural *A. cervicornis* out-plants, 3D-printed *A. cervicornis* out-plants, mixed natural and 3D-printed out-plants, and controls (no intervention). This study provides timely information on the short-term (one year) impacts of hybrid coral restoration interventions.

2. Materials and Methods

2.1. Study Locations

This study was conducted on the southwestern coast of the island municipality of Culebra, Puerto Rico (Figure 1). It is located approximately 27 km off eastern Puerto Rico, in the northeastern Caribbean Sea, and spans approximately 11 × 7 km. Experimental plots were located within two general locations exposed to similar environmental conditions, depth distribution, exposure to surface currents, and occasional runoff and pollution pulses: Punta Tampico (TAM), which included Bahía Sardinas, Punta Tampico, and Playa Dátiles (centroid: 18.297882° N, −65.302582° W), and Punta de Maguey (MAG), including Punta de Maguey, Playa Cascajo, and Cayo Ahogado (centroid; 18.292634° N, −65.297451° W). Both regions are dominated by a mixture of patch reefs and colonized pavements separated by a mixture of sand, rubble, and seagrass bottoms. The maximum diameter of each of the two locations was roughly 1 km. Experimental study sites were separated somewhere between 200 and 300 m from each other.

2.2. Experimental Design

A total of 12 replicate sampling sites were randomly selected within representative coral reef habitats at each location (N = 24) (Figure 2). Experimental treatments were randomly assigned to triplicate sites per treatment as follows: (a) natural colonies of *A. cervicornis*; (b) 3D-printed colonies of *A. cervicornis*; (c) mixed stands of natural and 3D-printed colonies of *A. cervicornis*; and (d) control plots (no intervention) (Figure 3). Four replicate 10 × 10 m (100 m^2) plots were established adjacent (10 m apart) to each other per site on each location. Out-planting was conducted at a density of one colony per m^2 (100 colonies per 100 m^2 plot). In the mixed out-planting treatment, 50% were natural and 50% 3D-printed colonies. The 3D-printed corals were made of polylactic acid (PLA) filaments and were 20 cm high, with a main branch and four additional branches, matching the average size of natural corals six months post-out-planting. PLA is known to degrade over time in marine environments influenced by factors such as temperature, salinity, and microbial activity [99,100]. Natural *A. cervicornis* colonies were raised in in situ coral nurseries adjacent to the out-planting sites. Out-planting was conducted using masonry nails and plastic ties. Natural out-plants ranged in size from ~15 to ~25 cm.

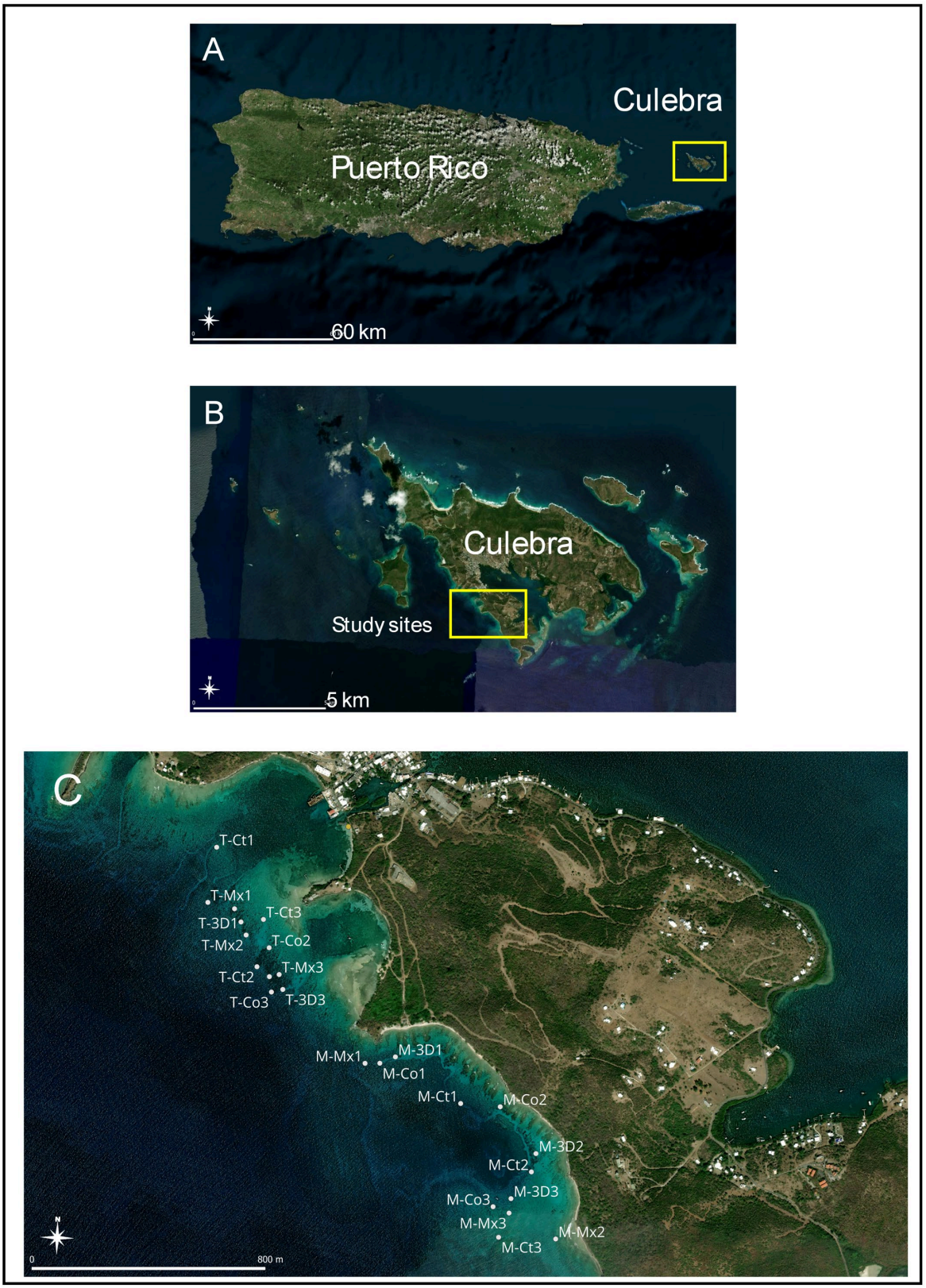

Figure 1. Study sites in Culebra Island, Puerto Rico: (**A**) General location of Puerto Rico and Culebra; (**B**) detailed view of Culebra and the location of study sites; (**C**) detailed view of coral out-planting and control plots at Punta Tampico (T) and at Punta Maguey (M) Culebra; T = TAM, M = MAG; Co = coral out-plants; 3D = 3D-printed out-plants; Mx = mixed out-plants; Ct = controls.

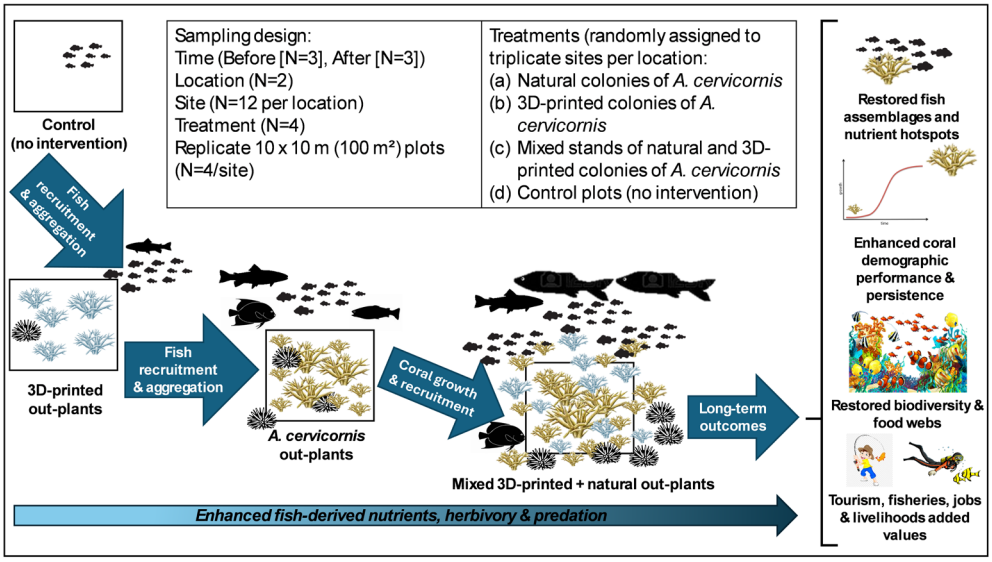

Figure 2. Conceptual experimental design and long-term outcomes of the project.

(**a**) (**b**)

(**c**) (**d**)

Figure 3. Detailed views of different experimental restoration treatments: (**a**) Natural *Acropora cervicornis* out-plants; (**b**) 3D-printed *A. cervicornis* out-plants; (**c**) mixed natural and 3D-printed out-plants; (**d**) control (no-intervention) plot.

2.3. Fish Community Sampling

The impact of the experimental coral restoration intervention on fish community structure was quantified using a slight modification of standard stationary visual fish counts [101]. Briefly, fish assemblages were quantitatively characterized before and after an experimental coral reef ecological restoration intervention within two locations and the four experimental treatments in triplicates per location, within four replicate 100 m^2 plots per treatment before coral out-planting and one year after out-planting (2 locations, 4 treatments per location, 3 randomly replicated sites per treatment, 4 replicate plots per treatment; N = 96 plots per sampling effort). Sampling was conducted three times before and three times after the ecological restoration experimental intervention using 10 min counts within each plot. All fish were identified to the lowest taxon possible, counted, and size determined by a single diver (EAHD). The method provides quantitative data on frequency of occurrence, fish length, abundance, and community composition at the species, genera, and family level, but also at the trophic functional group level and at the fisheries target species level.

Size distributions were determined for individual species based on length data. Fish length data were obtained during fish counts using a cm-calibrated stick as a scale bar. An index of biomass was obtained from length data for each species by multiplying abundance estimates by weight based on empirically derived, species-specific length–weight relationships [102]. Weight–length relationships were calculated by fitting a regression line to the equation: $log\ w = log\ a + b\ log\ L$, which is equivalent to the equation: $W = aL^b$, where W is weight in grams, L is length converted to millimeters, and a and b are constants [102]. Mean length data can be used directly to compare average stock sizes between habitats, reefs, and through time. Minimum lengths may be useful indicators of recruitment size for sampled habitats, while maximum lengths may be useful indicators of fishing pressure [101].

2.4. Spatio-Temporal Variation in Fish Community Structure

Spatio-temporal variation in fish community structure was quantified between 2022 and 2023 following a before-after-control-impact (BACI) design and a three-way permutational analysis of variance (PERMANOVA) [103], with time (before, one year after), treatment (natural *A. cervicornis*, 3D-printed *A. cewrvicornis*, mixed out-plants, control plots), and location (TAM, MAG) as main variables, following 9999 permutations of $\sqrt{}$-transformed data and on Bray Curtis resemblance [104]. Data were first analyzed for fish community parameters: (a) species richness, (b) total abundance, (c) total biomass; (d) species diversity index (H'_n), and (e) evenness (J'_n). Spatio-temporal variation in trophic functional group abundance and biomass was tested as above for the following guilds: (a) total carnivores, (b) generalist invertivores, (c) piscivores, (d) planktivores, (e) omnivores; (f) total herbivores, (g) non-denuder herbivores, (h) browser herbivores, and (i) scraper herbivores. Spatio-temporal variation in trophic functional group biomass were also tested as above. Fish species trophic functional classification was based on historical databases obtained from Puerto Rico [105]. Fish community structure spatio-temporal dynamics were tested as above using trophic group $\sqrt{}$-transformed abundance and biomass data. Principal coordinates ordination (PCO) was used to project spatio-temporal variation in fish community trajectory based in $\sqrt{}$-transformed abundance data and on Bray–Curtis resemblance [104] following 9999 permutations [106]. This allowed identifying which trophic groups explained observed patterns of variation. Also, variation in abundance data from experimental plots was projected using a dominance curve [106]. Abundance–biomass comparison (ABC) plots based on trophic functional group abundance and biomass were used to test for disturbance effects [106].

Spatio-temporal variation in fishery target species abundance, percent abundance, biomass, and percent biomass were similarly analyzed for those species that are often targeted by artisanal fishing. Fish species-level data was also used to determine spatio-temporal variation in fish community structure as above. This allowed identifying which species may best explain observed spatio-temporal variation among treatments and between locations. Similarity percentages (SIMPER) analysis was used on fish species-level $\sqrt{}$-transformed abundance data to identify indicator species of spatio-temporal variation in fish assemblages [106]. All multivariate testing was conducted in PRIMER v.7.0.23 + PERMANOVA v1 (PRIMER-e, Quest Research, Ltd., Auckland, New Zealand).

An analysis of the fishes' hierarchical preference by treatment was also conducted based on the abundance of 12 indicator species to determine their spatio-temporal variation following [92]. The abundance ratios were calculated comparing all treatments before and after the restoration intervention and comparing controls and impacted plots (experimental treatments).

2.5. Spatio-Temporal Variation in Fish Biodiversity and Phylogenetic Dynamics

2.5.1. Taxonomic Diversity (Delta, Δ)

The Δ is the average 'taxonomic distance apart' of every pair of individuals in a sample or the expected taxonomic path length between any two individuals chosen at random [106]. The Δ is a natural extension of the Simpson diversity index where 0 = same species, 20 = different species in the same genus, 40 = different genera but same family, etc. The higher the Δ value, the higher the taxonomic complexity is.

2.5.2. Taxonomic Distinctness (Delta*, Δ*)

The Δ* is calculated by dividing the Δ by the Simpson diversity index to remove the dominating effect of the species abundance distribution [107]. The Δ* measures the expected taxonomic distance apart from any two individuals chosen at random from a sample, provided those two individuals are not from the same species. The taxonomic/phylogenetic distinctness of a community summarizes features of the overall hierarchical structure of an assemblage (the spread, unevenness etc. of the classification tree). The larger the spread and unevenness, the higher the biodiversity.

2.5.3. Average Taxonomic Distinctness—AvTD (Delta$^+$, Δ^+)

The Δ^+ is the average taxonomic distance apart from all its pairs of species [107]. Δ^+ is a very intuitive definition of biodiversity, as average taxonomic breadth of a sample, which is totally independent of sampling effort.

2.5.4. Total Taxonomic Distinctness—TTD (sDelta$^+$, sΔ^+)

The sΔ^+ is analogous to phylogenetic diversity (PD), which is the cumulative branch length of the full taxonomic tree. sΔ^+ is a useful measure of total taxonomic breadth of an assemblage, as a modification of S which allows for the species inter-relatedness, so that it would be possible, for example, for an assemblage of 20 closely related species to be deemed less 'rich' than one of 10 distantly related species [106].

2.5.5. Variation in Taxonomic Distinctness—VarTD (Lambda$^+$, Λ^+)

The Λ^+ is the variance of the taxonomic distances between each pair of species *i* and *j*, about their mean distance Δ^+ [106]. It has the potential to distinguish differences in taxonomic structure resulting, for example, in assemblages with some genera becoming highly species-rich while a range of other higher taxa are represented by only one (or very few) species. In that case, average TD may be unchanged but Λ^+ will be greatly increased. Λ^+ has a lack of dependence of its mean value on sampling effort.

2.5.6. Average Phylogenetic Diversity—AvPD (Φ^+)

The Φ^+ is the analogue of Δ^+, both being ways of measuring the average taxonomic breadth of an assemblage (a species list), for a given number of species [106]. Φ^+ will give the same value (on average) whatever that number of species; Δ^+ will not. Φ^+ is the result of PD/S.

2.5.7. Total Phylogenetic Diversity—Faith's PD ($s\Phi^+$)

The $s\Phi^+$ is a measure based on known branch lengths: PD is simply the cumulative branch length of the full tree [108,109]. PD itself is a total rather than average property; as new species are added to the list, it always increases [106]. This makes PD highly dependent on *S* and thus sampling effort. A better equivalent to Δ^+ would be Φ^+.

All calculations of TD indices were conducted using multivariate routine DIVERSE and using $\sqrt{}$-transformed fish abundance data [106]. The construction of TD indices departure from a master list of species within defined taxonomic boundaries and encompassing the appropriate area, from which the species found at one location can be thought of as drawn, creating a framework within which TD measures can be tested for departure from 'expectation'. Joint AvTD (Δ^+) and VarTD (Λ^+) analyses were performed using multivariate routine TAXDTEST. TD spatio-temporal variation was tested following a BACI design and using a three-way PERMANOVA [103], with time, treatment, and location as main variables, and using 9999 permutations. Δ^+ and Λ^+ results were projected using funnel plots.

2.6. Benthic Structural Complexity (Rugosity Index)

The structural complexity of surveyed reef substrates, which is known to have an important influence on fish community structure [110], was evaluated following a six-point scale based on [111]: 0, no vertical relief; 1, low and sparse relief; 2, low but widespread relief; 3, moderately complex; 4, very complex with numerous caves and fissures, and 5, exceptionally complex with high coral cover and numerous caves and overhangs. Visual estimates were made on each replicate plot and averaged for each sampling site. Log_{10}-transformed and normalized data were tested following a two-way PERMANOVA with treatment and location as main factors [103]. Multivariate correlation (RELATE) was used following 9999 permutations to correlate the calculated rugosity index with fish variables [106].

3. Results

3.1. Spatio-Temporal Variation in Fish Community Parameters

The integration of 3D-printed corals and natural *A. cervicornis* out-planting contributed to enhancing fish assemblages and their ecological functions. Demographic performance of natural out-plants was quantified on a separate study. However, coral survival remained superior to 80% through this study, while 3D-printed coral stability remained higher than 90% through the study. There was a significant temporal increase in species richness ($p < 0.0001$) (Figure 4a, Table 1). Species richness showed variation among all restoration treatment interventions, with higher values on coral, 3D-printed, and mixed interventions ($p = 0.0094$), and showed significantly higher values at MAG ($p < 0.0001$). It also showed a marginally significant time × treatment interaction ($p = 0.0526$) and a significant treatment × location interaction ($p = 0.0002$). There was a significant temporal increase in species richness within each experimental treatment, except for controls (Figure 4a, Table S1).

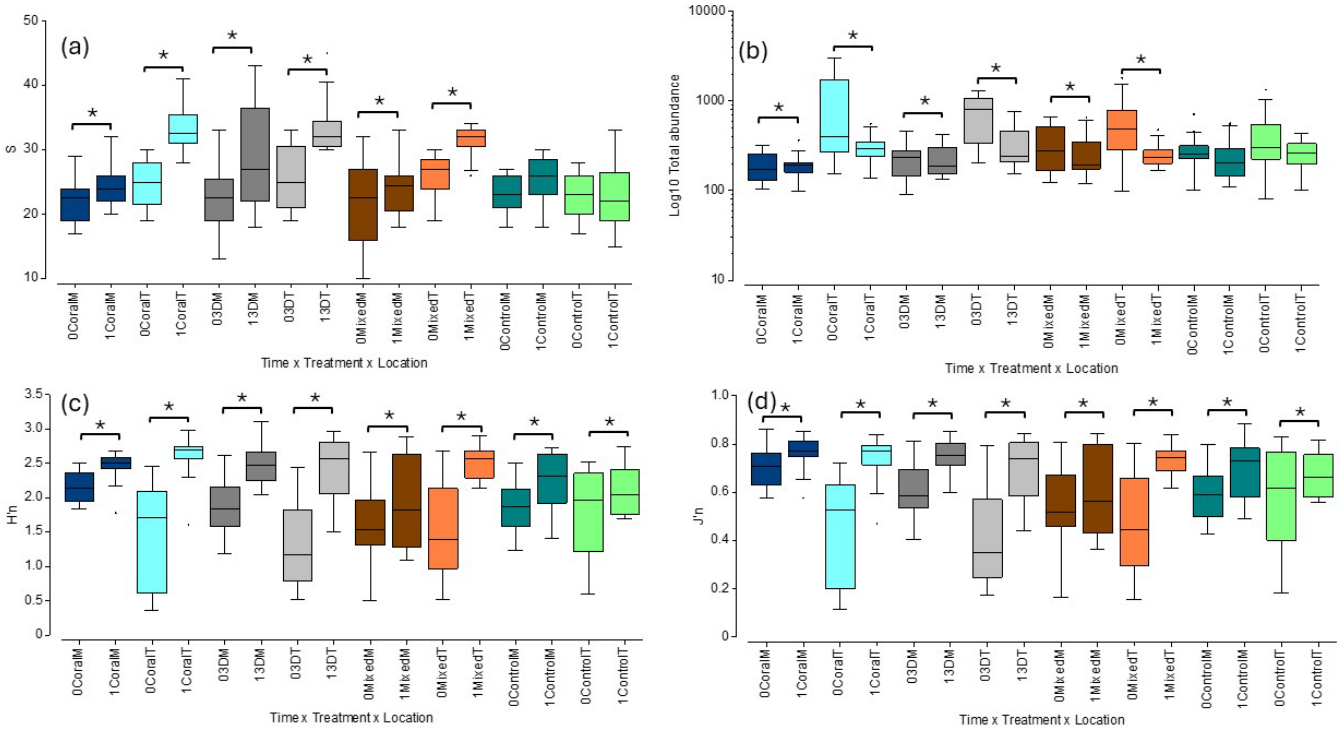

Figure 4. Box-plot diagram of BACI spatio-temporal variation in fish community parameters: (**a**) species richness; (**b**) total abundance; (**c**) species diversity index (H'_n); (**d**) evenness (J'_n). 0 = before; 1 = after. M = Maguey (darker tones); T = Tampico (lighter tones). Blue = coral; gray = 3D-printed; brown = mixed; green = control plots (no intervention). Asterisks illustrate significant temporal differences ($p < 0.0500$).

Table 1. Summary of a BACI three-way crossed PERMANOVA test of the spatio-temporal variation in fish community parameters in restored and control plots.

Source [1]	df	S	Total Abundance	H'_n	J'_n
Time	1	36.90 *	15.81	62.61 *	49.34 *
		<0.0001	**<0.0001**	**<0.0001**	**<0.0001**
Treatment	3	3.84	0.87	1.69	1.77
		0.0094	0.4707	0.1624	0.1466
Location	1	24.38	32.30 *	6.1	11.69
		<0.0001	**<0.0001**	**0.0109**	**0.0008**
Time × Treatment	3	2.56	0.4	1.62	1.04
		0.0526	0.8063	0.1792	0.3736
Time × Location	1	0.88	8.49	13.8	14.23
		0.3549	**0.0029**	**0.0002**	**0.0002**
Treat. × Location	3	6.62	3.55	3.21	3.32
		0.0002	**0.0094**	**0.0179**	**0.0196**
Time × Treat. × Loc.	3	1.11	0.9	1.58	1.24
		0.3508	0.4411	0.1936	0.2956
Residual	176				

[1] Based on 9999 permutations; Data = Pseudo-F statistic, *p* value. * Dominant component of variation.

Total fish abundance declined after the interventions ($p < 0.0001$) (Figure 4b, Table 1), largely due to the widespread sea surface warming-related decline in *Coryphopterus personatus*, the most abundant species before interventions. Decline was consistent among treatments ($p = 0.4707$) but was significantly higher at TAM ($p < 0.0001$), where *C. personatus* used to be more abundant. It also showed significant time × location ($p = 0.0029$) and treat-

ment × location interactions ($p = 0.0094$). There was a significant temporal decline in total abundance within each experimental treatment, except for controls (Figure 4b, Table S1).

Species diversity index (H'_n) showed significant temporal increase ($p < 0.0001$) (Figure 4c, Table 1) and significantly higher values at TAM ($p = 0.0109$). It also showed a significant time × location interaction ($p = 0.0002$) and a significant treatment × location interaction ($p = 0.0179$). There was a significant temporal increase in H'_n within each experimental treatment, including controls (Figure 4c, Table S1).

Species evenness (J'_n) showed significant temporal increase ($p < 0.0001$), following the climate-related decline in dominant *C. personatus* populations (Figure 4d, Table 1). There were significantly higher values at TAM ($p = 0.0008$). It also showed a significant time × location interaction ($p = 0.0002$) and a significant treatment × location interaction ($p = 0.0196$). There was a significant temporal increase in J'_n within each experimental treatment, including controls (Figure 4d, Table S1).

3.2. Spatio-Temporal Variation in Trophic Functional Group Abundance

There was a general significant temporal increase in total herbivore abundance ($p < 0.0001$), with significantly higher abundance in out-planted live coral and 3D plots ($p = 0.0036$) (Figure 5a, Table 2). Total herbivore abundance was also significantly higher at TAM ($p < 0.0001$). No significant interactions were documented. There was a significant temporal increase in total herbivore abundance within each experimental treatment, except for controls (Figure 3a, Table S2). No significant temporal or treatment effects were observed in non-denuder herbivores (Pomacentridae) (Figure 5b, Table 2). However, non-denuder herbivore abundance was significantly higher at TAM ($p < 0.0001$). No significant interactions were documented either. No significant temporal variation was documented within individual treatments, nor within controls (Figure 5b, Table S2).

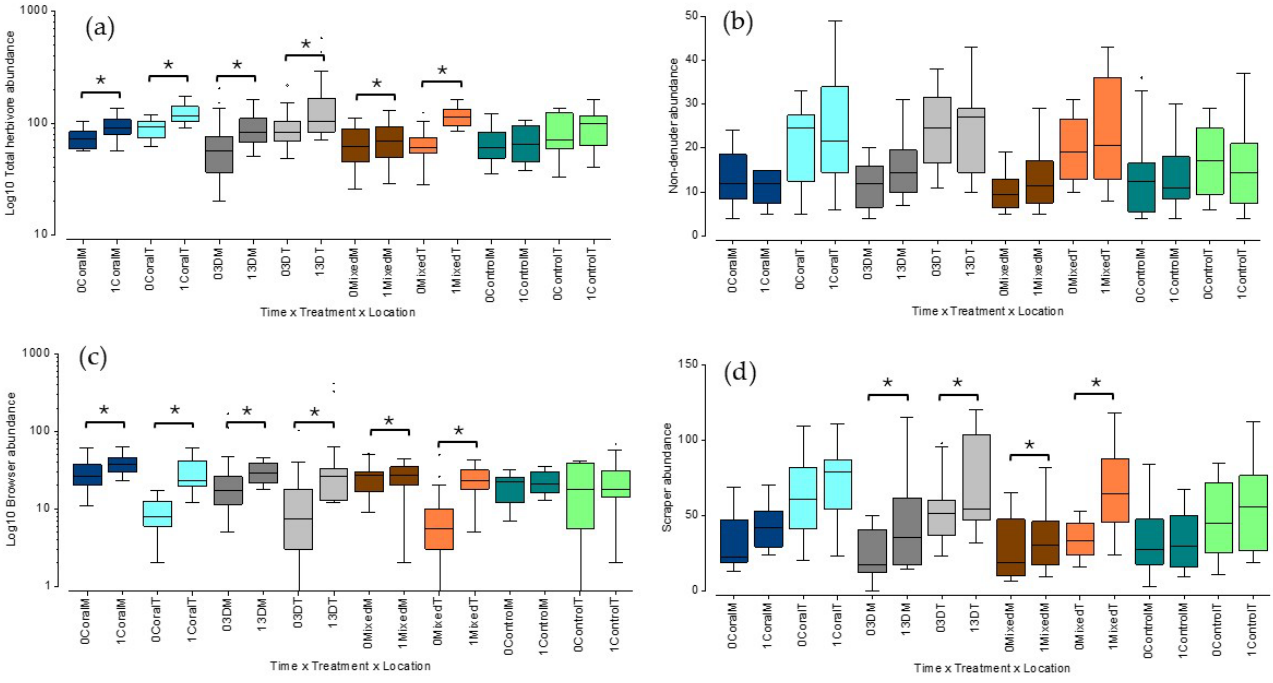

Figure 5. Box-plot diagram of BACI spatio-temporal variation in herbivore fish functional group abundance: (**a**) total herbivores; (**b**) non-denuders; (**c**) browsers; (**d**) scrapers. 0 = before; 1 = after. M = Maguey (darker tones); T = Tampico (lighter tones). Blue = coral; gray = 3D-printed; brown = mixed; green = control plots (no intervention). Asterisks illustrate significant temporal differences ($p < 0.0500$).

Table 2. Summary of a BACI three-way crossed PERMANOVA test of the spatio-temporal variation in herbivore fish functional group abundance in restored and control plots.

Source [1]	df	Herb [2]	NDN	Br	Sc
Time	1	20.91	0.68	24.41 *	10.27
		<0.0001	0.4197	**<0.0001**	**0.0009**
Treatment	3	4.36	1.87	1.28	1.84
		0.0036	0.122	0.2606	0.1163
Location	1	24.05 *	41.28 *	20.27	39.51 *
		<0.0001	**<0.0001**	**<0.0001**	**<0.0001**
Time × Treatment	3	1.58	0.37	1.24	0.92
		0.1845	0.8121	0.2772	0.441
Time × Location	1	2.48	0.79	9.84	0.99
		0.1044	0.3862	**0.0004**	0.333
Treat. × Location	3	0.36	1.29	1.32	0.76
		0.8274	0.277	0.2422	0.5473
Time × Treat. × Loc.	3	1.16	0.67	1.25	1.02
		0.3221	0.5815	0.275	0.3950
Residual	176				

[1] Based on 9999 permutations; Data = Pseudo-F statistic, *p* value. [2] Herb = Total herbivores; NDN = Non-denuders; Br = Browsers; Sc = Scrapers. * Dominant component of variation.

There was a significant temporal increase in browser herbivore (Acanthuridae) abundance ($p < 0.0001$), with significantly higher abundance at MAG ($p < 0.0001$) (Figure 5c, Table 2). There was no significant variation among treatments. There was also a significant time × location interaction ($p = 0.0004$). There was a significant temporal increase in browser herbivore abundance within each experimental treatment, except for controls (Figure 5c, Table S2). A significant temporal increase in scraper herbivore (Scaridae) abundance ($p = 0.0009$) was also observed, with significantly higher abundance at TAM ($p < 0.0001$) (Figure 5d, Table 2). There was no significant variation among treatments either. No significant interactions were documented. There was a significant temporal increase in scraper herbivore abundance within 3D-printed and mixed experimental treatments, but not within the coral treatment or the controls (Figure 5d, Table S2).

Total carnivore abundance showed no significant variation in time, treatment, and location (Figure 6a, Table 3). There was a significant time × location interaction ($p = 0.0287$). No significant temporal variation was observed in total carnivore abundance within individual treatments, nor within controls (Figure 6a, Table S3). No significant temporal, treatment or location effects were observed either in generalist invertivores (Figure 6b, Table 3). However, there were significant time × location ($p = 0.0212$) and treatment × location interactions ($p = 0.0104$). There was no significant temporal variation in generalist invertivore abundance within individual treatments, nor within controls (Figure 6b, Table S3). Piscivores showed a significant ($p = 0.0005$) temporal increase in abundance and significantly higher abundance at TAM ($p = 0.0316$) (Figure 6c, Table 3). There was a significant time × treatment × location interaction ($p = 0.0067$). There was a significant temporal increase in piscivore abundance within the 3D-printed treatment, but none within other treatments or controls (Figure 6c, Table S3).

Planktivores were significantly ($p = 0.0010$) more abundant also at TAM (Figure 6d, Table 3). There was no significant variation in time and among treatments. There was also a significant treatment × location interaction ($p = 0.0119$). There was a significant temporal increase in planktivore abundance within the coral treatment, but none within other treatments or controls (Figure 6d, Table S3). A significant temporal decline in omnivore abundance ($p < 0.0001$) was observed following the climate-related decline in *C. personatus* populations (Figure 6e, Table 3). Despite that decline, omnivores were

significantly more abundant at the live out-planted corals and at the 3D-printed coral plots ($p = 0.0085$), and at TAM ($p < 0.0001$). There were also significant time × location ($p = 0.0004$) and treatment × location interactions ($p = 0.0017$). A significant temporal decline in omnivore abundance was found within all experimental treatments, except for controls (Figure 6e, Table S3).

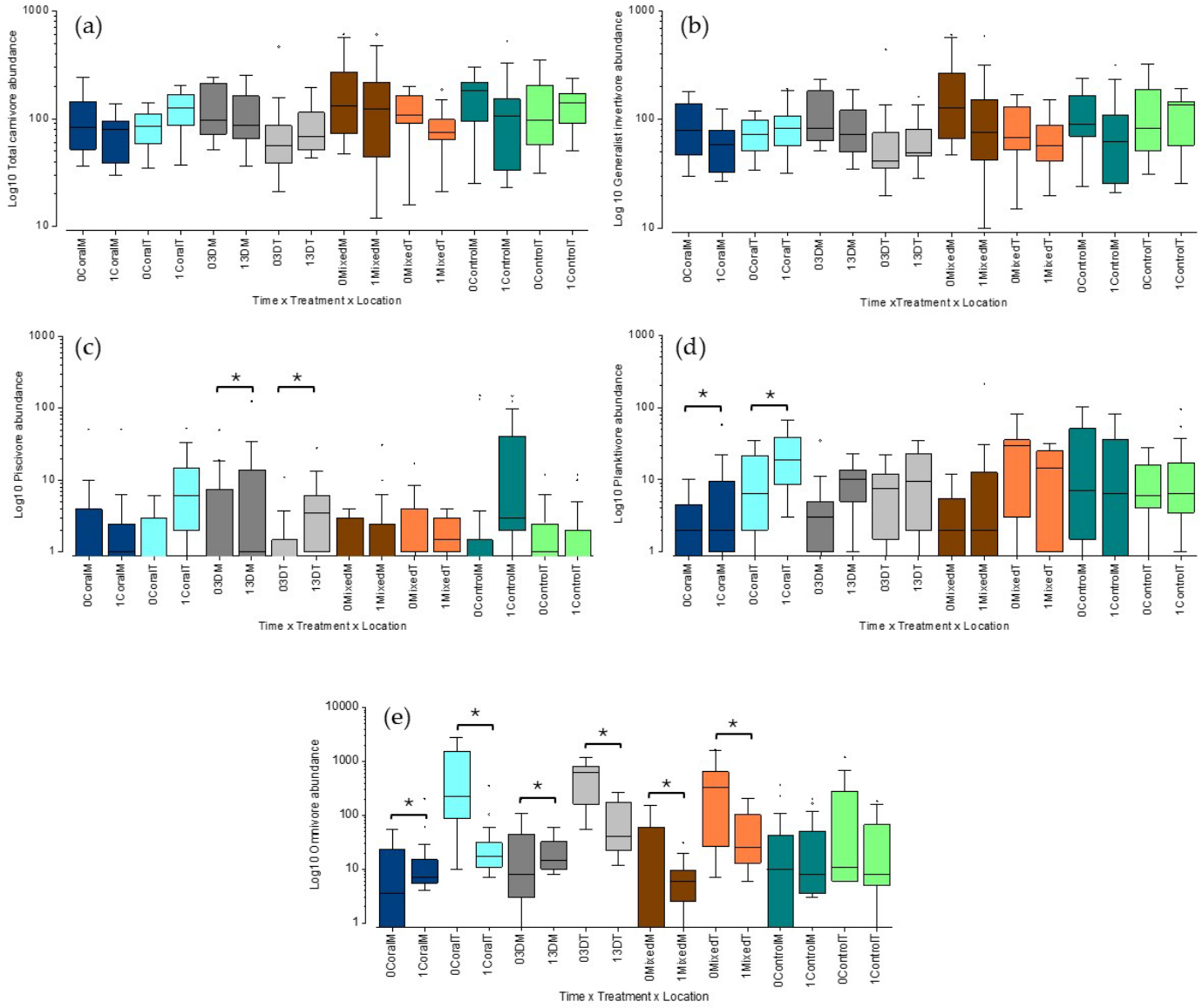

Figure 6. Box-plot diagram of spatio-temporal variation in carnivore fish functional groups abundance: (**a**) Total carnivores; (**b**) generalist invertivores; (**c**) piscivores; (**d**) planktivores; (**e**) omnivores. 0 = before; 1 = after. M = Maguey (darker tones); T = Tampico (lighter tones). Blue = coral; Gray = 3D-printed; brown = mixed; green = control plots (no intervention). Asterisks illustrate significant temporal differences ($p < 0.0500$).

3.3. Spatio-Temporal Variation in Trophic Functional Group Biomass

There was a significant temporal increase in total fish biomass ($p = 0.0025$), but no difference among treatments and locations (Figure 7a, Table 4). However, there was a significant treatment × location interaction ($p = 0.0002$). There was also a significant temporal increase in total fish biomass within the coral treatment, but none within other treatments or controls (Figure 7a, Table S4). There was a significant temporal increase in total herbivore biomass ($p = 0.0003$) but no difference among treatments (Figure 7b, Table 4). Total herbivore biomass was also significantly higher at TAM ($p = 0.0102$). There was a

significant time × location interaction ($p = 0.0208$). A significant temporal increase in total herbivore biomass was documented within the coral and 3D treatments, but none within other treatments or controls (Figure 7b, Table S4). No significant temporal or treatment effects were observed in non-denuder herbivore (Pomacentridae) biomass (Figure 7c, Table 4). However, non-denuder herbivore biomass was significantly higher at TAM ($p < 0.0001$). There was also a significant treatment × location interaction ($p = 0.0029$). No significant temporal variation in non-denuder herbivore biomass was found within any of the treatments or controls (Figure 7c, Table S4).

Table 3. Summary of a BACI three-way crossed PERMANOVA test of the spatio-temporal variation in carnivore fish functional group abundance in restored and control plots.

Source [1]	df	Carn [2]	Gen	Pisc	Plank	Omn
Time	1	0.99	3.69	10.3	2.39	18.47
		0.3241	0.0522	**0.0005**	0.1041	**<0.0001**
Treatment	3	2.4	1.55	0.66	0.98	2.92
		0.0553	0.1889	0.6313	0.4137	**0.0085**
Location	1	2.23	2.48	3.88	10.29 *	38.79 *
		0.1261	0.1116	**0.0316**	**0.001**	**<0.0001**
Time × Treatment	3	0.83	0.52	0.78	1.05	0.64
		0.4963	0.6964	0.551	0.3677	0.7036
Time × Location	1	4.43 *	4.96	0.03	0.05	11.28
		0.0287	**0.0212**	0.9737	0.9562	**0.0004**
Treat. × Location	3	2.44	3.70*	2.02	3.21	4.09
		0.0515	**0.0104**	0.0848	**0.0119**	**0.0017**
Time × Treat. × Loc.	3	0.56	0.18	3.53 *	0.89	0.94
		0.6789	0.9455	**0.0067**	0.4681	0.4579
Residual	176					

[1] Based on 9999 permutations; Data = Pseudo-F statistic, p value. [2] Carn = total carnivores; Gen = generalist invertivores; Pisc = piscivores; Plank = planktivores; Omn = omnivores. * Dominant component of variation.

Table 4. Summary of BACI three-way crossed PERMANOVA test of the spatio-temporal variation in herbivore fish functional group biomass in restored and control plots.

Source [1]	df	Total Biomass [2]	Herb	NDN	Br	Sc
Time	1	9.12	11.48 *	2.26	18.46 *	5.9
		0.0025	**0.0003**	0.1208	**<0.0001**	**0.0059**
Treatment	3	0.23	2.07	1.97	1.37	1.48
		0.9374	0.0815	0.1005	0.2038	0.1865
Location	1	2.41	5.78	67.88 *	4.71	9.01 *
		0.108	**0.0102**	**<0.0001**	**0.0066**	**0.0008**
Time × Treatment	3	1.07	1.56	0.35	1.05	1.72
		0.3621	0.1751	0.8615	0.3871	0.1242
Time × Location	1	0.46	4.57	2.21	0.8	3.65
		0.5421	**0.0208**	0.124	0.4637	**0.0315**
Treat. × Location	3	6.86 *	0.48	4.32	0.59	0.95
		0.0002	0.7629	**0.0029**	0.787	0.4346
Time × Treat. × Loc.	3	0.88	0.95	0.5	1.68	0.54
		0.4609	0.4333	0.7376	0.1061	0.7671
Residual	176					

[1] Based on 9999 permutations; Data = pseudo-F statistic, p value. [2] Herb = total herbivores; NDN = non-denuders; Br = browsers; Sc = scrapers. * Dominant component of variation.

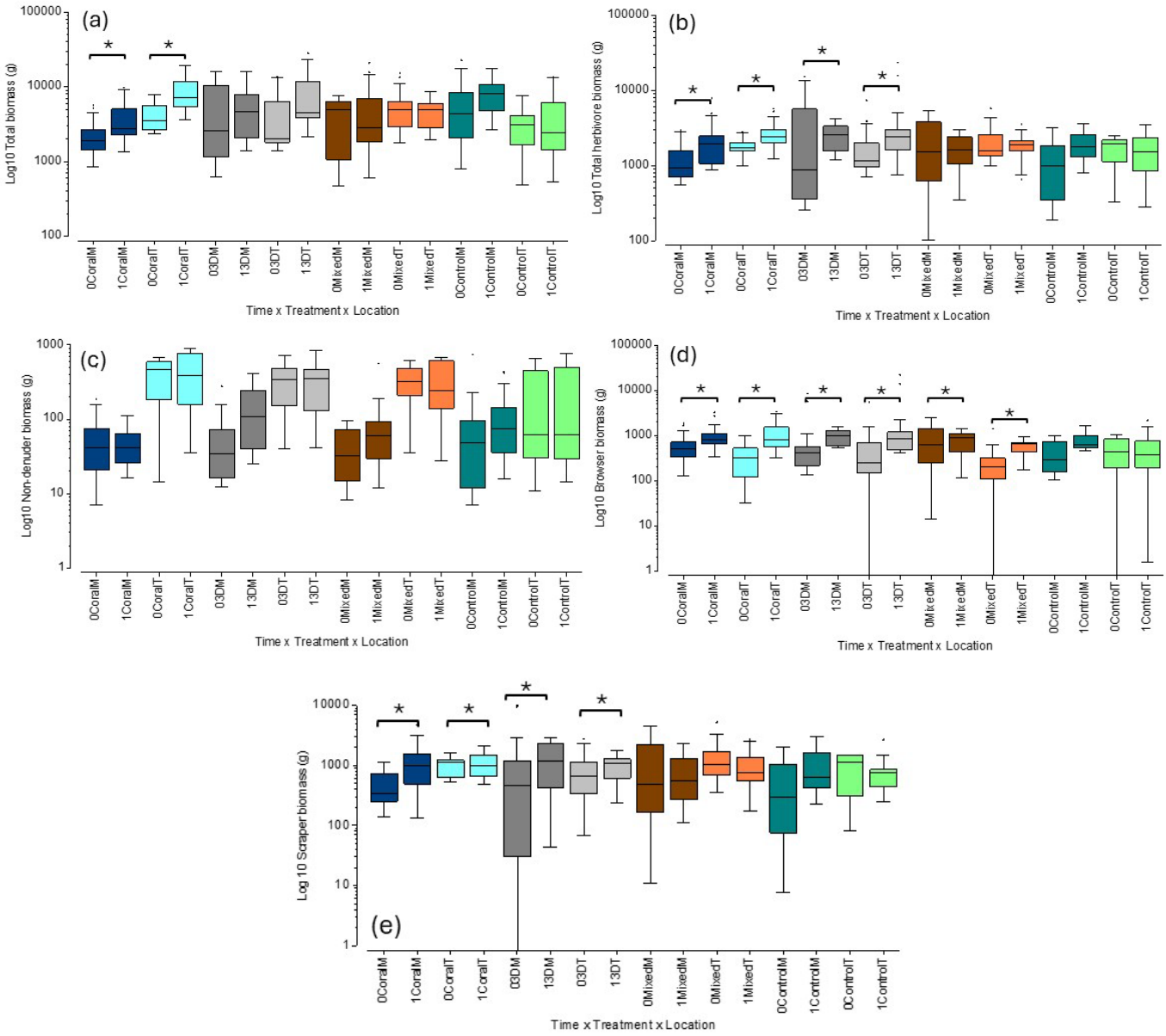

Figure 7. Box-plot diagram of spatio-temporal variation in herbivore fish functional groups biomass: (**a**) total biomass; (**b**) total herbivores; (**c**) non-denuders; (**d**) browsers; (**e**) scrapers. 0 = before; 1 = after. M = Maguey (darker tones); T = Tampico (lighter tones). Blue = coral; gray = 3D-printed; brown = mixed; green = control plots (no intervention). Asterisks illustrate significant temporal differences ($p < 0.0500$).

Browser herbivore (Acanthuridae) biomass showed a significant temporal increase ($p < 0.0001$), but no treatment effects were documented (Figure 7d, Table 4). There was a significantly higher biomass at MAG ($p = 0.0066$). There were no significant interaction effects. There was a significant temporal increase in browser biomass within all experimental treatments, except for controls (Figure 7d, Table S4). A significant temporal increase in scraper herbivore (Scaridae) biomass ($p = 0.0009$) was documented ($p = 0.0059$), but there were no significant treatment effects (Figure 7d, Table 4).

There was significantly higher scraper biomass at TAM ($p = 0.0008$), and a significant time × location effect ($p = 0.0315$). A significant temporal increase in scraper biomass was observed within coral and 3D treatments, but none for other treatments or controls (Figure 7e, Table S4).

There was a significant temporal increase in total carnivore biomass ($p = 0.0173$) and a significantly higher biomass at TAM ($p = 0.0355$) (Figure 8a, Table 5). There were no significant treatment effects. A significant treatment × location interaction ($p < 0.0001$) was observed. A significant temporal increase in total carnivore biomass was observed within coral treatment, but none for other treatments or controls (Figure 8a, Table S5). Generalist invertivore biomass significantly increased through time ($p = 0.0258$), particularly across TAM ($p = 0.0035$) (Figure 8b, Table 5). There were no significant treatment effects. There was significant time × location ($p = 0.0014$), and treatment × location interaction effects ($p = 0.0017$). No significant temporal variation in generalist invertivore biomass was observed within any experimental treatment, nor controls (Figure 6b, Table S5). Piscivore biomass showed a significant ($p = 0.0007$) temporal increase and significantly higher biomass at TAM ($p = 0.0086$) (Figure 8c, Table 5). There was a significant time × treatment × location interaction effect ($p = 0.0102$). A significant temporal increase in piscivore biomass was observed within coral and 3D treatments, but none for other treatments or controls (Figure 8c, Table S5).

Table 5. Summary of a BACI three-way crossed PERMANOVA test of the spatio-temporal variation in carnivore fish functional group biomass in restored and control plots.

Source [1]	df	Carn [2]	Gen	Pisc	Plank	Omn
Time	1	4.98	4.47	10.31	0.37	1.71
		0.0173	**0.0258**	**0.0007**	0.7182	0.1693
Treatment	3	0.42	0.14	0.28	1.4	3.8
		0.8019	0.9833	0.9345	0.2044	**0.0019**
Location	1	4.06	7.4	5.81	19.95 *	34.86 *
		0.0355	**0.0035**	**0.0086**	**<0.0001**	**<0.0001**
Time × Treatment	3	0.72	0.3	1.09	0.67	0.36
		0.5706	0.8926	0.3512	0.6742	0.9161
Time × Location	1	1.49	5.43	0.1	1.27	5.23
		0.2205	**0.0014**	0.9244	0.2711	**0.0078**
Treat. × Location	3	7.72 *	4.97 *	2.04	3.83	2.28
		<0.0001	**0.0017**	0.0737	**0.001**	**0.0391**
Time × Treat. × Loc.	3	1.69	0.72	3.40 *	1.32	0.31
		0.1466	0.569	**0.0102**	0.231	0.9478
Residual	176					

[1] Based on 9999 permutations; data = Pseudo-F statistic, *p* value. [2] Carn = total carnivores; Gen = generalist invertivores; Pisc = piscivores; Plank = planktivores; Omn = omnivores. * Dominant component of variation.

Planktivore biomass was significantly higher at TAM ($p < 0.0001$) (Figure 8d, Table 5). There was no significant biomass variation in time and among treatments. There was a significant treatment × location interaction ($p = 0.0010$). No significant temporal variation in planktivore biomass was observed within any experimental treatment, nor controls (Figure 8d, Table S5). Omnivore biomass showed a significant increase within live coral out-plants and within 3D-printed out-plant plots ($p = 0.0019$), with also significantly higher biomass at TAM ($p < 0.0001$) (Figure 8e, Table 5). There was also significant time × location ($p = 0.0078$) and treatment × location interaction effects ($p = 0.0391$). No significant temporal variation in omnivore biomass was observed within any experimental treatment, nor controls (Figure 8e, Table S5).

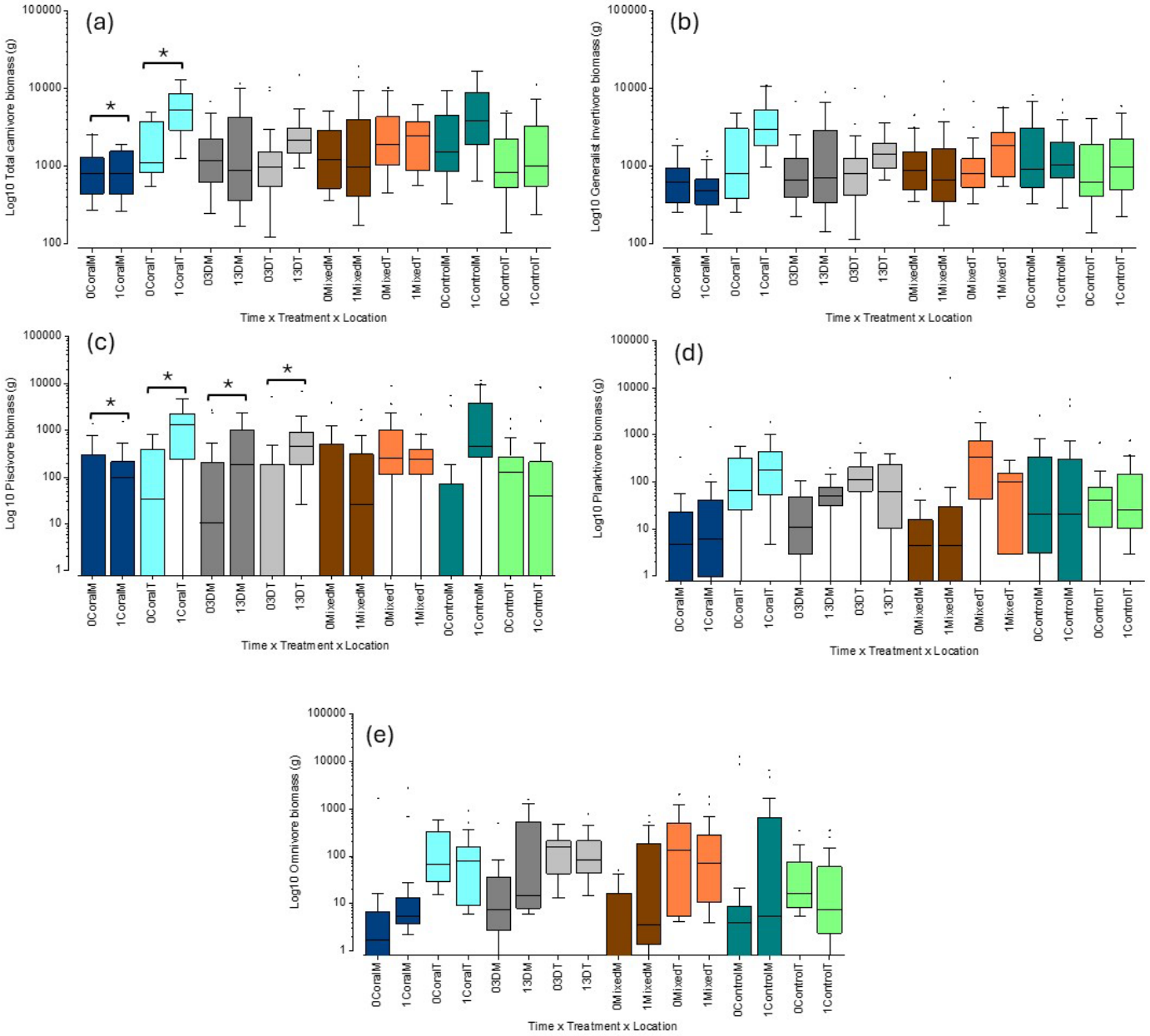

Figure 8. Box-plot diagram of spatio-temporal variation in carnivore fish functional groups biomass: (**a**) total carnivores; (**b**) generalist invertivores; (**c**) Log_{10} piscivores; (**d**) planktivores; (**e**) omnivores. 0 = before; 1 = after. M = Maguey (darker tones); T = Tampico (lighter tones). Blue = coral; gray = 3D-printed; brown = mixed; green = control plots (no intervention). Asterisks illustrate significant temporal differences ($p < 0.0500$).

3.4. Spatio-Temporal Variation in Fishery Target Species Parameters

Fishery target species density showed a significant temporal increase ($p = 0.0010$) that was marginally significant at locations with live coral out-plants and with 3D-printed coral out-plants ($p = 0.0618$) (Figure 9a, Table 6). Fishery target species density was significantly higher at TAM ($p < 0.0001$). There was a significant treatment × location interaction effect ($p < 0.0001$). A significant temporal increase in fishery target species density was observed within coral and mixed treatments, with a marginal increase in the 3D treatment but none for controls (Figure 9a, Table S6). Fishery target species percent abundance showed a significant temporal increase ($p < 0.0001$) that was also significant at locations with live coral out-plants and with 3D-printed coral out-plants ($p = 0.0031$) (Figure 9b,

Table 6). No significant difference between locations was observed. There was a significant time × location (p = 0.0012) and treatment × location interaction effect (p = 0.0266). A significant temporal increase in fishery target species percent abundance was observed within all experimental treatments, except for controls (Figure 9b, Table S6).

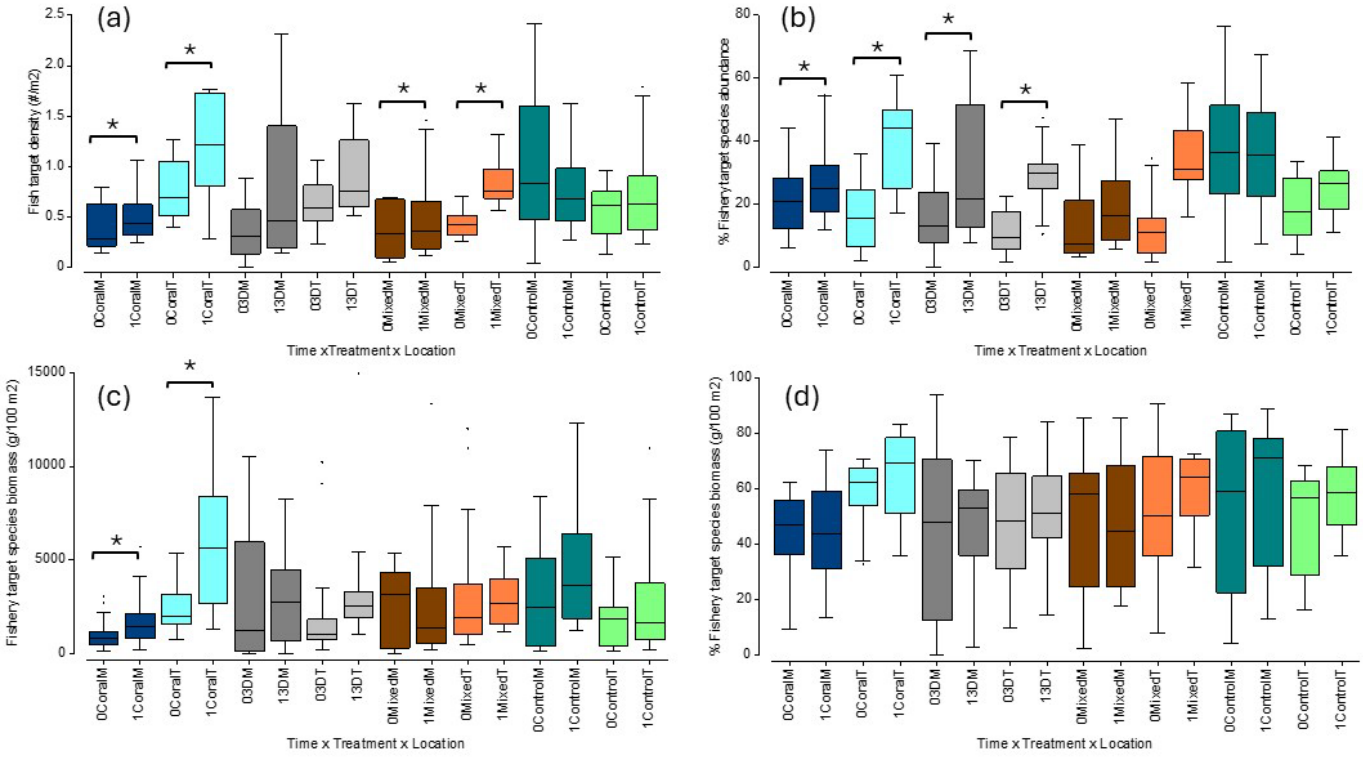

Figure 9. Box-plot diagram of spatio-temporal variation in fishery target species parameters: (**a**) Abundance; (**b**) percent abundance; (**c**) biomass; (**d**) percent biomass. 0 = before; 1 = after. M = Maguey (darker tones); T = Tampico (lighter tones). Blue = coral; gray = 3D-printed; brown = mixed; green = control plots (no intervention). Asterisks illustrate significant temporal differences (p < 0.0500).

Table 6. Summary of a BACI three-way crossed PERMANOVA test of the spatio-temporal variation in fishery target species parameters in restored and control plots.

Source [1]	df	Abund	% Abund	Biomass	% Biomass
Time	1	9.1	35.53	5.95	2.01
		0.001	**<0.0001**	**0.0058**	0.1261
Treatment	3	2.13	3.81	0.43	1.15
		0.0618	**0.0031**	0.8763	0.3151
Location	1	16.24	0.27	4.66	5.86 *
		<0.0001	0.8113	**0.0159**	**0.0053**
Time × Treatment	3	1.08	1.62	0.73	0.37
		0.35	0.1411	0.6172	0.9229
Time × Location	1	2.17	8.19 *	0.95	0.58
		0.1104	**0.0012**	0.3695	0.5479
Treat. × Location	3	5.17 *	2.56	4.92 *	0.86
		<0.0001	**0.0266**	**0.0003**	0.4986
Time × Treat. × Loc.	3	0.45	0.4	0.83	0.26
		0.8493	0.8951	0.5223	0.9835
Residual	176				

[1] Based on 9999 permutations; Data = pseudo-F statistic, p value. * Dominant component of variation.

Fishery target species biomass showed a significant temporal increase ($p = 0.0058$), but no significant treatment effects (Figure 9c, Table 6). Fishery target species biomass was significantly higher at TAM. There was a significant treatment × location interaction effect ($p = 0.0003$). A significant temporal increase in fishery target species biomass was observed within the coral treatment, but none for other treatments or controls (Figure 9c, Table S6). No significant temporal or treatment effects were observed in percentage fishery target species biomass (Figure 9d, Table 6). However, TAM supported a significantly higher ($p = 0.0053$) percent fishery target species biomass. No interaction effects were documented. No significant temporal variation in percent fishery target species biomass was observed within any experimental treatment, nor controls (Figure 9d, Table S6).

3.5. Spatio-Temporal Variation in Fish Functional Group Community Structure

Fish community structure (based on fish functional group abundance) showed a significant temporal change ($p < 0.0001$), with marginally significant treatment effects ($p = 0.0546$) (Table 7). Observed variation in fish community structure was significantly different between locations ($p < 0.0001$). There was significant time × location ($p < 0.0001$) and treatment × location interaction effects ($p = 0.0004$). A significant change in fish community structure based on abundance data was documented within all treatment groups, except for controls (Table S7).

Table 7. Summary of a BACI three-way crossed PERMANOVA test of the spatio-temporal variation in fish community structure in restored and control plots based on fish functional groups.

Source [1]	df	Abundance	Biomass
Time	1	11.57	5.91
		<0.0001	**0.0003**
Treatment	3	1.73	0.84
		0.0546	0.6303
Location	1	32.44 *	13.90 *
		<0.0001	**<0.0001**
Time × Treatment	3	0.55	0.82
		0.8905	0.6485
Time × Location	1	10.05	2.76
		<0.0001	**0.0193**
Treat. × Location	3	3.44	3.56
		0.0004	**0.0003**
Time × Treat. × Loc.	3	1.2	1.29
		0.2684	0.2004
Residual	176		

[1] Based on 9999 permutations; data = pseudo-F statistic, *p* value. * Dominant component of variation.

Fish community structure (based on fish functional group biomass) also showed a significant temporal change ($p = 0.0003$), but no significant treatment effects (Table 7). Observed variation in fish community structure by biomass was significantly different between locations ($p < 0.0001$). There were significant time × location ($p = 0.0193$) and treatment × location interaction effects ($p = 0.0003$). A significant change in fish community structure based on biomass data was documented within coral and 3D-printed treatment groups, but none for the mixed treatment or controls (Table S7).

Principal coordinate ordination analysis (PCO) based on fish abundance showed significant spatio-temporal variation and three distinctive clustering patterns (Figure 10). There was a small cluster on the left composed of live coral, 3D-printed, and mixed (live coral + 3D-printed) out-planting plots before restoration interventions. This cluster was largely explained by omnivore, non-denuder herbivore, scraper herbivore, and planktivore

abundance. A second cluster was composed of control plots before restoration and of 3D-printed and mixed plots after restoration. It was mostly explained by piscivore, browser, and generalist invertivore abundance. The final cluster was constituted by a combination of all restored locations, with before and after sampling efforts. This was mostly composed of locations at MAG that showed less variation in fish abundance after restoration interventions than at TAM. This PCO solution explains 86% of the observed spatio-temporal variation and clearly shows that restoration interventions resulted in a significant variation in fish assemblages after restoration interventions, but also shows spatial variations at the level of locations, suggesting that those locations with greater habitat complexity at TAM showed a stronger response than locations with flatter, more homogenous benthic community structures at MAG.

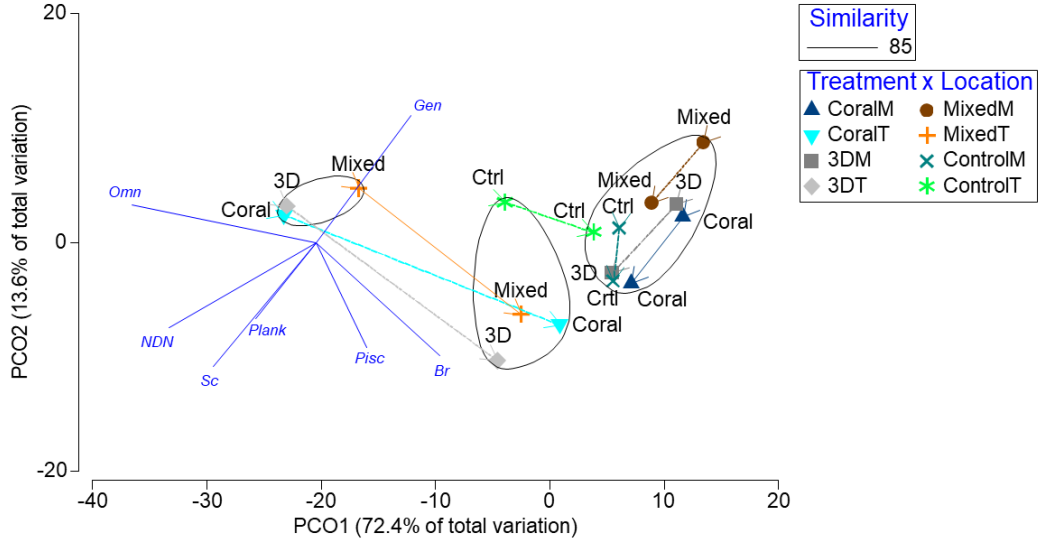

Figure 10. Principal coordinates ordination (PCO) analysis of the spatio-temporal variation in fish community structure based on fish functional group $\sqrt{}$-transformed abundance. NDN = non-denuders; Br = browsers; Sc = scrapers; Gen = generalist invertivores; Pisc = piscivores; Plank = planktivores; Omn = omnivores. M = Maguey (darker tones); T = Tampico (lighter tones). Blue = coral; gray = 3D-printed; brown = mixed; green = control plots (no intervention). Trajectories move from time 0 (before intervention) to time 1 (after intervention). This model explains 86% of the observed variation.

A dominance plot of the spatio-temporal variation in fish functional group abundance on restoration and control plots clearly shows that fish assemblage became increasingly complex and diverse following the restoration interventions (Figure 11). This effect was particularly more significant within live coral out-plantings and within 3D-printed out-plantings, followed by mixed out-plantings, in comparison to observed spatio-temporal variation in control plots.

Abundance–biomass comparison (ABC) plots based on fish functional group abundance and biomass show a consistent change in the disturbed status of fish assemblages before restoration interventions of fish abundance *k*-dominance curve falling above the biomass curve through its length across all different restoration interventions, namely live coral out-planting, 3D-printed out-planting, and mixed live coral + 3D-printed out-planting plots (Figure 12). In comparison, fish assemblages after all out-planting showed a reversed trend of the fish biomass *k*-dominance curve falling above the abundance curve. There was no significant change in the case of control locations, where both curves were similarly lined up before and after interventions.

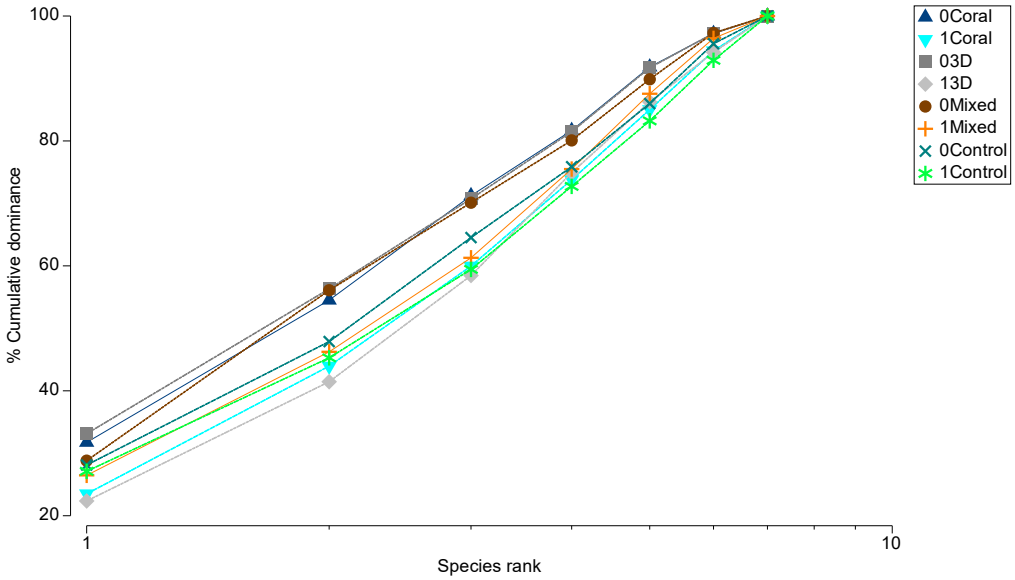

Figure 11. Dominance plot of the spatio-temporal variation in fish functional groups on restoration and control plots based on √-transformed abundance. Time zero (before intervention) = darker tones; Time 1 (after intervention) = lighter tones. Blue = coral; gray = 3D-printed; brown = mixed; green = control plots (no intervention).

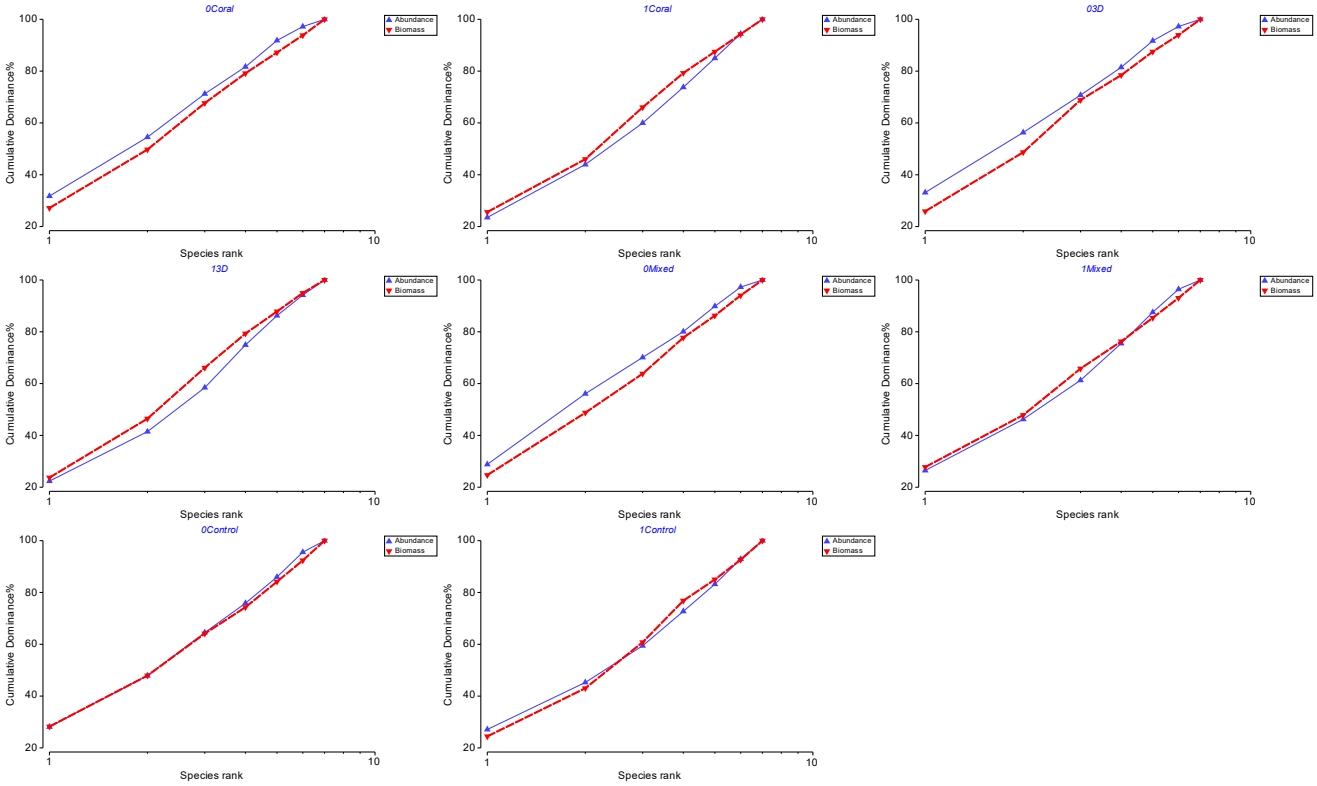

Figure 12. Abundance–biomass comparison (ABC) plots of the spatio-temporal variation in fish functional groups on restoration and control plots based on √-transformed abundance (blue) and biomass (red). 0 = Time 0 (before intervention); 1 = Time 1 (after intervention). Coral = living coral; 3D = 3D-printed; Mixed = coral + 3D-printed; Control = non-restored plots (no intervention).

3.6. Spatio-Temporal Variation in Fish Species Distribution

There was a highly significant temporal difference in fish community structure when data were analyzed at the species-level abundance (Pseudo-F = 17.66; $p < 0.0001$), with a significant treatment effect (Pseudo-F = 1.88; $p = 0.0031$). Temporal variation was sig-

nificant ($p < 0.0001$) within all experimental interventions, but not within control plots ($p = 0.0802$). There was a significant difference in fish community structure based on fish species distribution between corals and 3D-printed corals ($p = 0.0071$) and between 3D-printed and control plots ($p = 0.0071$), and marginal between 3D-printed and mixed corals ($p = 0.0580$). Other combinations of treatments were non-significant. There was a significant location effect (Pseudo-F = 31.00; $p < 0.0001$). There was no significant time × treatment interaction (Pseudo-F = 1.23; $p = 0.1516$). There were significant time × location (Pseudo-F = 4.99; $p < 0.0001$) and treatment × location interactions (Pseudo-F = 4.20; $p < 0.0001$). Time × treatment × location interaction was not significant (Pseudo-F = 1.07; $p = 0.3223$).

A PCO analysis showed significant spatio-temporal variation in fish assemblages (Figure 13). Community trajectories evidenced first a significant before-after change in fish community composition, but also a significant split in trajectories between both study locations, which were explained by different species composition. On the left, a cluster was composed of coral, 3D-printed, and mixed corals at TAM before interventions. These were mostly explained by the abundance of *C. personatus*, *Priacanthus arenatus*, and *Hypoplectrus indigo*. The trajectories of this group of experimental treatments after intervention formed a separate cluster mostly explained by *Bathygobius soporator*, juveniles of *Sparisoma chrysopterum*, *Acanthurus tractus*, and *Scarus iseri*. Also, *Stegastes planifrons*, *H. puella*, and *Chromis cyanea* explained most of the observed spatio-temporal variation. Bubble plots of showing the spatio-temporal variation of the sixteen most abundant species through this study are illustrated in the Supplementary Results (Figures S1–S16).

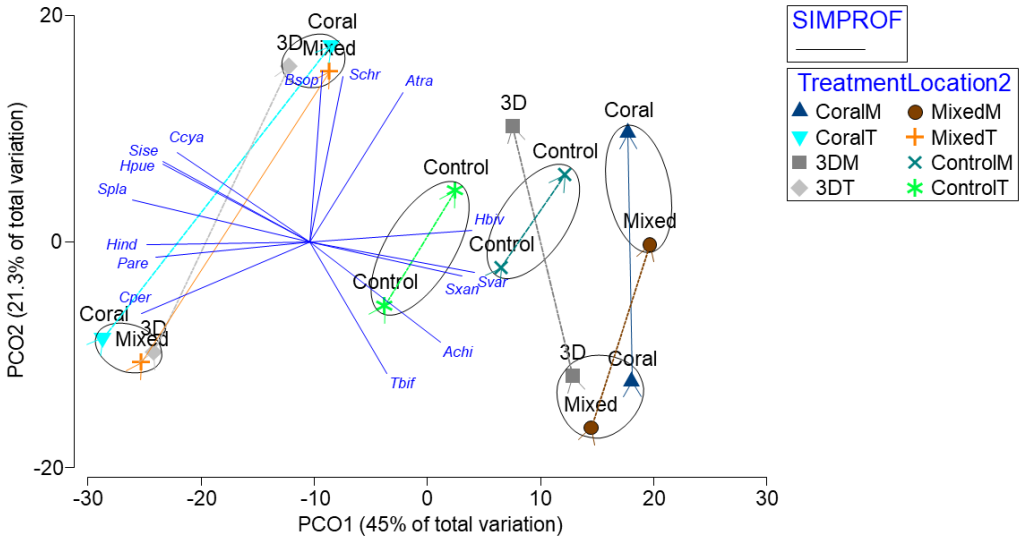

Figure 13. Principal coordinates ordination (PCO) analysis of the spatio-temporal variation in fish community structure based on $\sqrt{}$-transformed abundance of fish species. Vectorial analysis based on 90% correlation level. Clustering patterns based on SIMPROF test. Achi = *A. chirurgus*; Atra = *A. tractus*; Bsop = *bathygobius soporator*; Ccya = *Chromis cyanea*; Cper = *Coryphopterus personatus*; Hbiv = *Halichoeres bivittatus*; Hind = *Hypoplectrus indigo*; Hpue = *H. puella*; Pare = *Priacanthus arenatus*; Sise = *Scarus iseri*; Schr = *Sparisoma chrysopterum*; Spla = *Stegastes planifrons*; Svar = *S. variabilis*; Sxan = *S. xanthurus*; Tbif = *Thalassoma bifasciatum*. Trajectories are from time zero (before intervention) to time 1 (after intervention). Blue = coral; gray = 3D-printed; brown = mixed; green = control plots (no intervention). M = Maguey (darker tones); T = Tampico (lighter tones). Vector analysis based on a minimum correlation level of 0.80. This solution explains 72.8% of the observed variation.

On the right of Figure 13, there was also a cluster formed by coral, 3D-printed, and mixed corals at MAG before interventions. These were mostly explained by *Thalassoma bifasciatum* and juveniles of *A. chirurgus*. Trajectories of this group of experimental treat-

ments after intervention formed a separate cluster mostly explained by *S. xanthurus*, *S. variabilis*, and by juveniles of *Halichoeres bivittatus* and *A. tractus*. Control plots before and after interventions at TAM formed an individual cluster with limited temporal variation. Similarly, control plots at MAG formed a separate cluster with limited temporal variation. Control plots were mostly explained by *S. xanthurus*, *S. variabilis*, and by juveniles of *A. chirugus* and *H. bivittatus*. This solution explained 66.3% of the observed spatio-temporal variation.

Spatio-temporal variation in fish species composition showed remarkable differences. Similarity percentages (SIMPER) analysis showed that net species richness increased from 23.4 before interventions to 28.2 species per count after interventions. It also revealed an increase from 23.5 before interventions to 29.0 species per count within the coral out-planting plots after interventions, and from 23.9 before interventions to 31.0 species per count within the 3D-printed coral out-planting plots after interventions. There was also an increase from 23.3 before interventions to 28.3 species per count within the mixed out-planting plots after interventions, and a non-significant increase from 23.0 before interventions to 24.3 species per count within the control plots after interventions. There was also a temporal increase from 22.2 before interventions to 26.0 species per count within MAG after interventions, and an increase from 24.6 before interventions to 30.4 species per count within TAM after interventions.

SIMPER analysis also showed that *T. bifasciatum*, *S. iseri*, *C. personatus*, *A. coeruleus*, and *A. tractus* were the five most abundant fish species before interventions, explaining 57% of the observed abundance (Table S8). Meanwhile, *T. bifasciatum*, *S. iseri*, *A. tractus*, *A. coeruleus*, and *B. soporator* were the five most abundant fish species after interventions, explaining 48% of the observed abundance (Table S9). Before–after variation in fish species abundance was mostly explained by declining *C. personatus* and *T. bifasciatum* and by increased *H. flavolineatum*, *S. iseri*, and *A. tractus*, which explained 30% of the observed variation (Table S10). Fish assemblages also showed significant temporal variation between the two study locations. Before–after variation within MAG was mostly explained by declining *T. bifasciatum*, *C. personatus*, and *H. flavolineatum*, and by increased *Abudefduf saxtilis* and *Caranx ruber*, explaining 24% of the observed variation (Table S11). Before–after variation within TAM was mostly explained by declining *C. personatus* and *T. bifasciatum*, and by increased *A. tractus*, *H. flavolineatum*, and *Chromis multilineata*, explaining 35% of the observed variation (Table S12).

SIMPER analysis showed that *T. bifasciatum*, *S. iseri*, *C. personatus*, *A. coeruleus*, and *Sparisoma aurofrenatum*, were the most abundant species within the coral treatment, explaining 58% of the observed abundance before restoration (Table S13). In the case of the 3D-printed treatment, *T. bifasciatum*, *C. personatus*, *S. iseri*, *A. tractus*, and *A. coeruleus* were the most abundant, explaining 57% of the observed abundance before restoration (Table S14). *Thalassoma bifasciatum*, *C. personatus*, *S. iseri*, *A. coeruleus*, and *A. tractus* were the most abundant within the mixed treatment, explaining 59% of the observed abundance before restoration (Table S15). Meanwhile, *T. bifasciatum*, *S. iseri*, *A. coeruleus*, *A. tractus*, and *S. viride* were the most abundant within control plots, explaining 55% of the observed abundance before restoration (Table S16).

A higher abundance of *C. personatus* within 3D-printed plots, in comparison to coral plots explained the observed difference between both treatments before restoration (21%) (Table S17). A higher abundance of *C. personatus* within coral plots, in comparison to mixed plots explained the observed difference between both treatments (20%) before restoration (Table S18). A higher abundance of *C. personatus* within coral plots in comparison to control plots explained the observed difference between both treatments (17%) before restoration (Table S19). A higher abundance of *C. personatus* within 3D-printed plots in comparison

to mixed plots explained the observed difference between both treatments (19%) before restoration (Table S20). A higher abundance of *C. personatus* within 3D-printed plots in comparison to control plots explained the observed difference between both treatments (17%) before restoration (Table S21). A higher abundance of *C. personatus* within mixed plots in comparison to control plots explained the observed difference between both treatments (15%) before restoration (Table S22).

SIMPER analysis showed that *T. bifasciatum*, *S. iseri*, *A. tractus*, *A. coeruleus*, and *C. personatus* were the most abundant species within the coral treatment, explaining 50% of the observed abundance after restoration (Table S23). Also, *T. bifasciatum*, *S. iseri*, *C. personatus*, *A. tractus*, and *A. coeruleus* were the most abundant within the 3D-printed treatment, explaining 49% of the observed abundance after restoration (Table S24). *Thalassoma bifasciatum*, *S. iseri*, *C. personatus*, *A. tractus*, and *A. coeruleus* were the most abundant within the mixed treatment, explaining 50% of the observed abundance after restoration (Table S25). Meanwhile, *T. bifasciatum*, *S. iseri*, *A. tractus*, *A. coeruleus*, and *S. aurofrenatum* were the most abundant within control plots, explaining 53% of the observed abundance after restoration (Table S26).

A higher abundance of *C. personatus* within 3D-printed plots in comparison to coral plots explained the observed difference between both treatments after restoration (14%) (Table S27). A higher abundance of *C. personatus* within coral in comparison to mixed plots explained the observed difference between both treatments (13%) after restoration (Table S28). A higher abundance of *C. personatus* within coral plots in comparison to control plots explained the observed difference between both treatments (11%) after restoration (Table S29). A higher abundance of *C. personatus* within 3D-printed plots in comparison to mixed plots explained the observed difference between both treatments (13%) after restoration (Table S30). A higher abundance of *C. personatus* within 3D-printed plots in comparison to control plots explained the observed difference between both treatments (12%) after restoration (Table S31). A higher abundance of *C. personatus* within mixed plots in comparison to control plots explained the observed difference between both treatments (11%) after restoration (Table S32).

SIMPER analysis also revealed temporal variation in species composition within individual experimental treatments. Temporal variation within the coral treatment was mostly explained by declining *C. personatus* and *T. bifasciatum* and by increased *A. tractus*, *S. planifrons*, and *H. flavolineatum*, explaining the observed difference (29%) after restoration (Table S33). Temporal variation within the 3D-printed treatment was mostly explained by declining *C. personatus* and *T. bifasciatum* and by increased *A. coeruleus*, *S. iseri*, and *A. tractus*, explaining the observed difference (31%) after restoration (Table S34). Temporal variation within the mixed treatment was mostly explained by declining *C. personatus* and *T. bifasciatum* and by increased *S. iseri*, *H. bivittatus*, and *A. tractus*, explaining the observed difference (32%) after restoration (Table S35). Temporal variation within controls was mostly explained by declining *C. personatus*, *T. bifasciatum*, and *H. flavolineatum* and by increased *A. saxatilis* and *C. ruber*, explaining the observed difference (29%) after restoration (Table S36).

3.7. Spatio-Temporal Variation in the Hierarchical Preference of Fish Distribution by Treatment

An analysis of the fishes' hierarchical preference by treatment was conducted based on the abundance of 12 indicator species to determine their spatio-temporal variation (Table S37). The abundance ratios were calculated comparing all treatments before and after the restoration intervention. The analysis showed that important fishery target species such as *Epinephelus adsencionis*, *Lutjanus apodus*, *Ocyurus chrysurus*, and *Haemulon flavolineatum* showed a significant increase in abundance after intervention, particularly within the

coral and 3D-printed treatments. Non-denuder herbivore *Stegastes adustus*, planktivore *Abudefduf saxatilis*, and scraper herbivores *S. chrysopterum*, *S. aurofrenatum*, *Scarus vetula*, and *S. taeniopterus* showed several orders of magnitude increased juvenile abundances following restoration. The number of juveniles of browser herbivores, *A. coeruleus* and *A. tractus*, also increased following restoration. All combined average fish abundance ratios are shown in Figure 14, and evidence suggests that all experimental treatments showed increased fish abundance ratios following restoration: coral (2.70), 3D-printed (2.53), mixed (2.30), and even controls (1.14). Also, overall fish abundance ratios were higher within coral and 3D-printed treatments after restoration, in comparison to the mixed treatment and controls.

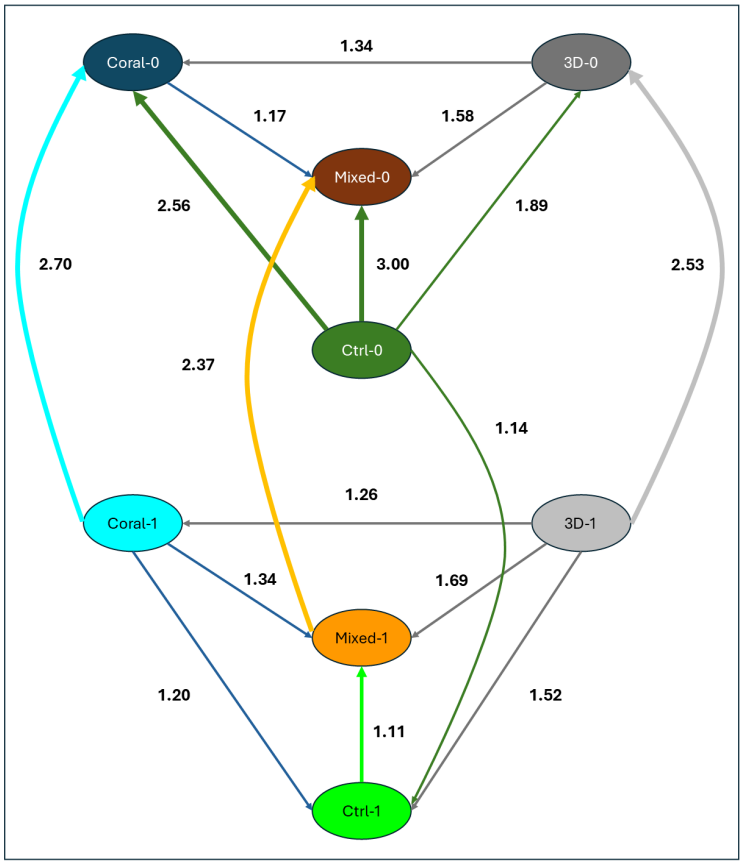

Figure 14. Hierarchal chart of fishes' preference based on the abundance of fishes of 12 indicator species * that preferred each experimental treatment before (0) and after (1) restoration interventions. The direction of the arrows indicates the most dominant to the less dominant treatments. The width of the arrows is proportional to the percentage of dominance, and the numbers next to each arrow are the ratio of more dominant to the less dominant treatment. * = Indicator species included in the analysis: *Epinephelus adsencionis*, *Lutjanus apodus*, *Ocyurus chrysurus*, *Haemulon flavolineatum*, *Stegastes adustus*, *Abudefduf saxatilis*, *Sparisoma chrysopterum*, *Sparisoma aurofrenatum*, *Scarus vetula*, *Scarus taeniopterus*, *Acanthurus coeruleus*, *Acanthurus tractus*.

3.8. Spatio-Temporal Variation in Fish Biodiversity and Phylogenetic Dynamics

Fish biodiversity was significantly enhanced after the experimental restoration interventions. Taxonomic diversity (Delta, Δ) increased from 66 to 68 in the coral treatment, from 66 to 70 in 3D-printed plots, from 65 to 68 in mixed plots, and from 66 to 67 in controls, suggesting enhanced taxonomic complexity (Table 8). Delta showed a significant temporal variation ($p < 0.0001$) and significant time × location ($p = 0.0088$) and time × treatment × location interactions ($p = 0.0270$) (Table 9).

Table 8. Spatio-temporal variation in annual mean fish biodiversity measures (taxonomic distinctness and phylogenetic diversity) in control and restored plots.

Variables [1]	Cor-0	Cor-1	3D-0	3D-1	Mix-0	Mix-1	Ctr-0	Ctr-1
Tax Div (Delta, Δ)	65.81 ± 1.95	68.44 ± 0.70	65.67 ± 1.52	69.5 ± 0.57	64.72 ± 1.32	67.56 ± 1.10	65.96 ± 0.96	67.17 ± 1.03
TD (Delta*, Δ*)	72.44 ± 0.77	71.32 ± 0.62	72.6 ± 0.73	72.53 ± 0.46	72.07 ± 1.03	71.04 ± 0.68	71.49 ± 0.83	71.18 ± 0.77
AvTD ($Delta^+$, Δ^+)	72.76 ± 0.53	72.44 ± 0.55	72.17 ± 0.48	73.16 ± 0.46	71.96 ± 0.79	72.23 ± 0.67	71.89 ± 0.63	71.83 ± 0.54
TTD ($sDelta^+$, $s\Delta^+$)	1710.27 ± 112.90	2107.47 ± 176.53	1731.05 ± 170.54	2274.41 ± 208.04	1682.37 ± 172.76	2045.61 ± 153.89	1654.81 ± 103.43	1748.23 ± 143.40
VarTD ($Lambda^+$, Λ^+)	280.75 ± 23.33	259.37 ± 17.95	277.03 ± 17.91	243.73 ± 15.94	292.06 ± 33.10	264.27 ± 22.82	297.38 ± 22.06	289.43 ± 20.13
AvPD (Φ^+)	47.25 ± 1.55	45.57 ± 1.12	47.38 ± 0.97	45.69 ± 1.14	47.33 ± 1.61	45.56 ± 0.98	45.85 ± 1.24	45.52 ± 0.90
Faith's PD ($s\Phi^+$)	1103.33 ± 61.11	1316.67 ± 96.90	1130 ± 103.23	1410 ± 114.92	1095 ± 103.85	1288.33 ± 95.61	1053.33 ± 66.72	1105 ± 88.23

[1] Mean ± 95% confidence intervals. (a) Taxonomic diversity (Delta, Δ); (b) taxonomic distinctness—TD (Delta*, Δ*); (c) average taxonomic distinctness—AvTD ($Delta^+$, Δ^+); (d) total taxonomic distinctness—TTD ($sDelta^+$, $s\Delta^+$); (e) variation in taxonomic distinctness—VarTD ($Lambda^+$, Λ^+); (f) average phylogenetic diversity—AvPD (Φ^+); (g) total phylogenetic diversity—Faith's PD ($s\Phi^+$).

Table 9. Summary of a two-way crossed PERMANOVA test of the spatio-temporal variation in Log_{10}-transformed fish biodiversity measures in restored and control plots.

Source [1]	df	Δ [2]	Δ*	Δ^+	$s\Delta^+$	Λ^+
Time	1	38.17 *	6.81	1.18	43.27 *	8.82
		<0.0001	**0.0105**	0.2780	**<0.0001**	**0.0034**
Treatment	3	2.11	5.05	3.78	5.15	3.46
		0.0982	**0.0027**	**0.0136**	**0.0021**	**0.0161**
Location	1	0.07	29.74 *	18.78 *	26.32	24.45 *
		0.7936	**<0.0001**	**<0.0001**	**<0.0001**	**<0.0001**
Time × Treatment	3	1.63	1.16	1.95	3.05	0.58
		0.1855	0.3152	0.1246	**0.0285**	0.6234
Time × Location	1	2.89	10.89	0.0006	1.28	0.14
		0.0945	**0.0012**	0.9798	0.2546	0.7090
Treat. × Location	3	3.85	5.41	1.41	6.05	1.91
		0.0088	**0.0019**	0.2417	**0.0007**	0.1284
Time × Treat. × Loc.	3	3.18	0.65	2.66	1.61	0.63
		0.0270	0.5773	0.0517	0.1913	0.5939
Residual	176					

[1] Based on 9999 permutations; data = pseudo-F statistic, *p* value. [2] Δ = taxonomic diversity (Delta); Δ* = taxonomic distinctness (Delta*); Δ^+ = average taxonomic distinctness—AvTD ($Delta^+$); $s\Delta^+$ = total taxonomic distinctness—TTD ($sDelta^+$); Λ^+ = variation in taxonomic distinctness—VarTD ($Lambda^+$). * Dominant component of variation.

Taxonomic distinctness (Delta*, Δ*) showed a slight but significant decline through time across all treatments (Table 8). It was significantly higher before restoration interventions ($p = 0.0105$) (Table 9). There were also significant differences among treatments ($p = 0.0027$) and between locations ($p < 0.0001$). There were also significant time × location ($p = 0.0012$) and treatment × location interactions ($p = 0.0019$).

Average taxonomic distinctness—AvTD ($Delta^+$, Δ^+) showed significant variation among treatments ($p = 0.0136$) and between locations ($p < 0.0001$) (Table 9). No significant interactions were documented.

Total taxonomic distinctness—TTD ($sDelta^+$, $s\Delta^+$) increased from 1710 to 2107 in the coral treatment, from 1731 to 2274 in 3D-printed plots, from 1682 to 2046 in mixed plots, and from 1655 to 1748 in controls (Table 8). $sDelta^+$ showed a significant temporal increase ($p < 0.0001$), and significant variation among treatments ($p = 0.0021$) and between locations ($p < 0.0001$) (Table 9). There was also a significant treatment × location interaction ($p = 0.0007$).

Variation in taxonomic distinctness—VarTD ($Lambda^+$, Λ^+) declined from 281 to 259 in the coral treatment, from 277 to 244 in 3D-printed plots, from 292 to 264 in mixed plots,

and from 297 to 289 in controls (Table 8). Lambda$^+$ showed a significant temporal decline ($p = 0.0034$) and significant variation among treatments ($p = 0.0161$) and between locations ($p < 0.0001$) (Table 9). There were no significant interactions.

Average phylogenetic diversity—AvPD (Φ^+) showed a slight but significant ($p = 0.0023$) decline through time across all treatments (Tables 8 and 10). No significant interaction effects were observed.

Table 10. Summary of a two-way crossed PERMANOVA test of the spatio-temporal variation in Log_{10}-transformed fish phylogenetic diversity measures in restored and control plots.

Source [1]	df	Φ^+ [2]	$s\Phi^+$
Time	1	9.38 *	34.08 *
		0.0023	**<0.0001**
Treatment	3	0.78	6.11
		0.5037	**0.0003**
Location	1	3.08	19.55
		0.0812	**0.0002**
Time × Treatment	3	0.62	2.28
		0.6018	0.0850
Time × Location	1	0.38	0.77
		0.5382	0.3827
Treat. × Location	3	0.85	5.9
		0.4779	**0.0004**
Time × Treat. × Loc.	3	0.22	1.75
		0.8836	0.1655
Residual	176		

[1] Based on 9999 permutations; Data = pseudo-F statistic, p value. [2] Φ^+ = average phylogenetic diversity—AvPD; $s\Phi^+$ = total phylogenetic diversity—Faith's PD. * Dominant component of variation.

Total phylogenetic diversity—Faith's PD ($s\Phi^+$) increased from 1103 to 1317 in the coral treatment, from 1130 to 1410 in 3D-printed plots, from 1095 to 1288 in mixed plots, and from 1053 to 1105 in controls (Table 8). $s\Phi^+$ showed a significant temporal increase ($p < 0.0001$) (Table 10). There was also significant variation among treatments ($p = 0.0003$) and between locations ($p = 0.0002$), and a significant treatment × location effect ($p = 0.0004$).

Superimposing the real Δ^+ values for the before–after variation in fish assemblages across all treatments, several features are apparent. There was no significant before–after variation in Δ^+ values, but there was significant variation among all treatments (Figure 15). Coral and 3D-printed treatments showed consistently slightly lower average distinctness and Δ^+ values slightly closer to that of the species master list. There was also a slight decline in Δ^+ values within mixed plots but with higher dispersion of values after restoration. There was no variation in Δ^+ values within control plots. Figure 16 for simulated variation in Λ^+ shows also several findings. There was a significant before–after variation in Λ^+ values and a significant variation among all treatments. Dispersion was also higher in Λ^+ values from the mixed treatment and controls.

3.9. Spatio-Temporal Correlations Between Fish Community Structure Reef Rugosity Index

Figure 17 shows the spatial variation of the reef rugosity index scale. There was no significant difference in benthic habitat complexity among treatments (d.f. = 3; Pseudo-F = 0.53; $p = 0.5283$), but the rugosity index scale was significantly higher at TAM (d.f. = 1; Pseudo-F = 10.22; $p = 0.0047$). No significant treatment × location interaction was observed (d.f. = 3; Pseudo-F = 1.60; $p = 0.2179$).

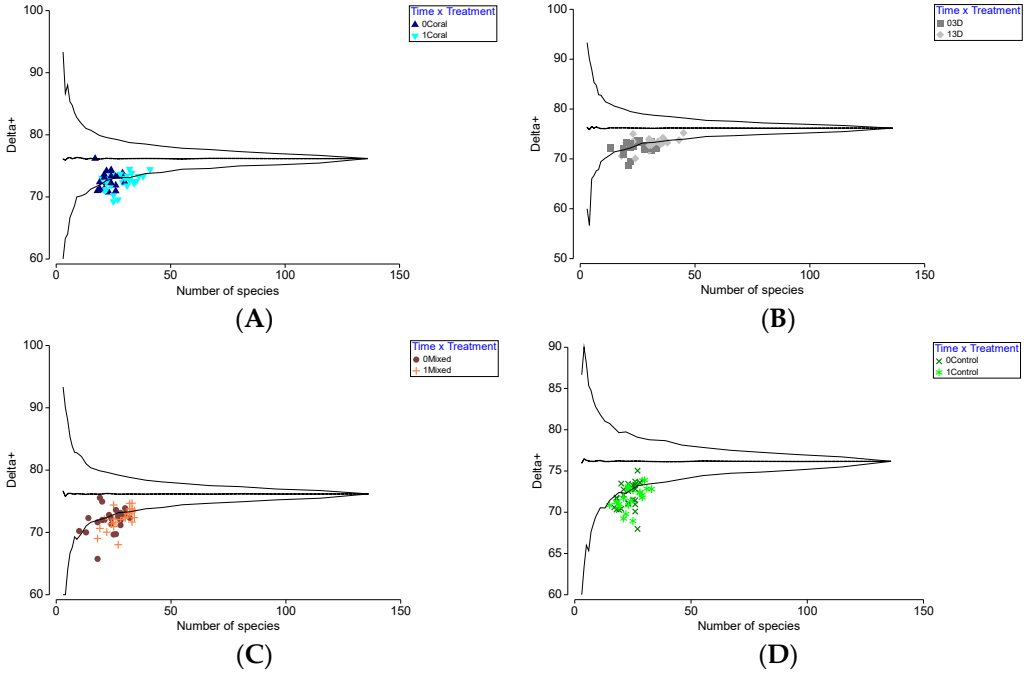

Figure 15. Funnel plot for simulated average taxonomic distinctness—AvTD (Δ^+) before and after coral restoration intervention: (**A**) coral; (**B**) 3D; (**C**) mixed; (**D**) control. The horizontal line indicates the mean Δ^+ of the master species list, which is not a function of S. The boundary lines indicate the limits within which 95% of simulated Δ^+ values lie. Points are the true temporal variation in AvTD (y-axis) for the before and after samples. 0 = before restoration; 1 = after restoration interventions.

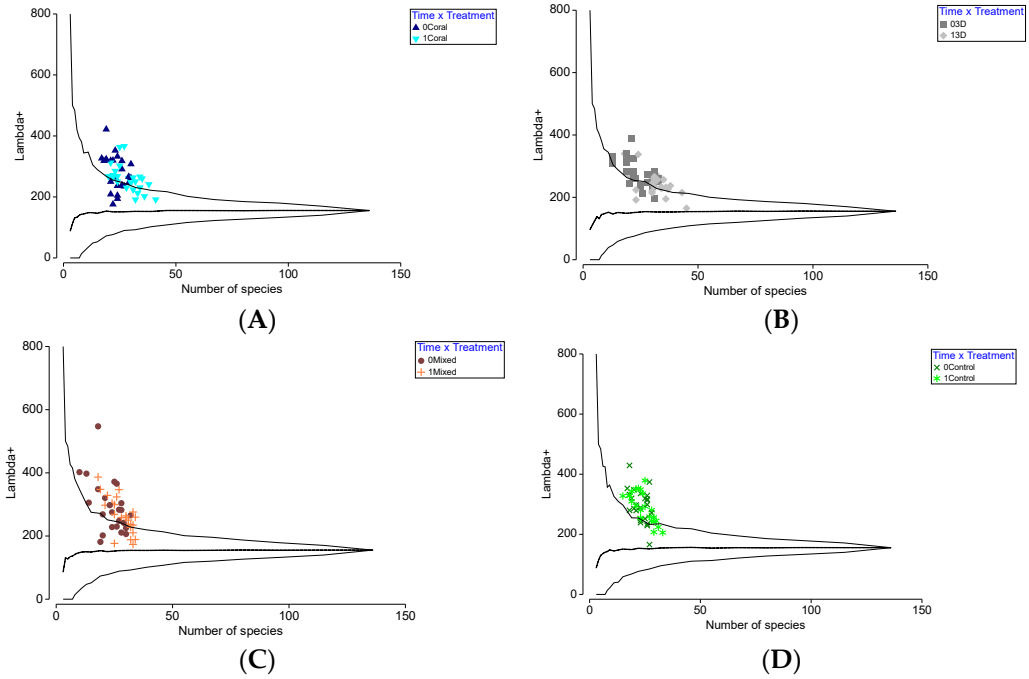

Figure 16. Funnel plot for simulated variation in taxonomic distinctness—VarTD (Lambda$^+$, Λ^+) before and after coral restoration intervention: (**A**) coral; (**B**) 3D; (**C**) mixed; (**D**) control. The horizontal line indicates the mean Λ^+ of the master species list, which is not a function of S. The boundary lines indicate the limits within which 95% of simulated Λ^+ values lie. Points are the true temporal variation in VarTD (y-axis) for the before and after samples. 0 = before restoration; 1 = after restoration interventions.

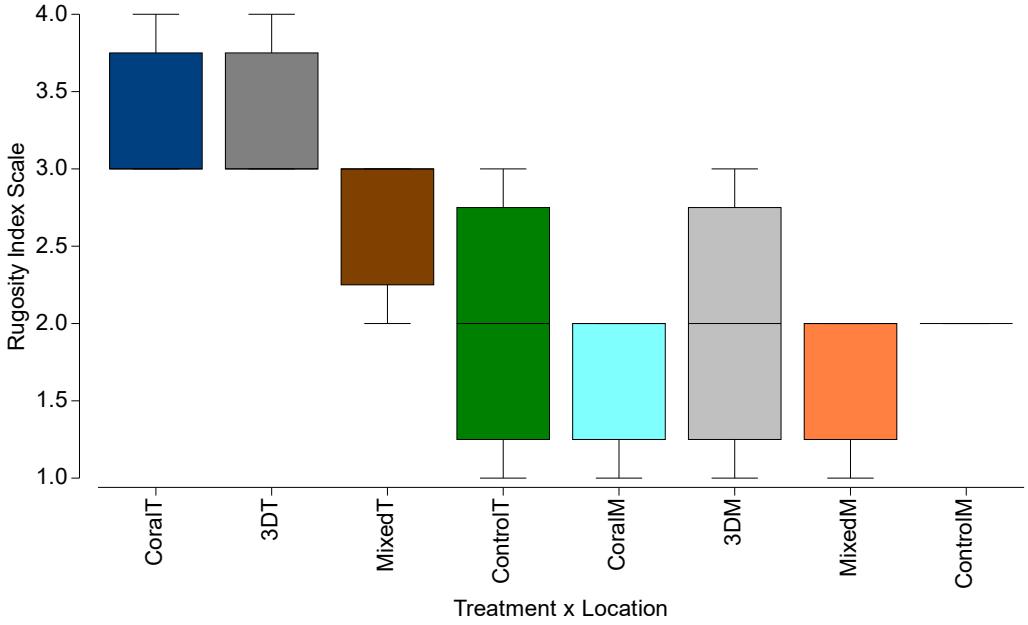

Figure 17. Mean rugosity index scale calculated for all treatment × location combinations. Blue = Coral; Gray = 3D-printed; Brown = Mixed; Green = Control plots (no intervention). M = Maguey; T = Tampico.

A significant positive multivariate correlation was observed between reef rugosity and species richness (Rho = 0.803; $p = 0.0010$), total fish abundance (Rho = 0.804; $p = 0.0018$), total herbivore abundance (Rho = 0.555; $p = 0.0123$), non-denuder herbivore abundance (Rho = 0.838; $p = 0.0040$), scraper herbivore abundance (Rho = 0.643; $p = 0.0067$), omnivore abundance (Rho = 0.756; $p = 0.0017$), and non-denuder herbivore biomass (Rho = 0.655; $p = 0.0050$) (Table S38). No other individual fish abundance or biomass parameter correlated with reef rugosity. There was a significant correlation between reef rugosity and fish functional group community structure based on abundance data (Rho = 0.777; $p = 0.0016$), but there was none with fish functional group community structure based on biomass data (Rho = 0.060; $p = 0.3624$). There was also a significant correlation between reef rugosity and fish functional group community structure based on individual species abundance data (Rho = 0.712; $p = 0.0011$). There were also significant correlations between reef rugosity and Δ^* (Rho = 0.810; $p = 0.0008$), Δ^+ (Rho = 0.620; $p = 0.0047$), $s\Delta^+$ (Rho = 0.824; $p = 0.0014$), Λ^+ (Rho = 0.757; $p = 0.0028$), and $s\Phi^+$ (Rho = 0.724; $p = 0.0045$) (Table S39).

4. Discussion

This study investigated the short-term impacts of various coral restoration interventions on reef fish assemblages in Culebra Island, Puerto Rico. The interventions included natural *A. cervicornis* out-plants, 3D-printed *A. cervicornis* structures, mixed natural and 3D-printed out-plants, and control sites with no intervention. The findings provide valuable insights into how different restoration strategies influence fish communities and their ecological functions. Important factors such as enhanced benthic spatial complexity, enhanced fish recruitment and attraction of different fish functional groups, particularly, herbivore guilds, were the most conspicuous results of the restoration intervention. Natural out-plants and mixed interventions showed the most significant effects of fish assemblage enhancement.

4.1. Effects of Coral and 3D-Printed Coral on Fish Assemblages: The Role of Structural Complexity

The integration of 3D-printed corals in coral restoration efforts offers significant benefits for ecological restoration, structural stability, and the functional enhancement of coral reefs. This innovative approach enables rapid and customizable restoration, promoting

biodiversity, enhancing ecosystem services at the intervention spatial scale, and providing sustainable and ethical solutions to address coral reef decline due to human impacts and climate change. The results indicated that both natural and 3D-printed *A. cervicornis* structures positively influenced fish species' richness, abundance, biomass, and diversity, compared to control sites. Notably, sites with mixed natural and 3D-printed out-plants exhibited the highest metrics in most parameters, suggesting a possible synergistic effect between natural and artificial corals. This aligns with previous research demonstrating that artificial structures can effectively mimic natural coral habitats, providing refuge and foraging opportunities for various fish species [32,112,113]. For instance, a previous study in Culebra Island found that 3D-printed corals mimicking *A. cervicornis* attracted similar fish assemblages as natural corals, highlighting their potential as complementary tools in reef restoration efforts [86]. Elsewhere, fish abundance and diversity increased significantly in areas with 3D-printed structures compared to control sites, stressing the potential of 3D printing in reef restoration efforts [112]. An experimental study manipulated habitat complexity using artificial structures, including 3D-printed modules, to assess their impact on fish diversity, demonstrating that increased structural complexity positively influences fish community composition [113]. Also, the effectiveness of artificial reefs, including 3D-printed structures, in sediment-impacted areas suggests that these structures can enhance coral recruitment and support diverse fish assemblages even under significantly degraded environmental conditions [114].

Furthermore, certain fish species appear to show preferences for specific colors and shapes of the 3D-printed models, suggesting that these structures can substitute for live corals in providing habitat for certain reef fish [92]. Another study found that blue-green damselfish (*Chromis viridis*) did not exhibit altered behavior when exposed to 3D-printed coral models compared to natural coral skeletons, and that larval stages of mustard hill coral (*Porites astreoides*) settled on 3D-printed substrates at rates comparable to natural substrates, indicating that 3D-printed materials are not inherently harmful to these reef organisms [88]. The use of artificial structures like 3D-printed corals have also had overall positive impacts in fostering increased abundance and biomass and fish assemblages, with important socio-economic implications for local fishing communities [115].

The integration of 3D-printed corals and natural *A. cervicornis* out-planting in this study contributed to enhancing fish assemblage biodiversity and their ecological functions one year after interventions. This resulted in increased fish species richness, H'_n and J'_n within natural *A. cervicornis*, 3D-printed, and mixed treatments, particularly within TAM, the location with the highest benthic spatial relief. Total fish abundance declined after the interventions, largely due to the impact of abnormally high sea surface temperature (SST) and the widespread mass coral bleaching event during 2023 in *C. personatus*, the most abundant species before interventions. Decline was consistent among treatments but was significantly higher at TAM, which was associated with higher benthic spatial heterogeneity and higher *C. personatus* populations. However, total fish biomass showed a significant increase, particularly within the natural coral restoration plots and at studied reefs at TAM. This location exhibited the highest mean rugosity index. Several studies collectively underscore the critical role of benthic spatial relief and structural complexity in enhancing fish abundance, biomass, and diversity on coral reefs.

Structural complexity, or rugosity, is a critical factor influencing fish community composition. The 3D-printed structures in this study were designed to mimic the branching morphology of *A. cervicornis*, enhancing habitat complexity at the intervention plot scales. The positive response of fish assemblages to these structures underscores the importance of physical habitat features in reef restoration. Complex structures provide niches for various species, reduce predation pressure, and increase resource availability, thereby

supporting higher biodiversity and taxonomic complexity. This finding is supported by previous research demonstrating that increased habitat complexity by corals is associated with greater fish abundance and diversity on reefs [116]. A combination of biotic factors and multi-scale abiotic factors, such as structural complexity, significantly influence habitat quality, which in turn affects the distribution and abundance of coral reef fishes [117]. Habitat biodiversity, closely linked to structural complexity, is also a crucial determinant of fish community structure, influencing species richness and abundance [118].

Benthic rugosity, or the structural complexity of the seafloor is a crucial factor influencing the diversity and abundance of coral reef fish assemblages. High rugosity provides a variety of microhabitats, shelters, and foraging opportunities, which support a wide range of fish species and life stages. Complex structures offer habitat provision, numerous niches, and protection from strong currents and wave action, allowing coexistence of diverse species by reducing competition and promoting predator avoidance. Crevices and overhangs serve as refuges for smaller fish, enhancing survival rates. Varied surfaces support diverse algae and invertebrate communities, providing abundant food resources. Certain fish species also rely on specific structural features for spawning. Structural complexity is a strong predictor of fish species richness and abundance on coral reefs [119] and biomass [120], significantly influencing fish community structure [121–124], benthic and fish diversity patterns [125–129], and behavior and distribution [130]. It plays a vital role in promoting reef fish sheltering dynamics [131], particularly on reefs with a higher percentage of branching and tabulate live coral cover [132,133]. Artificial reefs with high structural complexity share similar characteristics as higher rugosity reefs [118].

More structurally complex reefs provide a greater variety of habitats, which in turn support higher fish diversity and biomass [119], including up to 20–30% higher abundance, ~20% higher species richness, and nearly twice the biomass compared to other habitats [134]. They also support higher juvenile densities [135,136] and higher survival of juveniles [137]. Complex reef architecture supports higher abundances of small-bodied fishes and longer food chains, becoming a key determinant of fish community composition and trophic interactions [138], therefore enhancing overall coastal productivity. However, significant coral reef habitat degradation can lead to declining fish assemblages [139]. A long-term region-wide decline in the structural complexity of Caribbean coral reefs correlated with habitat loss and a "flattening" effect with reductions in fish diversity and biomass [140–142]. Another study explored how the loss of structural complexity can lead to declines in reef fish abundance and diversity, emphasizing the importance of maintaining reef architecture for fisheries sustainability [143]. However, a study observed that reefs in the Seychelles with greater structural complexity showed higher rates of fish species richness and abundance during recovery periods following bleaching events, highlighting the resilience provided by complex habitats [144]. Structural complexity is a key factor influencing the recovery potential of coral reef fish communities, with more complex reefs supporting higher biomass and diversity [145]. These findings underscore the importance of structural complexity in enhancing fish community metrics and in fostering enhanced natural recovery ability following disturbance and promoting high ecosystem resilience.

4.2. Trophic Functional Group Responses: The Importance of Restoring Herbivores and Piscivores

Analysis of trophic functional groups revealed that herbivores and omnivores were more abundant in restored sites, particularly in mixed out-planting areas. There was an increased abundance and biomass of browsers (Acanthuridae) and scrapers (Scaridae). Non-denuders (Pomacentridae) showed no temporal increase, but scrapers and non-denuders were more abundant at TAM, which sustained reefs with higher structural complexity, while browsers were more abundant at MAG, with reefs with lower structural complexity.

Total herbivore biomass, particularly scrapers, significantly increased within the coral and 3D treatments. These results are consistent with previous restoration studies that showed increased herbivore abundance or biomass following coral restoration interventions and a consequent enhancing of structural complexity [146]. In addition, fish recurrently impacted by mass coral bleaching and mortality, such as the study sites in this project, have shown significant regime shifts in fish assemblages enhancing dominance by herbivore guilds and affecting fish catches [147].

Two potential mechanisms involving positive and negative feedbacks might control reef resilience recovery: coral restoration and enhanced benthic spatial relief lead to enhanced herbivore attraction and enhanced herbivore guilds lead to important algal control, opening substrates for coral larval settlement and for asexual fragments reattachment, promoting natural recovery. Enhancing structural complexity through restoration can attract herbivorous fishes, thereby increase herbivory rates and benefiting coral out-plants by reducing algal competition [148]. Restoration efforts focusing on herbivore management can enhance coral recovery by controlling algal growth [149]. Long-term Elkhorn coral (*A. palmata*) restoration in Puerto Rico resulted in significantly augmented benthic spatial heterogeneity and diverse herbivore guilds enhancement in a shallow, high-energy reef [85]. Different herbivorous fish species have varying effects on algal communities and coral growth, suggesting that restoration efforts should aim to support a diverse herbivore population to optimize coral reef recovery [149]. Different herbivorous fish guilds influence algal succession, emphasizing the importance of diverse herbivore assemblages in maintaining coral-dominated reef states, which is crucial for restoration success [150].

Herbivorous fish play a fundamental role in controlling algal growth, thereby facilitating long-term coral recruitment and growth. The increase in herbivore populations suggests that restoration efforts may enhance essential ecological processes, promoting reef resilience. This observation is consistent with findings from a study in the Dominican Republic, where restored areas showed increased fish biomass, particularly of the herbivorous parrotfish *S. iseri*, underscoring the functional importance of *A. cervicornis* in reef ecosystems [151]. *Scarus iseri* was also a paramount species within restored areas in this study. Increased herbivory resulting from effective restoration can reduce harmful seaweed proliferation, thereby aiding coral health and resilience [152]. An experimental reduction in herbivory hampered coral recovery, highlighting the necessity of protecting herbivores in restoration strategies [153]. On the other hand, marine reserves, by protecting herbivorous fish populations, facilitate coral recovery through increased grazing pressure, underscoring the importance of herbivore management in restoration efforts [154]. The protection of herbivorous fishes leads to trophic cascades that benefit coral communities, suggesting that restoration projects should consider herbivore conservation to promote reef health [155]. Furthermore, maintaining herbivorous fish populations above certain thresholds is vital for preventing phase shifts to algal-dominated reefs [156]. The importance of herbivory in preventing phase shifts to algal-dominated states on coral reefs suggests that restoration efforts should include strategies to enhance herbivory to bolster reef resilience against climate change [157]. This emphasizes the importance of implementing 3D-printed coral structures in combination with natural out-plants to accelerate herbivore fish attractiveness.

Piscivores also showed a significant increase in abundance and biomass, particularly in natural and in mixed out-planting areas. ABC analysis evidenced a consistent change in the disturbed status of fish assemblages before restoration interventions with the fish abundance *k*-dominance curve falling above the biomass curve through its length across all different restoration interventions. This is consistent with previous studies suggesting strong fishing impacts [158–160]. Ecological restoration can be used as an alternative to help reverse fishing impacts and promote fish assemblage recovery.

Temporal variation in fish community structure was also significant within all experimental interventions, but not within control plots. These findings clearly point out the rapid enhancement of fish assemblages of different functional groups. Coral restoration efforts can enhance habitat complexity, potentially leading to increased abundance and biomass of piscivorous fishes and improved recruitment rates [32]. A previous study explored how chemical cues from restored coral habitats influence the settlement and recruitment of fish larvae, including those of piscivorous species [161]. Findings suggest that successful coral restoration can enhance larval attraction and subsequent recruitment, further contributing to fish assemblage recovery.

4.3. Fishery Target Species Recovery: Coral Restoration as a Fishery Management Tool

The study noted a significant increase in the abundance of fishery target species, such as snappers (Lutjanidae), grunts (Haemulidae), groupers (Serranidae), and parrotfishes (Scaridae) in restored sites. The presence of structurally complex habitats, provided by both natural and artificial corals, likely offers shelter and hunting grounds for these commercially important species, supporting their recovery and sustainability. A study evaluated the effectiveness of coral transplantation onto artificial structures in restoring fish communities [114]. Results indicated that fish abundance and diversity increased significantly in areas with restored habitats, including species targeted by fisheries. There is also evidence that supports the use of complex structures in increasing the abundance of fishery-targeted species in degraded reef areas [112]. This enhancement has both ecological and economic implications, as these species are vital for local fisheries and contribute to the overall health of reef ecosystems and to locally support food security.

4.4. Implications of Mass Coral Bleaching During 2023

Marine heatwaves (MHWs) in the tropical Atlantic have increased in frequency and intensity [27,162,163], leading to widespread coral bleaching and potential long-term impacts on reef-associated fish populations [164,165]. Culebra Island has been significantly impacted by mass bleaching events in 1987, 1998, 2005, 2010, 2019, 2021, 2023, and 2024. The 2005, 2023, and 2024 events caused significant mortality in numerous coral species. The 2023 event partially affected the final sampling efforts in this study, becoming a potentially compounded factor that might have influenced the after out-planting results. Coral bleaching can result in the decline of some vulnerable, coral-dependent fish species. It is argued that declining small-sized coral-dependent omnivores, such as the masked goby (*C. personatus*), was related to the abnormally elevated SST (up to 33 °C). This might have had a temporal negative effect on fish abundance in this species. Observed coral mortality during the 2023 bleaching event (data not part of this study) might have contributed to the observed decline. Fish species richness and abundance are positively correlated with percent coral cover and structural complexity, emphasizing the importance of healthy coral reefs for maintaining fish communities. However, coral bleaching often leads to significant declines in the abundance of coral-dependent fish species, particularly those with specialized habitat requirements [164]. *Coryphopterus personatus* and other small-bodied, reef-associated fish species in the Caribbean are particularly vulnerable to the impacts of MHWs, coral bleaching, and mortality [164]. These climate-induced events lead to significant declines in coral cover and structural complexity, which are essential for the survival of such species. Bleaching-related coral mortality results in the degradation of reef structures, leading to the loss of shelter and breeding grounds for small, site-attached fish like *C. personatus*. The loss of structural complexity results in reduced fish diversity and abundance, with small-bodied species being the most affected [165]. The decline in coral health often leads to food web disruption, affecting the abundance of invertebrates and

other food sources, impacting the diet of these fish. Simplified reef structures also offer fewer hiding spots, making small fish more susceptible to predators.

Increased temperatures and recurrent mass bleaching events disrupt the reproductive success of corals, leading to long-term declines in percent coral cover and associated reef fish populations [166]. In turn, mass bleaching events often result in reduced fish abundance and diversity, particularly among species that rely heavily on live coral habitats [164–166]. Structural complexity of coral reefs is diminished by bleaching events and declining coral recruitment [167,168] and can be a critical determinant of fish size distributions, leading to declines in larger-bodied fish species [169]. A previous study documented delayed effects of the 1998 mass coral bleaching event in the Indian Ocean on reef fish communities that affected fish diversity and abundance, particularly among coral-dependent species, several years post-bleaching [170]. Following the 2016 mass bleaching event on the Great Barrier Reef, there were significant changes in fish community composition, with declines in species richness and shifts towards more herbivorous species as coral cover decreased [171]. Mass bleaching events lead to a homogenization of reef fish communities, characterized by reduced diversity and the dominance of generalist species, less dependent on live coral [172]. Another study indicated that while some recovery is possible, repeated disturbances and elevated temperatures hinder the resilience of reef fish assemblages [173]. Significant warming is projected to occur over the next decades across the Wider Caribbean and Eastern Tropical Pacific regions over the next few decades, with significant adverse impacts on coral reef conservation and restoration outcomes [27]. Potential future impacts of climate change-induced coral bleaching on reef fish communities predict declines in abundance and diversity, especially among species with high dependence on live coral habitats [174]. Bleaching impacts during this study apparently had a significant impact on some small-bodied, coral-dependent taxa, which we were probably not able to address due to the original sampling design. However, despite the significant warming trends during 2023, restoration interventions in this study had a net positive impact on the overall community structure, probably buffering some of the coral bleaching and mortality effects observed at the end of the study.

4.5. Implications for Future Restoration Strategies of Severely Degraded Coral Reef Ecosystems

While some studies have reported limited short-term impacts of coral restoration on fish communities, particularly in isolated or less disturbed reefs, the present study observed notable positive effects at the experimental plot scales within a one-year period on severely disturbed reefs. This discrepancy may be attributed to differences in habitat environmental conditions, structural complexity, restoration methodologies, and the initial state of the fish communities. Coral reefs in Culebra Island have a long history of environmental disturbances by military maneuver, anchoring and bombing activities [175–177]. This resulted in the mechanical demolition of numerous reef structures, including some of our studied reefs. They have also been severely impacted by extreme rainfall events [29], recent hurricanes [178], invasive species [179], land-based source pollution [2,180–182]; sewage [8], eutrophication [183], and fishing [184]. They have also been affected by eight mass coral bleaching events between 1987 and 2024, which has resulted in significant coral loss [26], indirectly impacting fish assemblages. Synergistic interactions among these factors were largely possible, but these were not addressed in this study, particularly, interactions among temperature effects, pollution pulses, and fishing. Sewage and eutrophication have been documented to impact Culebra [8,183], often in combination with fishing [184]. These issues contribute to coral decline through various mechanisms, including nutrient enrichment, pathogen introduction, and habitat degradation. Excessive nutrients from sewage promote the proliferation of macroalgae, which can outcompete corals for space

and light, leading to shifts in reef community structure [185–187]. Elevated nutrient levels can enhance the virulence of coral pathogens, increasing the incidence of coral diseases [188]. Algal blooms resulting from nutrient-loaded and sediment-laden runoff and coastal eutrophication decrease water clarity, limiting the photosynthetic capacity of coral endosymbionts. Nutrient enrichment can also disrupt the balance of microbial communities associated with corals, potentially leading to increased susceptibility to disease. It is possible that local eutrophication gradient impacts might have contributed to affect fish distribution in this study, but this was not directly quantified.

Fish assemblage recovery from disturbance was documented in this study evidencing enhanced abundance and biomass on numerous species and on different functional groups, but particularly on some of the herbivore guilds. It was also documented through abundance–biomass comparison (ABC) analysis. The ABC method is a valuable tool for assessing the disturbance levels in fish assemblages by comparing species cumulative abundance and biomass. In a stable community, the biomass curve typically lies above the abundance curve, indicating dominance by larger, slower-growing species. Conversely, in disturbed communities, the abundance curve surpasses the biomass curve, reflecting a shift towards smaller, opportunistic species. The data observed in this study suggest that restoration interventions not only resulted in an overall enhancement of fish community biodiversity, taxonomic complexity and functional diversity, but also in the abundance and biomass of juvenile stages of numerous species and in the attraction of large-bodied 'climax' species. Studies have indicated that in heavily fished areas, the abundance curves were positioned above the biomass curves, signifying a disturbed community structure [158–160]. Studies conducted in Daya Bay, revealed that when the biomass curve was above the abundance curve, the community was stable and dominated by large-sized, "climax" species, but when the biomass curve felt below the abundance curve, it indicated a severely disturbed community dominated by small-sized species [159]. This supports the original hypothesis of this study that the role of coral reef habitat restoration should promote the recovery of depleted fish assemblages and enhance the natural role of fish in promoting enhanced coral growth and net long-term resilience.

The impacts of coral restoration on recovering depleted fish assemblages were also documented though changes in overall biodiversity. Average taxonomic distinctness (Δ^+) and its variation (Λ^+) are valuable metrics for assessing biodiversity and taxonomic complexity changes in reef fish communities, particularly in the context of coral restoration efforts. Δ^+ measures the mean taxonomic distance between all pairs of species within a community, reflecting the breadth of taxonomic complexity. In the context of this study, the observed variation in Δ^+ after restoration efforts suggests enhanced species richness and a broader range of taxonomic groups present, indicating a positive impact on taxonomic complexity and potentially in functional diversity and redundancy. Λ^+ quantifies the variability in taxonomic distances among species pairs, providing insight into the evenness of taxonomic representation. High Λ^+ values indicate uneven taxonomic representation before the restoration intervention, possibly due to dominance by a few taxonomic groups, while low Λ+ values suggest a more even distribution after restoration.

While direct studies linking coral reef restoration to changes in Δ^+ and Λ^+ in fish communities are limited. Existing research provides insights into how restoration efforts can influence these indices. Studies have shown that coral reef degradation, due to factors like bleaching and habitat loss, can lead to declines in both Δ^+ and Λ^+. For instance, research on Meiji Reef in the South China Sea observed reductions in these indices over time, suggesting a loss of taxonomic diversity and evenness in fish communities [189]. However, a pioneering study conducted in Puerto Rico showed that long-term restoration of *Acropora palmata* led to enhanced fish abundance, biomass and biodiversity indices, including Δ^+

and Λ^+ [85]. A study conducted in St. Croix, USVI, reported increases in fish abundance and species richness shortly after *A. cervicornis* restoration activities [190]. While this study did not directly measure Δ^+ and Λ^+, the observed enhancements in species richness and community composition suggest potential improvements in taxonomic distinctness metrics. Although direct empirical evidence linking coral restoration to changes in Δ^+ and Λ^+ is scarce, existing studies indicate that restoration efforts can positively influence fish community structure and diversity. Further research is needed to quantify these effects and to establish robust links between restoration practices and taxonomic distinctness indices across different biogeographic provinces and across different spatial scales.

The use of mixed natural out-planted corals and artificial structures in this study was novel and aimed to accelerate fish attraction and recruitment to promote higher fish densities. In turn, this was expected to promote the formation of nutrient hot spots as suggested in previous restoration studies [85]. This should in turn lead to enhanced demographic performance in out-planted corals. There are examples of previous studies showing successful fish recruitment and community enhancement on 3D-printed coral artificial units at the Gulf of Aqaba, which reached a steady state within one year [72]. Small-bodied fish species with high habitat specificity showed preferences for selected 3D-printed coral colors and morphologies, suggesting that 3D-printed corals can serve as functional substitutes for live corals in providing habitat for reef fish [92]. A study at Bahía Tamarindo Reef in Culebra, Puerto Rico, evaluated the effectiveness of 3D-printed corals in attracting reef fish [86]. The findings indicated that the number of fish associated with artificial and natural corals did not differ significantly. However, fish abundance was higher in corals with greater structural complexity, regardless of whether they were natural or 3D-printed. This underscores the importance of structural complexity in reef habitats and that 3D-printed units can mimic depleted natural corals. In laboratory experiments, the behavior of coral-associated damselfish (*Chromis viridis*) was assessed in the presence of 3D-printed coral models [88]. The study found no significant differences in fish behavior between natural and 3D-printed corals, suggesting that the artificial structures did not negatively impact the fish. This supports the potential use of 3D-printed corals in reef restoration without adverse effects on resident fish species. These studies collectively suggest that 3D-printed coral structures can play a valuable role in reef restoration efforts by providing suitable habitats for reef fish, thereby supporting the recovery and maintenance of fish assemblages in degraded reef ecosystems. This technology can be useful in reef futures largely depleted by projected climate change impacts.

4.6. The Future of Integrated Natural and 3D-Printed Corals

The novel integration of 3D-printed and natural corals promotes increased biodiversity, fish taxonomic complexity and ecosystem functionality. This combined strategy creates a variety of microhabitats that support a wider range of marine species, enhancing biodiversity. Spatial configurations can be designed to form a combination of shelters and natural corridors for juvenile fish and individuals of different size stages. Integrated 3D-printed models enhance essential shelter and breeding grounds for various fish species provided by natural corals, promoting enhanced habitat complexity and increased biodiversity. The ability to customize the design of 3D-printed corals allows for the accommodation of specific habitat preferences of different fish species, potentially aiding in targeted conservation efforts. In areas where natural coral recovery is slow or unfeasible, 3D-printed structures can serve as interim habitats, supporting fish populations and maintaining ecological functions until natural corals can reestablish via ecological restoration.

Natural corals contribute to essential ecosystem functions such as calcium carbonate production, nutrient cycling, and primary productivity. Meanwhile, 3D-printed corals

enhance habitat complexity and stability, increasing fish attraction, nutrient hotspot formation, bolstering coral demographic performance, and potentially providing substrate for coral larval settlement and growth. This integration also improves ecosystem resilience to environmental stressors. Depending on the materials used, reef zone deployment, unit size, and spatial configuration, the combined structural complexity of 3D-printed and natural corals can more effectively dissipate wave energy in the long term, protecting shorelines and reducing erosion. Furthermore, natural corals with enhanced resilience to thermal stress and ocean acidification can be integrated with 3D-printed corals to create more resilient reef systems. This innovative approach leverages the strengths of both artificial and natural elements to foster a more robust and diverse marine environment.

This combined approach can also enhance coral propagation and recruitment. Depending on the materials used, 3D-printed corals provide additional surfaces for coral larvae to settle, increasing the chances of successful recruitment and growth of natural corals. Depending on the materials used, microbial biofilms can develop on 3D-printed coral surfaces to promote coral larval settlement on these structures [191]. There is also an emergent technology of producing "bionic 3D-printed corals" capable of capable of harboring high densities of endosymbiotic microalgae [93]. Additionally, 3D-printed corals also provide habitat for transplanting clippings of natural corals, contributing to creating "natural coral nursery plots" that serve as potential sources of clippings for future restoration efforts through coral gardening strategies. Fragments of resilient coral species can be directly attached to open reef substrates or to 3D-printed structures, promoting the growth and spread of these species within the reef. There is evidence that fragments of *Acropora palmata* out-planted to natural reef substrates in Puerto Rico resulted in significant reattachment, colony survival and growth rates, and enhanced fish attraction [85]. These colonies also functioned as natural nursery plots providing thousands of natural fragments for further restoration activities for 15 years. Natural nursery plots can become a vital strategy to acclimatize corals to changing climate and environmental conditions, as well as to restore degraded urban reefs (Figure 18). Obviously, the success of natural nursery plots will depend on reef trophic conditions, algal and sediment dynamics, reef geomorphology, etc. But this is an important strategy to add to the coral restoration practice toolbox.

Integrated approaches also offer significant conservation and management benefits. They reduce the need to harvest natural corals from healthy reefs, mitigating the impact on existing ecosystems. This method allows for targeted restoration efforts in specific areas that have suffered significant degradation, optimizing resource use and effectiveness and enabling community-based integration. It also provides opportunities for controlled experimentation and research, facilitating monitoring and data collection, and supporting adaptive management.

The integration of 3D-printed and natural out-planted corals promotes vital community-based socio-economic benefits. Enhanced reef structures attract divers and snorkelers, boosting eco-tourism and supporting local economies. Additionally, this approach offers valuable educational opportunities for local communities and visitors, raising awareness about coral conservation. Combining 3D-printed corals with natural corals in reef restoration provides a comprehensive strategy that combines the immediate and temporal benefits of artificial structures with the long-term ecological functions of natural corals. This approach enhances habitat complexity, accelerates reef recovery through increased biodiversity, and promotes the formation of nutrient hotspots. It improves natural coral demographic performance and the resilience of coral reef ecosystems. By leveraging the strengths of both 3D-printed and natural corals, more effective and sustainable reef restoration efforts can be achieved, supporting both marine life and human communities.

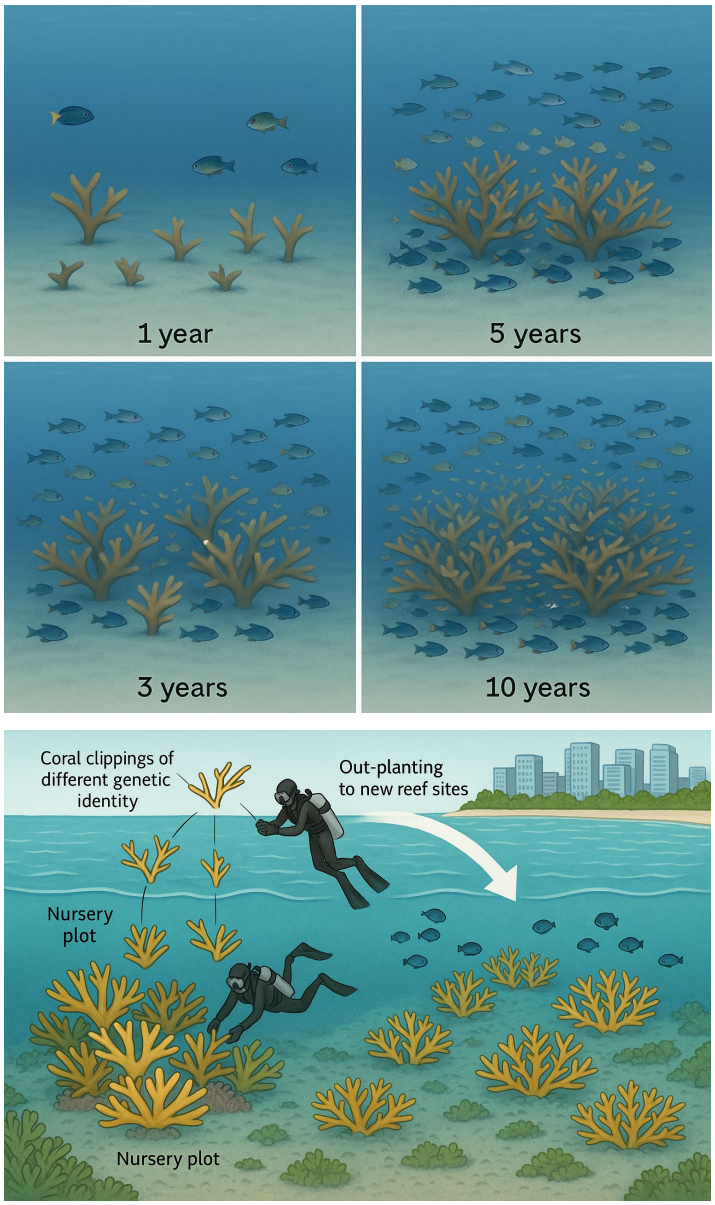

Figure 18. Conceptual design of natural coral nursery plots through time after 1, 3, 5, and 10 years of creation. Using appropriate genetic characterization, tagging, and mapping techniques, these nursery plots can continuously provide coral clippings of different genetic identities to promote restoration at new out-planting sites. They can also support acclimatization of corals to changing environments and climate variations, mitigate environmental impacts, restore urban coastlines, etc.

The use of 3D-printed corals offers several benefits for enhancing fish assemblages, which are crucial for maintaining the ecological balance and health of coral reef ecosystems:

1. Habitat creation and complexity—3D-printed corals can be designed to mimic the intricate structures of natural coral reefs, providing nooks, crannies, and overhangs that serve as hiding spots, breeding grounds, and feeding areas for fish. Different fish species have varying habitat preferences. Also, 3D-printed corals can be constructed of different materials and customized to create diverse microhabitats and spatial configurations, supporting a wider range of fish species and life stages.
2. Refuge and protection—The complex structures of 3D-printed corals offer refuge and biological corridors for smaller fish and juvenile stages of larger fish, helping them avoid predators. Secure environments within 3D-printed corals also provide

safe breeding spaces for fish to lay eggs and rear their young, contributing to higher survival rates.

3. Enhanced feeding opportunities—The surfaces of 3D-printed corals can support the growth of algae and sessile invertebrates, which are important food sources for many reef fish species. The intricate designs can also help trap plankton and detritus, providing additional feeding opportunities for filter-feeding fish.
4. Increased biodiversity and fish abundance—By providing a variety of habitats and resources, 3D-printed corals can attract a more diverse assemblage of fish species, increasing overall biodiversity, taxonomic complexity and functional diversity. Enhanced habitats can support larger populations of fish by providing the necessary resources for survival and reproduction.
5. Support for fish communities—Healthy fish assemblages contribute to the stability and resilience of coral reef ecosystems. Diverse fish communities play various roles, such as grazing on algae, which prevents algal overgrowth and supports coral health. Certain fish species play key roles in maintaining the balance of reef ecosystems. Also, some fish species are vital to support geo-ecological functions, such as sediment transport dynamics; 3D-printed corals help support these key species by providing suitable habitats and resources.
6. Facilitation of ecological interactions—Enhanced structures can facilitate symbiotic relationships between fish and other marine organisms, such as cleaner fish that remove parasites from larger fish. By attracting different trophic levels, 3D-printed corals help sustain complex food webs, supporting ecosystem functioning and productivity.
7. Conservation and restoration benefits—In areas where natural coral reefs have been damaged or destroyed (such as in this study), 3D-printed corals can help partially re-establish fish habitats and support the recovery of fish populations. In addition to restoring degraded areas, 3D-printed corals can be used to supplement existing reefs, enhancing their habitat complexity and fish-carrying capacity.
8. Research and monitoring opportunities—3D-printed corals provide standardized and replicable structures for scientific research, allowing for controlled studies on fish behavior, population dynamics, and ecological interactions. The use of 3D-printed corals facilitates easier monitoring of fish assemblages, enabling researchers to track changes over time and adapt restoration strategies accordingly.

5. Conclusions

This study has profound implications for future restoration strategies under projected climate changes. The findings suggest that integrating 3D-printed structures with natural coral out-plants can rapidly enhance fish assemblages (i.e., abundance, biomass, biodiversity) and their ecological functions (i.e., herbivory) in degraded reef areas by a possible combination of enhancing benthic complexity at the plot scale and by promoting the formation of nutrient hot spots on fish aggregations. Fish community enhancement resulting from the integrated out-planting of natural and 3D-printed *A. cervicornis* can lead to numerous benefits for corals such as nutrient subsidies and recycling, sediment removal, enhanced oxygenation, and protection against predators and parasites [192]. Greater fish densities support higher demographic performance of coral out-plants. These aspects require further investigation. This hybrid approach offers a promising strategy for reef restoration, particularly in regions where natural coral recruitment is limited, has collapsed following bleaching-related mass coral mortalities, where reef bottoms are flattened due to hurricane mechanical impacts, or where there is a need to rehabilitate herbivory. It would also be useful for restoring shallow urban coral reefs using combined green/grey infrastructure restoration approaches. Future efforts should consider the specific design

and placement of larger artificial or hybrid structures to maximize habitat complexity and ecological benefits. This would particularly enhance wave energy and runup attenuation in the long-term, while bolstering fisheries recovery. Additionally, long-term monitoring is essential to assess the persistence of these effects and to inform adaptive management practices.

This study also evidenced a potential compounded effect of mass coral bleaching and mortality in 2023. The increasing frequency and severity of mass coral bleaching and mortality associated with prolonged MHWs pose a significant threat to *C. personatus* and similar small-bodied, highly specialized Caribbean reef fish species. The loss of coral cover and structural complexity disrupts essential habitat and food resources, leading to declines in fish diversity and abundance, further disrupting fish ecological functions and food web integrity. Conservation efforts focusing on mitigating climate change impacts and protecting and restoring coral reef habitats are crucial for the sustainability of these vulnerable fish populations.

By creating complex, diverse, and sustainable habitats, depending on the materials used, 3D-printed corals offer significant benefits for enhancing fish assemblages. These structures support fish populations through increased refuge, feeding opportunities, and breeding grounds, leading to greater biodiversity and ecological resilience. By integrating 3D-printed corals into restoration and conservation efforts, we can promote a faster recovery of ecological processes and help maintain and enhance the health and productivity of coral reef ecosystems, benefiting both marine life and human communities that depend on these vital resources. These insights contribute to the growing body of knowledge on innovative restoration techniques and underscore the potential of hybrid approaches in supporting restored reef resilience and biodiversity. Furthermore, this project has also demonstrated again that participatory community-based conservation and restoration efforts have produced significant outcomes, in consistency with the literature that suggests that human stewardship is essential for driving conservation success, especially when different stakeholders work together in restoring marine life [193]. Reversing the trajectory of ecosystem loss towards repairing ocean health is feasible if appropriate strategies and stakeholder participation are made possible.

Supplementary Materials: The following are available online at https://www.mdpi.com/article/10.3390/d17070445/s1, Figure S1. Bubble plot of the spatio-temporal variation in the $\sqrt{}$-transformed abundance of *Scarus iseri* based on a PCO analysis of fish community structure; Figure S2. Bubble plot of the spatio-temporal variation in the $\sqrt{}$-transformed abundance of *Scarus taeniopterus* based on a PCO analysis of fish community structure; Figure S3. Bubble plot of the spatio-temporal variation in the $\sqrt{}$-transformed abundance of *Sparisoma chrysopterum* based on a PCO analysis of fish community structure; Figure S4. Bubble plot of the spatio-temporal variation in the $\sqrt{}$-transformed abundance of *Sparisoma viride* based on a PCO analysis of fish community structure; Figure S5. Bubble plot of the spatio-temporal variation in the $\sqrt{}$-transformed abundance of *Acanthurus tractus* based on a PCO analysis of fish community structure; Figure S6. Bubble plot of the spatio-temporal variation in the $\sqrt{}$-transformed abundance of *Stegastes partitus* based on a PCO analysis of fish community structure; Figure S7. Bubble plot of the spatio-temporal variation in the $\sqrt{}$-transformed abundance of *Epinephelus adsencionis* based on a PCO analysis of fish community structure; Figure S8. Bubble plot of the spatio-temporal variation in the $\sqrt{}$-transformed abundance of *Lutjanus apodus* based on a PCO analysis of fish community structure; Figure S9. Bubble plot of the spatio-temporal variation in the $\sqrt{}$-transformed abundance of *Ocyurus chrysurus* based on a PCO analysis of fish community structure; Figure S10. Bubble plot of the spatio-temporal variation in the $\sqrt{}$-transformed abundance of *Haemulon flavolineatum* based on a PCO analysis of fish community structure; Figure S11. Bubble plot of the spatio-temporal variation in the $\sqrt{}$-transformed abundance of *Haemulon parrai* based on a PCO analysis of fish community structure; Figure S12. Bubble plot of the spatio-

temporal variation in the √-transformed abundance of *Chaetodon capistratus* based on a PCO analysis of fish community structure; Figure S13. Bubble plot of the spatio-temporal variation in the √-transformed abundance of *Halichoeres bivittatus* based on a PCO analysis of fish community structure; Figure S14. Bubble plot of the spatio-temporal variation in the √-transformed abundance of *Bathygobius soporator* based on a PCO analysis of fish community structure; Figure S15. Bubble plot of the spatio-temporal variation in the √-transformed abundance of *Cophopterus personatus* based on a PCO analysis of fish community structure; Figure S16. Bubble plot of the spatio-temporal variation in the √-transformed abundance of *Elacatynus genie* based on a PCO analysis of fish community structure; Table S1. Summary of before–after pairwise two-way crossed PERMANOVA test of the spatio-temporal variation in fish community parameters among treatments; Table S2. Summary of before–after pairwise two-way crossed PERMANOVA test of the spatio-temporal variation in herbivore fish abundance among treatments; Table S3. Summary of before–after pairwise two-way crossed PERMANOVA test of the spatio-temporal variation in carnivore fish abundance among treatments; Table S4. Summary of before–after pairwise two-way crossed PERMANOVA test of the spatio-temporal variation in herbivore fish biomass among treatments; Table S5. Summary of before–after pairwise two-way crossed PERMANOVA test of the spatio-temporal variation in carnivore fish biomass among treatments; Table S6. Summary of before–after pairwise two-way crossed PERMANOVA test of the spatio-temporal variation in fishery target species abundance and biomass among treatments; Table S7. Summary of before–after pairwise two-way crossed PERMANOVA test of the spatio-temporal variation in fish community structure based in abundance and biomass among treatments; Table S8. SIMPER analysis of the dominant fish species before restoration interventions (Group 0); Table S9. SIMPER analysis of the dominant fish species after restoration interventions (Group 1); Table S10. SIMPER analysis of indicator fish species of the variation in community structure before (Group 0) and after (Group 1) the restoration interventions; Table S11. SIMPER analysis of indicator fish species of the variation in community structure before (Group 0) and after (Group 1) the restoration interventions within location MAG; Table S12. SIMPER analysis of indicator fish species of the variation in community structure before (Group 0) and after (Group 1) the restoration interventions within location TAM; Table S13. SIMPER analysis of the dominant fish species before restoration interventions within the Coral treatment group; Table S14. SIMPER analysis of the dominant fish species before restoration interventions within the 3D treatment group; Table S15. SIMPER analysis of the dominant fish species before restoration interventions within the Mixed treatment group; Table S16. SIMPER analysis of the dominant fish species before restoration interventions within the Control treatment group; Table S17. SIMPER analysis of indicator fish species of the variation in community structure before restoration interventions between groups Coral and 3D; Table S18. SIMPER analysis of indicator fish species of the variation in community structure before restoration interventions between groups Coral and Mixed; Table S19. SIMPER analysis of indicator fish species of the variation in community structure before restoration interventions between groups Coral and Control; Table S20. SIMPER analysis of indicator fish species of the variation in community structure before restoration interventions between groups 3D and Mixed; Table S21. SIMPER analysis of indicator fish species of the variation in community structure before restoration interventions between groups 3D and Control; Table S22. SIMPER analysis of indicator fish species of the variation in community structure after restoration interventions between groups Mixed and Control; Table S23. SIMPER analysis of the dominant fish species after restoration interventions within the Coral treatment group; Table S24. SIMPER analysis of the dominant fish species after restoration interventions within the 3D treatment group; Table S25. SIMPER analysis of the dominant fish species after restoration interventions within the Mixed treatment group; Table S26. SIMPER analysis of the dominant fish species after restoration interventions within the Control treatment group; Table S27. SIMPER analysis of indicator fish species of the variation in community structure after restoration interventions between groups Coral and 3D; Table S28. SIMPER analysis of indicator fish species of the variation in community structure after restoration interventions between groups Coral and Mixed; Table S29. SIMPER analysis of indicator fish species of the variation in community structure after restoration interventions between groups Coral and Control;

Table S30. SIMPER analysis of indicator fish species of the variation in community structure after restoration interventions between groups 3D and Mixed; Table S31. SIMPER analysis of indicator fish species of the variation in community structure after restoration interventions between groups 3D and Control; Table S32. SIMPER analysis of indicator fish species of the variation in community structure after restoration interventions between groups Mixed and Control; Table S33. SIMPER analysis of indicator fish species of the variation in community structure before (Time 0) and after (Time 1) restoration interventions within group Coral; Table S34. SIMPER analysis of indicator fish species of the variation in community structure before (Time 0) and after (Time 1) restoration interventions within group 3D; Table S35. SIMPER analysis of indicator fish species of the variation in community structure before (Time 0) and after (Time 1) restoration interventions within group Mixed; Table S36. SIMPER analysis of indicator fish species of the variation in community structure before (Time 0) and after (Time 1) restoration interventions within group Control; Table S37. Hierarchal preference based on the abundance of indicator fishes that preferred each experimental treatment before (0) and after (1) restoration interventions; Table S38. Summary of multivariate correlations between fish community parameters and the reef rugosity index; Table S39. Summary of multivariate correlations between fish biodiversity parameters and the reef rugosity index.

Author Contributions: Conceptualization, A.E.M.-M., S.E.S.-R. and E.A.H.-D.; methodology, E.A.H.-D., A.E.M.-M. and S.E.S.-R.; validation, E.A.H.-D.; formal analysis, E.A.H.-D.; investigation, E.A.H.-D. and J.S.F.-M.; resources, A.E.M.-M., S.E.S.-R. and E.A.H.-D.; data curation, E.A.H.-D.; writing—original draft preparation, E.A.H.-D.; writing—review and editing, E.A.H.-D., J.S.F.-M., A.E.M.-M. and S.E.S.-R.; visualization, E.A.H.-D.; supervision, A.E.M.-M. and S.E.S.-R.; project administration, A.E.M.-M. and S.E.S.-R.; funding acquisition, A.E.M.-M. and S.E.S.-R. All authors have read and agreed to the published version of the manuscript.

Funding: This research was supported by National Fish and Wildlife Foundation (NFWF), National Coastal Resilience Fund through grant 66113 to A.E.M.-M. and S.E.S.-R. (Sociedad Ambiente Marino).

Institutional Review Board Statement: Not applicable.

Data Availability Statement: The data presented in this study are available in the Supplementary File Hernandez-Delgado et al. 3D fish data*.xlsx.

Acknowledgments: This project was made possible by the extensive support provided by members and volunteers of Sociedad Ambiente Marino (SAM) and Captain Pedro Gómez (Asociación Pesquera de Culebra). The project was completed with the support of the Fideicomiso de Arquitectura (Fablab), University of Puerto Rico-Río Piedras, Alpha-Distributors, Centro Criollo de Ciencia y Tecnología (C3TEC), and Engine 4 for all 3D printing. This project was conducted under letter of agreement 2019-000007 between SAM and the Puerto Rico Department of Natural and Environmental Resources (PRDNER). It was also conducted under PRDNER research permit O-VS-PVS15-SJ-001159-24092020 and under US Army Corps of Engineer (USACE) permit SAJ-2020-00989. This publication is a contribution of SAM's Reef Conservation, Vitalization and Ecological Restoration (RECOVER) Program. Author E.A.H.D. is the Certified Ecological Restoration Practitioner #0670 (Society for Ecological Restoration). Special thanks to the three anonymous reviewers for their recommendations that significantly improved the manuscript.

Conflicts of Interest: The authors declare no conflicts of interest. The funders had no role in the design of the study; in the collection, analyses, or interpretation of data; in the writing of the manuscript, or in the decision to publish the results.

References

1. Rogers, C.S. Responses of coral reefs and reef organisms to sedimentation. *Mar. Ecol. Progr. Ser.* **1990**, *62*, 185–202. [CrossRef]
2. Otaño-Cruz, A.; Montañez-Acuña, A.A.; García-Rodríguez, N.M.; Díaz-Morales, D.M.; Benson, E.; Cuevas, E.; Ortiz-Zayas, J.; Hernández-Delgado, E.A. Caribbean near-shore coral reef benthic community response to changes on sedimentation dynamics and environmental conditions. *Front. Mar. Sci.* **2019**, *6*, 551. [CrossRef]
3. Rogers, C.S.; Ramos-Scharrón, C.E. Assessing effects of sediment delivery to coral reefs: A Caribbean watershed perspective. *Front. Mar. Sci.* **2022**, *8*, 773968. [CrossRef]

4. Freitas, L.M.; Oliveira, M.D.; Leão, Z.M.; Kikuchi, R.K. Effects of turbidity and depth on the bioconstruction of the Abrolhos reefs. *Coral Reefs* **2019**, *38*, 241–253. [CrossRef]
5. Cloern, J.E. Our evolving conceptual model of the coastal eutrophication problem. *Mar. Ecol. Progr. Ser.* **2001**, *210*, 223–253. [CrossRef]
6. Díaz-Ortega, G.; Hernández-Delgado, E.A. Unsustainable land-based source pollution in a climate of change: A roadblock to the conservation and recovery of Elkhorn Coral *Acropora palmata* (Lamarck 1816). *Nat. Res.* **2014**, *5*, 561–581. [CrossRef]
7. Ennis, R.S.; Brandt, M.E.; Grimes, K.R.; Smith, T.B. Coral reef health response to chronic and acute changes in water quality in St. Thomas, United States Virgin Islands. *Mar. Poll. Bull.* **2016**, *111*, 418–427. [CrossRef]
8. Hernández-Delgado, E.A.; Medina-Muñiz, J.L.; Mattei, H.; Norat-Ramírez, J. Unsustainable land use, sediment-laden runoff, and chronic raw sewage offset the benefits of coral reef ecosystems in a no-take marine protected area. *Env. Mgmt. Sust. Dev.* **2017**, *6*, 292. [CrossRef]
9. Hawkins, J.P.; Roberts, C.M. Effects of artisanal fishing on Caribbean coral reefs. *Conserv. Biol.* **2004**, *18*, 215–226. [CrossRef]
10. Wilson, S.K.; Fisher, R.; Pratchett, M.S.; Graham, N.A.; Dulvy, N.K.; Turner, R.A.; Cakacaka, A.; Polunin, N.V. Habitat degradation and fishing effects on the size structure of coral reef fish communities. *Ecol. Appl.* **2010**, *20*, 442–451. [CrossRef]
11. McWilliams, J.P.; Côté, I.M.; Gill, J.A.; Sutherland, W.J.; Watkinson, A.R. Accelerating impacts of temperature-Induced coral bleaching in the Caribbean. *Ecology* **2005**, *86*, 2055–2060. [CrossRef]
12. Burt, J.; Al-Harthi, S.; Al-Cibahy, A. Long-term impacts of coral bleaching events on the world's warmest reefs. *Mar. Env. Res.* **2011**, *72*, 225–229. [CrossRef] [PubMed]
13. Kleypas, J.A.; Yates, K.K. Coral reefs and ocean acidification. *Oceanography* **2009**, *22*, 108–117. [CrossRef]
14. Field, M.E.; Ogston, A.S.; Storlazzi, C.D. Rising sea level may cause decline of fringing coral reefs. *Eos. Tran. Am. Geophys. Union.* **2011**, *92*, 273–274. [CrossRef]
15. Elsner, J.B. Evidence in support of the climate change–Atlantic hurricane hypothesis. *Geophys. Res. Lett.* **2006**, *33*, L16705. [CrossRef]
16. Trenberth, K.E. Warmer oceans, stronger hurricanes. *Sci. Am.* **2007**, *297*, 44–51. [CrossRef]
17. Knutson, T.R.; Chung, M.V.; Vecchi, G.; Sun, J.; Hsieh, T.L.; Smith, A.J. Climate change is probably increasing the intensity of tropical cyclones. In *Critical Issues in Climate Change Science*; Tyndall Centre for Climate Change Research: Norwich, UK, 2021; Available online: https://tyndall.ac.uk/wp-content/uploads/2021/03/sciencebrief_review_cyclones_mar2021.pdf (accessed on 1 November 2024).
18. Ruiz-Allais, J.P.; Benayahu, Y.; Lasso-Alcalá, O.M. The invasive octocoral *Unomia stolonifera* (Alcyonacea, Xeniidae) is dominating the benthos in the Southeastern Caribbean Sea. *Mem. Fund. La. Salle Cien. Nat.* **2021**, *79*, 63–80.
19. Toledo-Rodríguez, D.A.; Veglia, A.; Marrero, N.M.; Gómez-Samot, J.M.; McFadden, C.S.; Weil, E.; Schizas, N.V. Shadows over Caribbean reefs: Identification of a new invasive soft coral species, *Xenia umbellata*, in southwest Puerto Rico. *bioRxiv* **2024**. [CrossRef]
20. Pueschel, C.M.; Saunders, G.W. *Ramicrusta textilis* sp. nov. (Peyssonneliaceae, Rhodophyta), an anatomically complex Caribbean alga that overgrows corals. *Phycologia* **2009**, *48*, 480–491. [CrossRef]
21. Altieri, A.H.; Harrison, S.B.; Seemann, J.; Collin, R.; Diaz, R.J.; Knowlton, N. Tropical dead zones and mass mortalities on coral reefs. *Proc. Natl. Acad. Sci. USA* **2017**, *114*, 3660–3665. [CrossRef]
22. Nelson, H.R.; Altieri, A.H. Oxygen: The universal currency on coral reefs. *Coral Reefs* **2019**, *38*, 177–198. [CrossRef]
23. Weil, E.; Rogers, C.S. Coral reef diseases in the Atlantic-Caribbean. In *Coral Reefs: An Ecosystem in Transition*; Dubinsky, Z., Stambler, N., Eds.; Springer: Dordrecht, The Netherlands, 2010; pp. 465–491.
24. Hewson, I.; Ritchie, I.T.; Evans, J.S.; Altera, A.; Behringer, D.; Bowman, E.; Brandt, M.; Budd, K.A.; Camacho, R.A.; Cornwell, T.O.; et al. A scuticociliate causes mass mortality of *Diadema antillarum* in the Caribbean Sea. *Science Adv.* **2023**, *9*, eadg3200. [CrossRef] [PubMed]
25. Miller, J.; Muller, E.; Rogers, C.; Waara, R.; Atkinson, A.; Whelan, K.R.; Patterson, M.; Witcher, B. Coral disease following massive bleaching in 2005 causes 60% decline in coral cover on reefs in the US Virgin Islands. *Coral Reefs* **2009**, *28*, 925–937. [CrossRef]
26. Hernández-Pacheco, R.; Hernández-Delgado, E.A.; Sabat, A.M. Demographics of bleaching in a major Caribbean reef-building coral: *Montastraea annularis*. *Ecosphere* **2011**, *2*, 1–13. [CrossRef]
27. Hernández-Delgado, E.A.; Rodríguez-González, Y.M. Runaway climate across the Wider Caribbean and Eastern Tropical Pacific in the Anthropocene: Threats to coral reef conservation, restoration, and social-ecological resilience. *Atmosphere* **2025**, *16*, 575. [CrossRef]
28. Cruz, D.W.; Villanueva, R.D.; Baria, M.V. Community-based, low-tech method of restoring a lost thicket of *Acropora* corals. *ICES J. Mar. Sci.* **2014**, *71*, 1866–1875. [CrossRef]

29. Hernández-Delgado, E.A.; Mercado-Molina, A.E.; Alejandro-Camis, P.J.; Candelas-Sánchez, F.; Fonseca-Miranda, J.S.; González-Ramos, C.M.; Guzmán-Rodríguez, R.; Mège, P.; Montañez-Acuña, A.A.; Maldonado, I.O.; et al. Community-based coral reef rehabilitation in a changing climate: Lessons learned from hurricanes, extreme rainfall, and changing land use impacts. *Open J. Ecol.* **2014**, *4*, 918. [CrossRef]
30. Young, C.N.; Schopmeyer, S.A.; Lirman, D. A review of reef restoration and coral propagation using the threatened genus *Acropora* in the Caribbean and Western Atlantic. *Bull. Mar. Sci.* **2012**, *88*, 1075–1098. [CrossRef]
31. Omori, M. Coral restoration research and technical developments: What we have learned so far. *Mar. Biol. Res.* **2019**, *15*, 377–409. [CrossRef]
32. Boström-Einarsson, L.; Babcock, R.C.; Bayraktarov, E.; Ceccarelli, D.; Cook, N.; Ferse, S.C.; Hancock, B.; Harrison, P.; Hein, M.; Shaver, E.; et al. Coral restoration–A systematic review of current methods, successes, failures and future directions. *PLoS ONE* **2020**, *15*, e0226631. [CrossRef]
33. Ceccarelli, D.M.; McLeod, I.M.; Boström-Einarsson, L.; Bryan, S.E.; Chartrand, K.M.; Emslie, M.J.; Gibbs, M.T.; González Rivero, M.; Hein, M.Y.; Heyward, A.; et al. Substrate stabilisation and small structures in coral restoration: State of knowledge, and considerations for management and implementation. *PLoS ONE* **2020**, *15*, e0240846. [CrossRef] [PubMed]
34. Mwaura, J.M.; Murage, D.; Karisa, J.F.; Otwoma, L.M.; Said, H.O. Artificial reef structures and coral transplantation as potential tools for enhancing locally-managed inshore reefs: A case study from Wasini Island, Kenya. *West. Indian Ocean J. Mar. Sci.* **2022**, *21*, 83–94. [CrossRef]
35. Rinkevich, B. Ecological engineering approaches in coral reef restoration. *ICES J. Mar. Sci.* **2021**, *78*, 410–420. [CrossRef]
36. Henry, J.A.; O'Neil, K.L.; Pilnick, A.R.; Patterson, J.T. Strategies for integrating sexually propagated corals into Caribbean reef restoration: Experimental results and considerations. *Coral Reefs* **2021**, *40*, 1667–1677. [CrossRef]
37. Page, C.A.; Muller, E.M.; Vaughan, D.E. Microfragmenting for the successful restoration of slow growing massive corals. *Ecol. Eng.* **2018**, *123*, 86–94. [CrossRef]
38. Knapp, I.S.; Forsman, Z.H.; Greene, A.; Johnston, E.C.; Bardin, C.E.; Chan, N.; Wolke, C.; Gulko, D.; Toonen, R.J. Coral micro-fragmentation assays for optimizing active reef restoration efforts. *Peer J.* **2022**, *10*, e13653. [CrossRef]
39. Chamberland, V.F.; Vermeij, M.J.; Brittsan, M.; Carl, M.; Schick, M.; Snowden, S.; Schrier, A.; Petersen, D. Restoration of critically endangered elkhorn coral (*Acropora palmata*) populations using larvae reared from wild-caught gametes. *Global Ecol. Cons.* **2015**, *4*, 526–537. [CrossRef]
40. Hagedorn, M.; Spindler, R.; Daly, J. Cryopreservation as a tool for reef restoration: 2019. *Adv. Exp. Med. Biol.* **2019**, *1200*, 489–505.
41. Toh, E.C.; Liu, K.L.; Tsai, S.; Lin, C. Cryopreservation and cryobanking of cells from 100 coral species. *Cells* **2022**, *11*, 2668. [CrossRef]
42. Hagedorn, M.; Page, C.A.; O'Neil, K.L.; Flores, D.M.; Tichy, L.; Conn, T.; Chamberland, V.F.; Lager, C.; Zuchowicz, N.; Lohr, K.; et al. Assisted gene flow using cryopreserved sperm in critically endangered coral. *Proc. Nat. Acad. Sci. USA* **2021**, *118*, e2110559118. [CrossRef]
43. Lin, C.C.; Li, H.H.; Tsai, S.; Lin, C. Tissue cryopreservation and cryobanking: Establishment of a cryogenic resource for coral reefs. *Biopreserv. Biobanking.* **2022**, *20*, 409–411. [CrossRef] [PubMed]
44. Hobbs, R.J.; O'Brien, J.K.; Bay, L.K.; Severati, A.; Spindler, R.; Henley, E.M.; Quigley, K.M.; Randall, C.J.; van Oppen, M.J.; Carter, V.; et al. A decade of coral biobanking science in Australia-transitioning into applied reef restoration. *Front. Mar. Sci.* **2022**, *9*, 960470. [CrossRef]
45. Schmidt-Roach, S.; Duarte, C.M.; Hauser, C.A.; Aranda, M. Beyond reef restoration: Next-generation techniques for coral gardening, landscaping, and outreach. *Front. Mar. Sci.* **2020**, *7*, 672. [CrossRef]
46. Rinkevich, B. The active reef restoration toolbox is a vehicle for coral resilience and adaptation in a changing world. *J. Mar. Sci. Eng.* **2019**, *7*, 201. [CrossRef]
47. Hernández-Delgado, E.A. Coastal restoration challenges and strategies for small island developing states in the face of sea level rise and climate change. *Coasts* **2024**, *4*, 235–286. [CrossRef]
48. Horoszowski-Fridman, Y.B.; Brêthes, J.-C.; Rahmani, N.; Rinkevich, B. Marine silviculture: Incorporating ecosystem engineering properties into reef restoration acts. *Ecol. Eng.* **2015**, *82*, 201–213. [CrossRef]
49. Hoegh-Guldberg, O.; Hughes, L.; McIntyre, S.; Lindenmayer, D.B.; Parmesan, C.; Possingham, H.P.; Thomas, C.D. Assisted colonization and rapid climate change. *Science* **2008**, *321*, 345–346. [CrossRef]
50. Coles, S.L.; Riegl, B.M. Thermal tolerances of reef corals in the Gulf: A review of the potential for increasing coral survival and adaptation to climate change through assisted translocation. *Mar. Pollut. Bull.* **2013**, *72*, 323–332. [CrossRef]
51. Van Oppen, M.J.; Oliver, J.K.; Putnam, H.M.; Gates, R.D. Building coral reef resilience through assisted evolution. *Proc. Natl. Acad. Sci. USA* **2015**, *112*, 2307–2313. [CrossRef]
52. Epstein, H.E.; Smith, H.A.; Torda, G.; van Oppen, M.J. Microbiome engineering: Enhancing climate resilience in corals. *Front. Ecol. Environ.* **2019**, *17*, 100–108. [CrossRef]

53. Rosado, P.M.; Leite, D.C.; Duarte, G.A.; Chaloub, R.M.; Jospin, G.; da Rocha, U.N.; Saraiva, J.P.; Dini-Andreote, F.; Eisen, J.A.; Bourne, D.G.; et al. Marine probiotics: Increasing coral resistance to bleaching through microbiome manipulation. *ISME J.* **2019**, *13*, 921–936. [CrossRef] [PubMed]
54. Palumbi, S.R.; Barshis, D.J.; Traylor-Knowles, N.; Bay, R.A. Mechanisms of reef coral resistance to future climate change. *Science* **2014**, *344*, 895–898. [CrossRef] [PubMed]
55. Liew, Y.J.; Zoccola, D.; Li, Y.; Tambutté, E.; Venn, A.A.; Michell, C.T.; Cui, G.; Deutekom, E.S.; Kaandorp, J.A.; Voolstra, C.R.; et al. Epigenome-associated phenotypic acclimatization to ocean acidification in a reef-building coral. *Sci. Adv.* **2018**, *4*, eaar8028. [CrossRef]
56. Rinkevich, B. Coral chimerism as an evolutionary rescue mechanism to mitigate global climate change impacts. *Glob. Change Biol.* **2019**, *25*, 1198–1206. [CrossRef]
57. Coe, W.R. Season of attachment and rate of growth of sedentary marine organisms at the pier of the Scripps Institution of Oceanography, La Jolla, California. *Bull. Scripps. Inst. Oceanogr. Tech. Ser.* **1932**, *3*, 37–86.
58. Coe, W.R.; Allen, W.E. Growth of sedentary marine organisms on experimental blocks and plates for nine successive years at the pier of the Scripps Institution of Oceanography. *Bull. Scripps. Inst. Oceanogr. Tech. Ser.* **1937**, *4*, 101–136.
59. Carlisle, J.G., Jr.; Turner, C.H.; Ebert, E.E. Artificial habitat in the marine environment. *Calif. Dept. Fish Game Fish Bull.* **1964**, *124*, 1–93.
60. Ogawa, Y. Experiments on the attractiveness of artificial reefs for marine fishes. VII. Attraction of fishes to the various sizes of model reefs. *Bull. Jap. Soc. Sci. Fish.* **1967**, *33*, 801–811. [CrossRef]
61. Bohnsack, J.A.; Sutherland, D.L. Artificial reef research: A review with recommendations for future priorities. *Bull. Mar. Sci.* **1985**, *37*, 11–39.
62. Alevizon, W.S.; Gorham, J.C. Effects of artificial reef deployment on nearby resident fishes. *Bull. Mar. Sci.* **1989**, *44*, 646–661.
63. Gorham, J.C.; Alevizon, W.S. Habitat complexity and the abundance of juvenile fishes residing on small scale artificial reefs. *Bull. Mar. Sci.* **1989**, *44*, 662–665.
64. Polovina, J.J. Fisheries applications and biological impacts of artificial habitats. In *Artificial Habitats for Marine and Freshwater Fisheries*; Academic Press, Inc.: Cambridge, MA, USA, 1991; pp. 153–176.
65. Pickering, H.; Whitmarsh, D. Artificial reefs and fisheries exploitation: A review of the 'attraction versus production' debate, the influence of design and its significance for policy. *Fish. Res.* **1997**, *31*, 39–59. [CrossRef]
66. Seaman, W. Artificial habitats and the restoration of degraded marine ecosystems and fisheries. *Hydrobiologia* **2007**, *580*, 143–155. [CrossRef]
67. Andrade Frehse, F.; Derviche, P.; Pereira, F.W.; Hostim-Silva, M.; Simões Vitule, J.R. Artificial aquatic hábitats: A systematic literature review and new perspectives. *Hydrobiologia* **2025**, *852*, 1997–2012. [CrossRef]
68. Lange, C.J.; Ratoi, L.; Co, D.L. Reformative coral habitats-Rethinking artificial coral reef structures through a robotic clay printing method. InRE: Anthropocene, Design in the Age of Humans. In Proceedings of the 25th International Conference of the Association for Computer-Aided Architectural Design Research, Singapore, 30 June–3 July 2020; CAADRIA: Hsinchu, China, 2020; Volume 2.
69. Avila-Ramírez, A.; Valle-Pérez, A.U.; Susapto, H.H.; Pérez-Pedroza, R.; Briola, G.R.; Alrashoudi, A.; Khan, Z.; Bilalis, P.; Hauser, C.A. Ecologically friendly biofunctional ink for reconstruction of rigid living systems under wet conditions. *Int. J. Bioprinting.* **2021**, *7*, 65–75. [CrossRef]
70. Hirsch, M.; Lucherini, L.; Zhao, R.; Saracho, A.C.; Amstad, E. 3D printing of living structural biocomposites. *Materials Today* **2023**, *62*, 21–32. [CrossRef]
71. Gutiérrez-Heredia, L.; Keogh, C.; Keaveney, S.; Reynaud, E.G. 3D printing solutions for coral studies, education and monitoring. *Reef Encounter.* **2016**, *31*, 39–44.
72. Oren, A.; Berman, O.; Neri, R.; Edery-Lutri, M.; Chernihovsky, N.; Tarazi, E.; Shashar, N. Ecological succession on 3D printed ceramic artificial reefs. *Sci. Total Environ.* **2024**, *954*, 176371. [CrossRef]
73. Albalawi, H.I.; Khan, Z.N.; Valle-Pérez, A.U.; Kahin, K.M.; Hountondji, M.; Alwazani, H.; Schmidt-Roach, S.; Bilalis, P.; Aranda, M.; Duarte, C.M.; et al. Sustainable and eco-friendly coral restoration through 3D printing and fabrication. *ACS Sust. Chem. Eng.* **2021**, *9*, 12634–12645. [CrossRef]
74. Good, A.M. Investigating the Influence of Additional Structural Complexity in Present Day Reef Restoration. Master's Thesis, University of Delaware, Delaware, NJ, USA, 2020; pp. 1–78.
75. Levy, N.; Simon-Blecher, N.; Ben-Ezra, S.; Yuval, M.; Doniger, T.; Leray, M.; Karako-Lampert, S.; Tarazi, E.; Levy, O. Evaluating biodiversity for coral reef reformation and monitoring on complex 3D structures using environmental DNA (eDNA) metabarcoding. *Sci. Total Env.* **2023**, *856*, 159051. [CrossRef]
76. Crawford, A.; Humanes, A.; Caldwell, G.; Guest, J.; van der Steeg, E. Architecture for coral restoration: Using clay-based digital fabrication to overcome bottlenecks to coral larval propagation. In *Structures and Architecture A Viable Urban Perspective?* CRC Press: Boca Raton, FL, USA, 2022; pp. 458–466.

77. Berman, O.; Levy, N.; Parnas, H.; Levy, O.; Tarazi, E. Exploring new frontiers in coral nurseries: Leveraging 3D printing technology to benefit coral growth and survival. *J. Mar. Sci. Eng.* **2023**, *11*, 1695. [CrossRef]
78. Muñoz-Maravilla, J.D.; Edmunds, P.J. Three-dimensional printing can provide opportunities to promote coral recruitment on disturbed reefs. *Bull. Mar. Sci.* **2024**, *101*, 283–296. [CrossRef]
79. Leonard, C.; Hédouin, L.; Lacorne, M.C.; Dalle, J.; Lapinski, M.; Blanc, P.; Nugues, M.M. Performance of innovative materials as recruitment substrates for coral restoration. *Rest. Ecol.* **2022**, *30*, e13625. [CrossRef]
80. Levenstein, M.A.; Gysbers, D.J.; Marhaver, K.L.; Kattom, S.; Tichy, L.; Quinlan, Z.; Tholen, H.M.; Wegley Kelly, L.; Vermeij, M.J.; Wagoner Johnson, A.J.; et al. Millimeter-scale topography facilitates coral larval settlement in wave-driven oscillatory flow. *PLoS ONE* **2022**, *17*, e0274088. [CrossRef] [PubMed]
81. Frau, L.; Marzeddu, A.; Dini, E.; Gracía, V.; Gironella, X.; Erioli, A.; Zomparelli, A.; Sánchez-Arcilla, A. Effects of ultra-porous 3D printed reefs on wave kinematics. *J. Coast. Res.* **2016**, *37*, 851–855. [CrossRef]
82. Geldard, J.; Lowe, R.; Draper, S.; Ghisalberti, M.; Westera, S.; Ellwood, G.; Cuttler, M.; Smith, D.; McArdle, A. Effectiveness of coral reef restoration in wave attenuation applications. *Coast. Eng. Proc.* **2022**, *37*, 90–91. [CrossRef]
83. Karim, F.; Nandasena, N.A. Experimental and numerical assessment of marine flood reduction by coral reefs. *Nat. Hazards Res.* **2023**, *3*, 35–41. [CrossRef]
84. Norris, B.K.; Storlazzi, C.D.; Pomeroy, A.W.; Reguero, B.G. Optimizing infragravity: Wave attenuation to improve coral reef restoration design for coastal defense. *J. Mar. Sci. Eng.* **2024**, *12*, 768. [CrossRef]
85. Hernández-Delgado, E.A.; Laureano, R. Bringing back reef fish: Sustainable impacts of community-based restoration of Elkhorn coral (*Acropora palmata*) in Vega Baja, Puerto Rico (2008–2023). *Sustainability* **2024**, *16*, 5985. [CrossRef]
86. Pérez-Pagán, B.S.; Mercado-Molina, A.E. Evaluation of the effectiveness of 3D-printed corals to attract coral reef fish at Tamarindo Reef, Culebra, Puerto Rico. *Conserv. Evid.* **2018**, *15*, 43–47.
87. Ruhl, E.J. Understanding the Importance of Habitat Complexity for Juvenile Fish and the Application of 3D Printed Corals for Reef Restoration. Master's Thesis, University of Delaware, Delaware, NJ, USA, 2018; pp. 1–92.
88. Ruhl, E.J.; Dixson, D.L. 3D printed objects do not impact the behavior of a coral-associated damselfish or survival of a settling stony coral. *PLoS ONE* **2019**, *14*, e0221157. [CrossRef] [PubMed]
89. Tarazi, E.; Parnas, H.; Lotan, O.; Zoabi, M.; Oren, A.; Josef, N.; Shashar, N. Nature-centered design: How design can support science to explore ways to restore coral reefs. *The Design J.* **2019**, *22* (Suppl. S1), 1619–1628. [CrossRef]
90. Garg, A.; Green, S.J. An integrative method for enhancing the ecological realism of aquatic artificial habitat designs using 3D scanning, printing, moulding and casting. *Front. Built Environ.* **2022**, *8*, 763315. [CrossRef]
91. Riera, E.; Hubas, C.; Ungermann, M.; Rigot, G.; Pey, A.; Francour, P.; Rossi, F. Artificial reef effectiveness changes among types as revealed by underwater hyperspectral imagery. *Rest. Ecol.* **2023**, *31*, e13978. [CrossRef]
92. Oren, A.; Berman, O.; Neri, R.; Tarazi, E.; Parnas, H.; Lotan, O.; Zoabi, M.; Josef, N.; Shashar, N. Three-dimensional-printed coral-like structures as a habitat for reef fish. *J. Mar. Sci. Eng.* **2023**, *11*, 882. [CrossRef]
93. Wangpraseurt, D.; You, S.; Azam, F.; Jacucci, G.; Gaidarenko, O.; Hildebrand, M.; Kühl, M.; Smith, A.G.; Davey, M.P.; Smith, A.; et al. Bionic 3D printed corals. *Nature Comm.* **2020**, *11*, 1748. [CrossRef]
94. Wangpraseurt, D.; Sun, Y.; You, S.; Chua, S.T.; Noel, S.K.; Willard, H.F.; Berry, D.B.; Clifford, A.M.; Plummer, S.; Xiang, Y.; et al. Bioprinted living coral microenvironments mimicking coral-algal symbiosis. *Adv. Funct. Mat.* **2022**, *32*, 2202273. [CrossRef]
95. Firmanda, A.; Syamsu, K.; Sari, Y.W.; Cabral, J.; Pletzer, D.; Mahadik, B.; Fisher, J.; Fahma, F. 3D printed cellulose based product applications. *Mat. Chem. Front.* **2022**, *6*, 254–279. [CrossRef]
96. Yoris-Nobile, A.I.; Slebi-Acevedo, C.J.; Lizasoain-Arteaga, E.; Indacoechea-Vega, I.; Blanco-Fernández, E.; Castro-Fresno, D.; Alonso-Estebanez, A.; Alonso-Cañón, S.; Real-Gutiérrez, C.; Boukhelf, F.; et al. Artificial reefs built by 3D printing: Systematisation in the design, material selection and fabrication. *Const. Building Mat.* **2023**, *362*, 129766. [CrossRef]
97. Shantz, A.A.; Ladd, M.C.; Schrack, E.; Burkepile, D.E. Fish-derived nutrient hotspots shape coral reef benthic communities. *Ecol. Appl.* **2015**, *25*, 2142–2152. [CrossRef]
98. Stuart, C.E.; Wedding, L.M.; Pittman, S.J.; Serafy, J.E.; Moura, A.; Bruckner, A.W.; Green, S.J. Seascape connectivity modeling predicts hotspots of fish-derived nutrient provisioning to restored coral reefs. *Mar. Ecol. Progr. Series.* **2023**, *731*, 179–196. [CrossRef]
99. Krasowska, K.; Heimowska, A. Degradability of polylactide in natural aqueous environments. *Water* **2023**, *15*, 198. [CrossRef]
100. Royer, S.J.; Greco, F.; Kogler, M.; Deheyn, D.D. Not so biodegradable: Polylactic acid and cellulose/plastic blend textiles lack fast biodegradation in marine waters. *PLoS ONE* **2023**, *18*, e0284681. [CrossRef]
101. Bohnsack, J.A.; Bannerot, S.P. A stationary visual census technique for quantitatively assessing community structure of coral reef fishes. *NOAA Tech. Rept. NMFS* **1986**, *41*, 1–15.
102. Bohnsack, J.A.; Harper, D.E. Length-weight relationships of selected marine reef fishes from the southeastern United States and the Caribbean. *NOAA Tech. Memo. NMFSSEFC* **1988**, *215*, 1–31.

103. Anderson, M.J.; Gorley, R.N.; Clarke, K.R. *PERMANOVA + for PRIMER: Guide to Software and Statistical Methods*; Massey University: Auckland, New Zealand; Palmerston, New Zealand; PRIMER-e Ltd.: Plymouth, UK, 2008.
104. Bray, J.R.; Curtis, J.T. An ordination of the upland forest communities of southern Wisconsin. *Ecol. Monogr.* **1957**, *27*, 325–349. [CrossRef]
105. Randall, J.E. Food habits of reef fishes of the West Indies. *Contrib. Inst. Mar. Biol. Univ. Puerto Rico, Mayagüez* **1967**, *5*, 665–847.
106. Clarke, K.R.; Gorley, R.N.; Somerfield, P.J.; Warwick, R.M. *Change in Marine Communities: An Approach to Statistical Analysis and Interpretation*, 3rd ed.; PRIMER-E: Plymouth, UK, 2014.
107. Warwick, R.M.; Clarke, K.R. New\'biodiversity\'measures reveal a decrease in taxonomic distinctness with increasing stress. *Mar. Ecol. Progr. Ser.* **1995**, *129*, 301–305. [CrossRef]
108. Faith, D.P. Conservation evaluation and phylogenetic diversity. *Biol. Conserv.* **1992**, *61*, 1–10. [CrossRef]
109. Faith, D.P. Phylogenetic pattern and the quantification of organismal biodiversity. *Phil. Trans. Royal Soc. London. Ser. B Biol. Sci.* **1994**, *345*, 45–58.
110. Roberts, C.M.; Ormond, R.F.G. Habitat complexity and coral reef fish diversity and abundance on Red Sea fringing reefs. *Mar. Ecol. Progr. Ser.* **1987**, *41*, 1–8. [CrossRef]
111. Hawkins, J.P.; Roberts, C.M.; Van'THof, T.; De Meyer, K.; Tratalos, J.; Aldam, C. Effects of recreational scuba diving on Caribbean coral and fish communities. *Conserv. Biol.* **1999**, *13*, 888–897. [CrossRef]
112. Clark, T.D.; Edwards, A.J. An evaluation of artificial reef structures as tools for marine habitat rehabilitation in the Maldives. *Aquat. Conserv. Mar. Freshw. Ecosyst.* **1999**, *9*, 5–21. [CrossRef]
113. Spieler, R.E.; Gilliam, D.S.; Sherman, R.L. Artificial substrate and coral reef restoration: What do we need to know to know what we need. *Bull. Mar. Sci.* **2001**, *69*, 1013–1030.
114. Fadli, N.; Campbell, S.J.; Ferguson, K.; Keyse, J.; Rudi, E.; Booth, D.J. The role of habitat creation in restoring fish communities: Coral transplantation and 3D-printed reefs. *Mar. Biol. Res.* **2012**, *8*, 765–772.
115. Heery, E.C.; Sebens, K.P.; Sebens, K.P. Experimental test of the effect of habitat complexity on the diversity of coral reef fishes. *Mar. Ecol. Progr. Ser.* **2014**, *511*, 169–184.
116. Ng, C.S.L.; Toh, T.C.; Chou, L.M. Artificial reefs as a reef restoration strategy in sediment-affected environments: Insights from long-term monitoring. *Aquat. Conserv. Mar. Freshw. Ecosyst.* **2016**, *26*, 331–345. [CrossRef]
117. Ferse, S.C.A.; Knittweis, L.; Krause, G.; Maddusila, A.; Glaser, M. Livelihoods of ornamental coral fishermen in South Sulawesi/Indonesia: Implications for management. *Coastal Mgmt.* **2013**, *40*, 525–555. [CrossRef]
118. Coker, D.J.; Wilson, S.K.; Pratchett, M.S. Importance of live coral habitat for reef fishes. *Rev. Fish Biol. Fish.* **2014**, *24*, 89–126. [CrossRef]
119. Harborne, A.R.; Mumby, P.J.; Kennedy, E.V.; Ferrari, R. Biotic and multi-scale abiotic controls of habitat quality: Their effect on coral-reef fishes. *Mar. Ecol. Progr. Ser.* **2011**, *437*, 201–214. [CrossRef]
120. Messmer, V.; Jones, G.P.; Munday, P.L.; Holbrook, S.J.; Schmitt, R.J.; Brooks, A.J. Habitat biodiversity as a determinant of fish community structure on coral reefs. *Ecology* **2011**, *92*, 2285–2298. [CrossRef] [PubMed]
121. Graham, N.A.J.; Nash, K.L. The importance of structural complexity in coral reef ecosystems. *Coral Reefs* **2013**, *32*, 315–326. [CrossRef]
122. Kerry, J.T.; Bellwood, D.R. Competition for shelter in a high-diversity system: Structure use by large reef fishes. *Coral Reefs* **2016**, *35*, 245–252. [CrossRef]
123. Chabanet, P.; Ralambondrainy, H.; Amanieu, M.; Faure, G.; Galzin, R. Relationships between coral reef substrata and fish. *Coral Reefs* **1997**, *16*, 93–102. [CrossRef]
124. Jones, G.P.; Syms, C. Disturbance, habitat structure and the ecology of fishes on coral reefs. *Austr. J. Ecol.* **1998**, *23*, 287–297. [CrossRef]
125. Pittman, S.J.; Christensen, J.D.; Caldow, C.; Menza, C.; Monaco, M.E. Predictive mapping of fish species richness across shallow-water seascapes in the Caribbean. *Ecol. Mod.* **2007**, *204*, 9–21. [CrossRef]
126. Wilson, S.K.; Graham, N.A.; Polunin, N.V. Appraisal of visual assessments of habitat complexity and benthic composition on coral reefs. *Mar. Biol.* **2007**, *151*, 1069–1076. [CrossRef]
127. Risk, M.J. Fish diversity on a coral reef in the Virgin Islands. *Atoll Res. Bull.* **1972**, *153*, 1–4. [CrossRef]
128. Luckhurst, B.E.; Luckhurst, K. Analysis of the influence of substrate variables on coral reef fish communities. *Mar. Biol.* **1978**, *49*, 317–323. [CrossRef]
129. Friedlander, A.M.; Parrish, J.D. Habitat characteristics affecting fish assemblages on a Hawaiian coral reef. *J. Exp. Mar. Biol. Ecol.* **1998**, *224*, 1–30. [CrossRef]
130. Darling, E.S.; Graham, N.A.; Januchowski-Hartley, F.A.; Nash, K.L.; Pratchett, M.S.; Wilson, S.K. Relationships between structural complexity, coral traits, and reef fish assemblages. *Coral. Reefs.* **2017**, *36*, 561–575. [CrossRef]
131. Mazzuco, A.C.; Stelzer, P.S.; Bernardino, A.F. Substrate rugosity and temperature matters: Patterns of benthic diversity at tropical intertidal reefs in the SW Atlantic. *Peer J.* **2020**, *8*, e8289. [CrossRef] [PubMed]

132. Ormond, R.F.; Roberts, J.M.; Jan, R.Q. Behavioural differences in microhabitat use by damselfishes (Pomacentridae): Implications for reef fish biodiveristy. *J. Exp. Mar. Biol. Ecol.* **1996**, *202*, 85–95. [CrossRef]
133. Kerry, J.T.; Bellwood, D.R. Environmental drivers of sheltering behaviour in large reef fishes. *Mar. Poll. Bull.* **2017**, *125*, 254–259. [CrossRef]
134. Komyakova, V.; Jones, G.P.; Munday, P.L. Strong effects of coral species on the diversity and structure of reef fish communities: A multi-scale analysis. *PLoS ONE* **2018**, *13*, e0202206. [CrossRef]
135. Komyakova, V.; Munday, P.L.; Jones, G.P. Relative importance of coral cover, habitat complexity and diversity in determining the structure of reef fish communities. *PLoS ONE* **2013**, *8*, e83178. [CrossRef]
136. Brandt, M.E.; Zurcher, N.; Acosta, A.; Ault, J.S.; Bohnsack, J.A.; Feeley, M.W.; Harper, D.E.; Hunt, J.; Kellison, G.T.; McClellan, D.B.; et al. Reef-fish abundance, biomass, and biodiversity inside and outside no-take marine zones in the Florida Keys National Marine Sanctuary: 1999–2018. *Oceanography* **2020**, *33*, 104–117.
137. Kerry, J.T.; Bellwood, D.R. The effect of coral morphology on shelter selection by coral reef fishes. *Coral Reefs* **2012**, *31*, 415–424. [CrossRef]
138. McCormick, M.I. Comparison of field methods for measuring surface topography and their associations with a tropical reef fish assemblage. *Mar. Ecol. Progr. Ser.* **1994**, *112*, 87–96. [CrossRef]
139. Hixon, M.A.; Beets, J.P. Predation, prey refuges, and the structure of coral-reef fish assemblages. *Ecol. Monogr.* **1993**, *63*, 77–101. [CrossRef]
140. Alvarez-Filip, L.; Gill, J.A.; Dulvy, N.K. Complex reef architecture supports more small-bodied fishes and longer food chains on Caribbean reefs. *Ecosphere* **2011**, *2*, 1–17. [CrossRef]
141. Alvarez-Filip, L.; Paddack, M.J.; Collen, B.; Robertson, D.R.; Côté, I.M. Simplification of Caribbean reef-fish assemblages over decades of coral reef degradation. *PLoS ONE* **2015**, *10*, e0126004. [CrossRef] [PubMed]
142. Alvarez-Filip, L.; Dulvy, N.K.; Gill, J.A.; Côté, I.M.; Watkinson, A.R. Flattening of Caribbean coral reefs: Region-wide declines in architectural complexity. *Proc. Royal Soc. B Biol. Sci.* **2009**, *276*, 3019–3025. [CrossRef] [PubMed]
143. Rogers, A.; Blanchard, J.L.; Mumby, P.J. Vulnerability of coral reef fisheries to a loss of structural complexity. *Current Biol.* **2014**, *24*, 1000–1005. [CrossRef]
144. Wilson, S.K.; Graham, N.A.J.; Polunin, N.V.C. Apparent recovery of a Seychelles coral reef following a severe bleaching event. *Mar. Ecol. Progr. Ser.* **2007**, *306*, 131–142.
145. MacNeil, M.A.; Graham, N.A.J.; Cinner, J.E.; Wilson, S.K.; Williams, I.D.; Maina, J.; Newman, S.; Friedlander, A.M.; Jupiter, S.; Polunin, N.V.C.; et al. Recovery potential of the world's coral reef fishes. *Nature* **2015**, *520*, 341–344. [CrossRef]
146. Ladd, M.C.; Shantz, A.A. Trophic interactions in coral reef restoration: A review. *Coral Reefs* **2020**, *39*, 1283–1297. [CrossRef]
147. Robinson, J.P.; Wilson, S.K.; Robinson, J.; Gerry, C.; Lucas, J.; Assan, C.; Govinden, R.; Jennings, S.; Graham, N.A. Productive instability of coral reef fisheries after climate-driven regime shifts. *Nature Ecol. Evol.* **2019**, *3*, 183–190. [CrossRef]
148. Adam, T.C.; Burkepile, D.E.; Ruttenberg, B.I.; Paddack, M.J. Herbivory and the resilience of Caribbean coral reefs: Knowledge gaps and implications for management. *Mar. Ecol. Progr. Ser.* **2015**, *520*, 1–20. [CrossRef]
149. Burkepile, D.E.; Hay, M.E. Impact of herbivore identity on algal succession and coral growth on a Caribbean reef. *PLoS ONE* **2010**, *5*, e8963. [CrossRef]
150. Ceccarelli, D.M.; Jones, G.P.; McCook, L.J. Interactions between herbivorous fish guilds and their influence on algal succession on a coastal coral reef. *J. Exp. Mar. Biol. Ecol.* **2011**, *399*, 60–67. [CrossRef]
151. Calle-Triviño, J.; Muñiz-Castillo, A.I.; Cortés-Useche, C.; Morikawa, M.; Sellares-Blasco, R.; Arias-González, J.E. Approach to the functional importance of *Acropora cervicornis* in outplanting sites in the Dominican Republic. *Front. Mar. Sci.* **2021**, *8*, 668325. [CrossRef]
152. Bonaldo, R.M.; Hay, M.E. Seaweed–coral interactions: Variance in seaweed allelopathy, coral susceptibility, and potential effects on coral resilience. *PLoS ONE* **2014**, *9*, e85786. [CrossRef] [PubMed]
153. Steneck, R.S.; Arnold, S.N.; Mumby, P.J. Experiment mimics fishing on parrotfish: Insights on coral reef recovery and alternative attractors. *Mar. Ecol. Progr. Ser.* **2014**, *506*, 115–127. [CrossRef]
154. Mumby, P.J.; Harborne, A.R. Marine reserves enhance the recovery of corals on Caribbean reefs. *PLoS ONE* **2010**, *5*, e8657. [CrossRef]
155. McClanahan, T.R.; Muthiga, N.A. Geographic extent and variation of a coral reef trophic cascade. *Ecology* **2016**, *97*, 1862–1872. [CrossRef]
156. Mumby, P.J.; Hastings, A.; Edwards, H.J. Thresholds and the resilience of Caribbean coral reefs. *Nature* **2007**, *450*, 98–101. [CrossRef]
157. Hughes, T.P.; Rodrigues, M.J.; Bellwood, D.R.; Ceccarelli, D.; Hoegh-Guldberg, O.; McCook, L.; Willis, B. Phase shifts, herbivory, and the resilience of coral reefs to climate change. *Curr. Biol.* **2007**, *17*, 360–365. [CrossRef]
158. Yemane, D.; Field, J.G.; Leslie, R.W. Exploring the effects of fishing on fish assemblages using Abundance Biomass Comparison (ABC) curves. *ICES J. Mar. Sci.* **2005**, *62*, 374–379. [CrossRef]

159. Xu, S.; Guo, J.; Liu, Y.; Fan, J.; Xiao, Y.; Xu, Y.; Li, C.; Barati, B. Evaluation of fish communities in Daya bay using biomass size spectrum and ABC curve. *Front. Environ. Sci.* **2021**, *9*, 663169. [CrossRef]
160. Wijeyaratne, M.J.S.; Bellanthudawa, B.K. Effectiveness of Biomass/Abundance Comparison (ABC) models in assessing fish community disturbances. *Water* **2022**, *14*, 2934.
161. Lecchini, D.; Nakamura, Y. Use of chemical cues by coral reef animal larvae for habitat selection. *Aquat. Biol.* **2013**, *19*, 231–238. [CrossRef]
162. Marcos, M.; Amores, A.; Agulles, M.; Robson, J.; Feng, X. Global warming drives a threefold increase in persistence and 1 °C rise in intensity of marine heatwaves. *Proc. Natnl. Acad. Sci. USA* **2025**, *122*, e2413505122. [CrossRef] [PubMed]
163. Rodrigues, R.R.; Gonçalves Neto, A.H.; Vieira, E.A.; Longo, G.O. The severe 2020 coral bleaching event in the tropical Atlantic linked to marine heatwaves. *Comm. Earth Environ.* **2025**, *6*, 208. [CrossRef]
164. Wilson, S.K.; Graham, N.A.J.; Pratchett, M.S.; Jones, G.P.; Polunin, N.V.C. Multiple disturbances and the global degradation of coral reefs: Are reef fishes at risk or resilient? *Global Change Biol.* **2006**, *12*, 2220–2234. [CrossRef]
165. Pratchett, M.S.; Munday, P.L.; Wilson, S.K.; Graham, N.A.J.; Cinner, J.E.; Bellwood, D.R.; McClanahan, T.R. Effects of climate-induced coral bleaching on coral-reef fishes: Ecological and economic consequences. *Oceanogr. Mar. Biol. Ann. Rev.* **2008**, *46*, 251–296.
166. Graham, N.A.; Wilson, S.K.; Jennings, S.; Polunin, N.V.; Bijoux, J.P.; Robinson, J. Dynamic fragility of oceanic coral reef ecosystems. *Proc. Natnl. Acad. Sci. USA* **2006**, *103*, 8425–8429. [CrossRef]
167. Hughes, T.P.; Kerry, J.T.; Baird, A.H.; Connolly, S.R.; Chase, T.J.; Dietzel, A.; Torda, G. Global warming impairs stock–recruitment dynamics of corals. *Nature* **2019**, *568*, 387–390. [CrossRef]
168. Bellwood, D.R.; Hughes, T.P.; Folke, C.; Nyström, M. Confronting the coral reef crisis. *Nature* **2004**, *429*, 827–833. [CrossRef]
169. Nash, K.L.; Graham, N.A.J.; Wilson, S.K.; Bellwood, D.R. Cross-scale habitat structure drives fish body size distributions on coral reefs. *Ecosystems* **2013**, *16*, 478–490. [CrossRef]
170. Graham, N.A.J.; Wilson, S.K.; Jennings, S.; Polunin, N.V.C.; Robinson, J.; Bijoux, J.P.; Daw, T.M. Lag effects in the impacts of mass coral bleaching on coral reef fish, fisheries, and ecosystems. *Conserv. Biol.* **2007**, *21*, 1291–1300. [CrossRef] [PubMed]
171. Stuart-Smith, R.D.; Brown, C.J.; Ceccarelli, D.M.; Edgar, G.J. Ecosystem restructuring along the Great Barrier Reef following mass coral bleaching. *Nature* **2018**, *560*, 92–96. [CrossRef] [PubMed]
172. Richardson, L.E.; Graham, N.A.J.; Pratchett, M.S.; Eurich, J.G.; Hoey, A.S. Mass coral bleaching causes biotic homogenization of reef fish assemblages. *Global Change Biol.* **2018**, *24*, 3117–3129. [CrossRef] [PubMed]
173. Emslie, M.J.; Logan, M.; Williamson, D.H.; Ayling, A.M.; MacNeil, M.A.; Ceccarelli, D.; Thompson, C.A. Recovery from disturbance: Coral reef dynamics under climate change. *Mar. Ecol. Progr. Ser.* **2020**, *625*, 177–191.
174. Munday, P.L.; Jones, G.P.; Pratchett, M.S.; Williams, A.J. Climate change and the future for coral reef fishes. *Fish Fisheries* **2008**, *9*, 261–285. [CrossRef]
175. Delgado Cintrón, C. *Culebra y la Marina de Estados Unidos*; Editorial Edil: San Juan, PR, USA, 1989; p. 346.
176. Feliciano, C.C. *Apuntes y Comentarios de la Colonización y Liberación de la Isla de Culebra*, 2nd ed.; Fundación de Culebra: Culebra, PR, USA, 2001; p. 278.
177. Hernández-Delgado, E.A.; Montañez-Acuña, A.; Otaño-Cruz, A.; Suleimán-Ramos, S.E. Bomb-cratered coral reefs in Puerto Rico, the untold story about a novel habitat: From reef destruction to community-based ecological rehabilitation. *Rev. Biol. Trop.* **2014**, *62*, 350–367.
178. Hernández-Delgado, E.A.; Alejandro-Camis, P.; Cabrera-Beauchamp, G.; Fonseca-Miranda, J.S.; Gómez-Andújar, N.X.; Gómez, P.; Guzmán-Rodríguez, R.; Olivo-Maldonado, I.; Suleimán-Ramos, S.E. Stronger hurricanes and climate change in the Caribbean Sea: Threats to the sustainability of endangered coral species. *Sustainability* **2024**, *16*, 1506. [CrossRef]
179. Hernández-Delgado, E.A.; Toledo-Hernández, C.; Ruíz-Díaz, C.P.; Gómez-Andújar, N.; Medina-Muñiz, J.L.; Canals-Silander, M.F.; Suleimán-Ramos, S.E. Hurricane impacts and the resilience of the invasive sea vine. *Halophila stipulacea*: A case study from Puerto Rico. *Est. Coasts* **2020**, *43*, 1263–1283.
180. Ramos-Scharrón, C.E.; Amador, J.M.; Hernández-Delgado, E.A. An interdisciplinary erosion mitigation approach for coral reef protection—A case study from the eastern Caribbean. In *Marine Ecosystems*; InTech Publications: London, UK, 2012; pp. 127–160.
181. Ramos-Scharrón, C.E.; McLaughlin, P.; Figueroa-Sánchez, Y. Impacts of unpaved roads on runoff and erosion in a dry tropical setting: Isla De Culebra, Puerto Rico. *J. Soils Sediments* **2024**, *24*, 1420–1430. [CrossRef]
182. Gómez-Andújar, N.X.; Hernandez-Delgado, E.A. Spatial benthic community analysis of shallow coral reefs to support coastal management in Culebra Island, Puerto Rico. *Peer J.* **2020**, *8*, e10080. [CrossRef]
183. Hernández-Delgado, E.A.; Ortiz-Flores, M.F. The long and winding road of coral reef recovery in the Anthropocene: A case study from Puerto Rico. *Diversity* **2022**, *14*, 804. [CrossRef]
184. Hernández-Delgado, E.A.; Rosado, B.J.; Sabat, A.M. Management failures and coral decline threatens fish functional groups recovery patterns in the Luis Peña Channel No-take Natural Reserve, Culebra Island, Puerto Rico. *Proc. Gulf Caribb. Fish. Inst.* **2006**, *57*, 577–605.

185. Lapointe, B.E.; Brewton, R.A.; Herren, L.W.; Porter, J.W.; Hu, C. Nitrogen enrichment, altered stoichiometry, and coral reef decline at Looe Key, Florida Keys, USA: A 3-decade study. *Mar. Biol.* **2019**, *166*, 108. [CrossRef]
186. Lesser, M.P. Eutrophication on coral reefs: What is the evidence for phase shifts, nutrient limitation and coral bleaching. *BioScience* **2021**, *71*, 1216–1233. [CrossRef]
187. Thanopoulou, Z.; Patus, J.; Sealey, K.S. Water quality negatively impacts coral occurrence in eutrophic nearshore environments of the Florida Keys. *Front. Mar. Sci.* **2022**, *9*, 1005036. [CrossRef]
188. Wear, S.L.; Vega Thurber, R. Sewage pollution: Mitigation is key for coral reef stewardship. *Ann. NY Acad. Sci.* **2015**, *1355*, 15–30. [CrossRef]
189. Gong, Y.; Zhang, J.; Chen, Z.; Cai, Y.; Yang, Y. Taxonomic diversity and interannual variation of fish in the lagoon of Meiji Reef (Mischief Reef), South China Sea. *Biology* **2024**, *13*, 740. [CrossRef]
190. Opel, A.H.; Cavanaugh, C.M.; Rotjan, R.D.; Nelson, J.P. The effect of coral restoration on Caribbean reef fish communities. *Mar. Biol.* **2017**, *164*, 221. [CrossRef]
191. Riera, E.; Lamy, D.; Goulard, C.; Francour, P.; Hubas, C. Biofilm monitoring as a tool to assess the efficiency of artificial reefs as substrates: Toward 3D printed reefs. *Ecol. Eng.* **2018**, *120*, 230–237. [CrossRef]
192. Stier, A.C.; Chase, T.J.; Osenberg, C.W. Fish services to corals: A review of how coral-associated fishes benefit corals. *Coral Reefs* **2025**, *44*, 825–834. [CrossRef]
193. Rossbach, S.; Steckbauer, A.; Klein, S.G.; Arossa, S.; Geraldi, N.R.; Lim, K.K.; Martin, C.; Rossbach, F.I.; Shellard, M.J.; Valluzzi, L.; et al. A tide of change: What we can learn from stories of marine conservation success. *One Earth* **2023**, *6*, 505–518. [CrossRef]